The Neurofascins orchestrate assembly and maintenance of axonal domains in the central nervous system

Barbara Zonta

Ph.D.
University of Edinburgh

2007

DECLARATION

I declare that this thesis and the work described in it are my own except where indicated and have not been submitted for any other degree.

Barbara Zonta
September 2007

ACKNOWLEDGEMENTS

CONTENTS

LIST OF FIGURES

LIST OF TABLES

ABBREVIATIONS

bp	base pairs
CAM	Cell-adhesion molecule
cDNA	complementary DNA
CNS	Central nervous system
d	days
DIV	Days *in vitro*
DTT	Dithiothreitol
EDTA	Ethylene diamine tetracetic acid
ES	Embryonic day
FITC	Fluorescein isothiocyanate
h	hour
HCl	Hydrochloric acid
HRP	Horseradish peroxidase
Ig	Immunoglobulin
kb	kilobases
kD	kiloDalton
Kv	Voltage-gated sodium channels
LB	Luria-Bertani medium
mA	milli-ampere
MAG	Myelin associated glycoprotein
MBP	Myelin Basic Protein
min	minutes
mm	millimeter
mM	millimolar
mRNA	messenger RNA
Nav	Voltage-gated sodium channels
NF	Neurofilament
Nfasc	Neurofascin
ng	nanogram
OCT	Optimal cutting temperature
OSP	Oligodendrocyte specific protein
P	Post-natal day
P0	Myelin protein zero
PAGE	Polyacrylamide gel electrophoresis
PB	Phosphate buffer
PBS	Phosphate buffer saline
PC	Purkinje cell
PCR	Polymerase chain reaction
PFA	Paraformaldehyde
PLP	Proteolipid protein
PMSF	Phenylmethanesulphonylfluoride
PNS	Peripheral Nervous System
ROI	Region Of Interest
s	seconds
SC	Schwann cell

SDS	Sodium dodecyl sulfate
TAE	Tris-acetate-EDTA
TESPA	3'Amino propyl tri ethoxy silane
TRIS	trishydroxymethylaminomethane
TRITC	Tetramethylrhodamine isothiocyanate
μm	micron
μl	microliter

ABSTRACT

Close interaction between oligodendrocytes and axons is essential to initiate myelination and to form specialised domains along myelinated fibres. These domains are characterised by the assembly of protein complexes at the axon-glia interface and key components of these complexes are the Neurofascins.

Neurofascins are transmembrane glycoproteins belonging to the L1 subgroup of the Immunoglobulin (Ig) superfamily of cell adhesion molecules. The *Neurofascin* (*Nfasc*) gene is subject to extensive alternative splicing. Two of the best characterised isoforms are Nfasc155 and Nfasc186, which are expressed in glia and neurons respectively. In myelinated fibres, Nfasc186 is the predominant isoform expressed at nodes of Ranvier and axon initial segments (AIS) in both the central and peripheral nervous system (CNS and PNS), whereas Nfasc155 resides on the glial side of the paranodal axoglial junction.

The *Neurofascin* gene has been inactivated by homologous recombination and Neurofascin-null mice die within the first week of postnatal life. The main focus of this work was to investigate the role of the Neurofascins in the developing CNS.

Similarly to what has been previously observed in the PNS, this study shows that in myelinated fibres of the spinal cord, nodal and paranodal markers are mislocalised and axoglial junctions do not form in the absence of the Neurofascins. In contrast to the PNS, where ensheathment of axons is unaffected, myelin proteins in the CNS are greatly reduced in the mutant. This appears to be due to the reduced ability of oligodendrocyte myelinating processes to extend along axons.

This work also shows that the role of Nfasc186 is to maintain the long term stability of the AIS rather than its assembly.

In the PNS, Nfasc186 was found to play an essential role in node assembly. However, PNS and CNS nodes are likely to assemble by different mechanisms. To investigate the relative contribution of the Neurofascin isoforms in CNS node assembly, this work made use of transgenic lines in which either neuronal Nfasc186 or glial Nfasc155 was expressed on a Neurofascin null background. Expression of either isoform was found to independently rescue the nodal complex and a model of how the Neurofascins cooperate in the assembly of the CNS node of Ranvier is proposed.

1. INTRODUCTION

1.1 Myelin biogenesis in the peripheral and central nervous system

The partnerships established between different cell types ensure proper functioning of the nervous system. This is particular true in the context of myelination, where an intricate and functional relationship between myelinating glial cells and neurons develops in a series of stages that result from reciprocal interactions. Our knowledge of how these complex relationships are established in the course of myelinogenesis has been gradually accumulating in the past decades.

Myelin is a lipid-rich membrane that acts as an electrical insulator. It is a unique feature of nervous system structure in vertebrates, since, from an evolutionary standpoint, it has conferred the advantage of increased speed of nerve impulse while minimising axon calibre and metabolic needs (Colman et al., 2001).

Specialised glial cells, Schwann cells (SCs) in the peripheral nervous system (PNS) and oligodendrocytes in the central nervous system (CNS) (Figure 1), form a myelin sheath by extending their plasma membrane and wrapping axons several times, and this sheath expands longitudinally and radially in proportion to the size and diameter of the axon (Sherman and Brophy, 2005).

Compact myelin is formed when the glial cytoplasm is extruded from the myelinating process, thus allowing for a close apposition of adjacent plasma membrane surfaces. The resulting multi-lamellar membrane forms as a periodic structure, with alternating concentric electron-dense and light layers (Scherer and Arroyo, 2002).

Myelinated axons are characterised by regularly spaced insulating segments, termed internodes, which can be up to 1.5 mm or more in length depending on the axon diameter and the specific fiber type (Salzer, 1997). The internodes are separated by regions where the axolemmal membrane is exposed to the extracellular environment. These bare regions of about 1-2 μm in length are known as nodes of Ranvier, and are the sites where action potentials are propagated (Ellisman et al., 2001). Similar to nodes of Ranvier, axon initial segments (AIS) are naked segments of 20-40 μm in length positioned at the very proximal end of the axon, where afferent input to the cell soma is integrated and where action potentials are initiated. Both the AIS and the nodes of

Ranvier are characterised by an extreme dense clustering of voltage-gated sodium (Nav) channels (Lai and Jan, 2006).

The high resistance and low capacitance of the myelin sheath, together with the fact that current spreads rapidly within the axon from node to node ensures that the nerve impulse travels rapidly down the axon, jumping from node to node, and this form of nerve conduction is described as saltatory (from the Latin *saltare*, to jump) (Kandel et al., 2000).
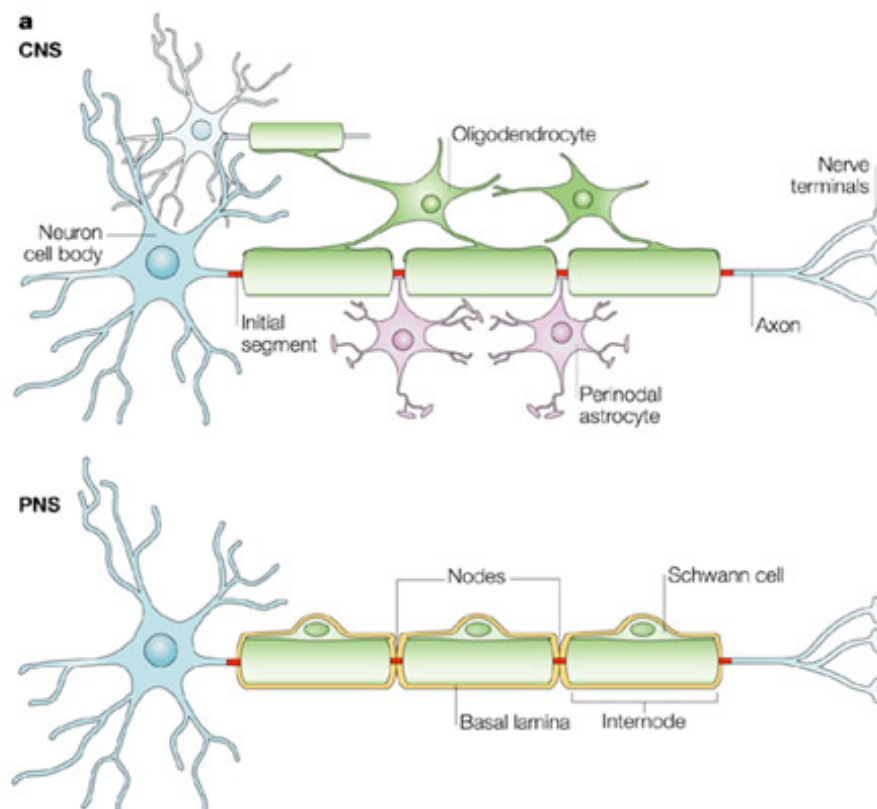
FIGURE 1. Structure of Myelinated Axons in the CNS and PNS
Compact myelin forms at regularly spaced intervals, internodes, leaving gaps, known as nodes of Ranvier. The initial segment is also a bare region positioned at the proximal end of the axon. In the CNS, oligodendrocytes myelinate multiple axons, whereas in the PNS Schwann cells myelinate one single axon. Schwann cells are also associated with a well-defined basal lamina, which is absent in the CNS (Source: Poliak and Peles, 2003).

The function of myelin in the PNS and CNS is similar, however there are differences in the cell biology of SCs and oligodendrocytes.

The first notable difference is that SCs myelinate a single internode, whereas oligodendrocytes can myelinate multiple axons and several internodes per axon, reaching as many as 40 in the optic nerve of rodents (Arroyo and Scherer, 2000). In addition, SCs are surrounded by a basal lamina, which is absent from the oligodendrocyte sheath, and they extend microvilli that encapsulate the node of Ranvier. The space between the axolemma and the basal lamina, i.e. the perinodal space, is also filled with a filamentous matrix. In the CNS, nodes may be contacted by perinodal astrocytes, but this is not a consistent feature of central nodes (Poliak and Peles, 2003).

Finally, ontogenetically PNS myelination precedes CNS myelination, and there are differences in myelin protein composition between PNS and CNS (Baumann and Pham-Dinh, 2001).

1.1.1 Schwann cell and oligodendrocyte lineages

Schwann cells (SCs) of spinal nerves derive from neural crest cells, which give rise to Schwann cell precursors (SCPs) and immature Schwann cells during embryogenesis. SCPs are already found to be closely associated with perinatal nerves early in murine embryonic life, at around embryonic day (E) 12-13, and their main function is not only to be the source of new SCs but also to provide trophic support to sensory and motor neurons. Immature SCs, which are generated at E13-15, are essential for normal nerve fasciculation. Their random association with axons of different calibres dictates the postnatal development of SCs to a mature identity. Mature SCs either ensheath multiple small axons, forming a Remak bundle, or sort larger axons (with a diameter of 1 μm or greater) into a 1:1 relationship that they subsequently myelinate. SC commitment to myelination is accompanied by a major change in their morphological and molecular phenotype that is driven by signals from the axon (Jessen and Mirsky, 2005) (Figure 2).

As mentioned previously, SCs are surrounded by a basal lamina, conferring to SCs a unique epithelial-like characteristic which is not shared by other glial cells

(Colman et al., 2001) and which also plays a critical role in myelin formation in the PNS (Salzer, 2003).
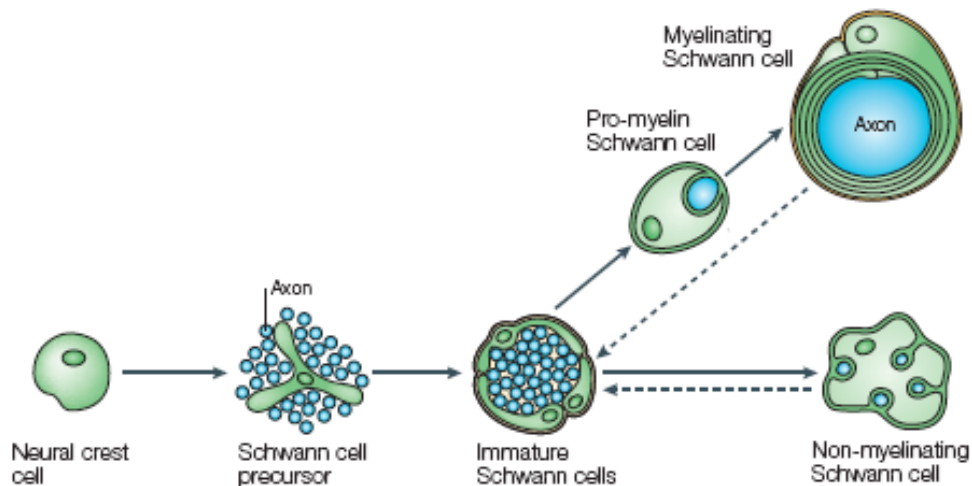
FIGURE 2. The Schwann Cell Lineage
Diagram showing the main cell types in Schwann cell development. Dashed arrows indicate the reversibility of the final, largely postnatal transition during which myelinating and non-myelinating cells are generated. Myelinating cells ensheath large diameter axons, whereas Schwann cells that envelop small diameter axons progress to become non-myelinating mature cells. (Source: Jessen and Mirsky, 2005).

Myelinating oligodendrocytes, like Schwann cells, have a neuroepithelial origin. Oligodendrocytes are one of the last cell types to differentiate in the CNS, accumulating mainly after birth in the rodent CNS. They derive from oligodendrocyte precursor cells (OPCs) that line the ventral lumen of the spinal cord and the sub-ventricular zone (SVZ) of the brain during embryonic life (Richardson, 2001). The OPCs then migrate and settle along the fibers of the future white matter tracts. There, they acquire new morphological and biochemical identities as pre-oligodendrocytes, though maintaining the property of cell division. Pre-oligodendrocytes become immature oligodendrocytes, which will develop into mature pro-myelinating oligodendrocytes. The latter have two

fates: only those oligodendrocytes that manage to ensheath axons survive, whereas those that fail degenerate (Trapp et al., 1997).

Similarly to what happens in the PNS, mature myelinating oligodendrocytes do not wrap their plasma membrane randomly around neuronal processes, but carefully select axons that attain a critical diameter of > 0.2 µm, excluding dendrites (Miller, 2002). The mature myelinating oligodendrocyte phenotype is established through the concurrent interaction with multiple axons, the expression and the targeting of myelin proteins to compact myelin (Richardson, 2001) (Figure 3).

At each stage of SC and oligodendrocyte development a unique complement of transcription factors and genes are expressed, accompanied by morphological changes, which in turn are triggered by extrinsic signals, including growth and trophic factors (Miller, 2002 ; Jessen and Mirsky, 2005).
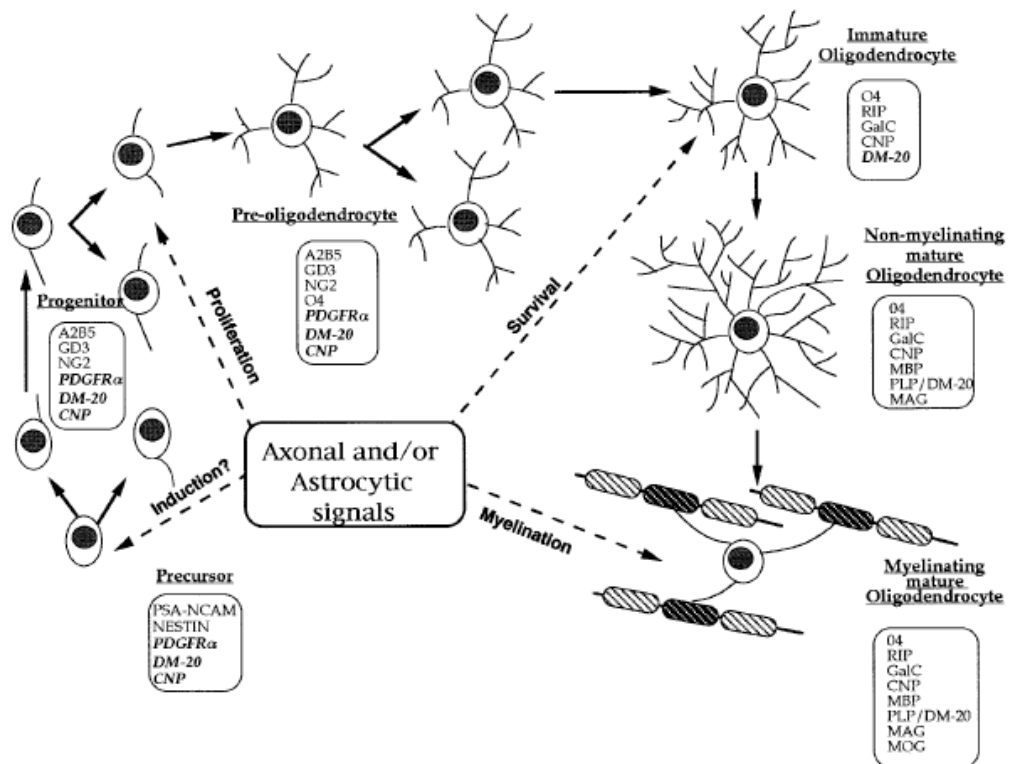
FIGURE 3. The Oligodendrocyte Cell Lineage.
Schematic representation of the developmental stages of the oligodendrocyte lineage and the accompanying morphological and genetic changes (Source: Baumann and Pham-Dinh, 2001)

1.1.2 Axonal signals involved in myelination

What are the signals that trigger axon ensheathment and myelination? Since the ensheathment of axons must occur at the appropriate time of neuronal development, reciprocal communication between neurons and myelinating glial cells is essential to coordinate myelin biogenesis.

It has become increasingly clear that the onset of myelination depends on a balance between positive and negative axonal signals, which control the timing of myelination and match the number of glial cells to the axonal surface requiring myelination (Coman et al., 2005; Simons and Trajkovic, 2006). In the PNS, it appears that, at all stages of Schwann cell maturation, axonal signals are mandatory, since proliferation, survival and differentiation of SCs do not occur in the absence of neurons (Jessen and Mirsky, 2005).

Conversely, oligodendrocytes appear to be less axon-dependent, since newly differentiated oligodendrocytes can synthesise myelin constituents and form myelin-like membrane in neuron-free cultures (Baumann and Pham-Dinh, 2001). Nevertheless, myelin formed *in vitro* in the absence of neurons is not as well compacted as when wrapped around axons, and the observation that, even in culture, oligodendrocytes myelinate solely axons suggests that a recognition signal on the axonal surface is likely to trigger ensheathment by oligodendrocyte processes (Lubetzki et al., 1993). In addition, axonal ensheathment appears to be significant for oligodendrocyte survival, since oligodendrocyte cell death occurs before any commitment to myelin formation (Trapp et al., 1997). Co-culture and *in vivo* experiments have also indicated that direct contact with axons increases myelin gene expression by oligodendrocytes (Matsuda et al., 1997). But what is the nature of these signals?

Cell adhesion molecules at the axon-glia interface have long been considered candidate molecules to convey the axonal signal to the myelin-forming cells. They not only bring the axon and glial cell in close proximity, but have the potential to transduce signals in a bidirectional way. For example, L1 and polysialylated NCAM (Neural Cell Adhesion Molecule) on the axonal surface appear to regulate myelination in both PNS and CNS (Sherman and Brophy, 2005). In myelinating co-cultures, antibodies against L1 have been shown to inhibit the earlier stages of myelination (Wood et al., 1990), whereas disappearance of polysialylated NCAM from the axonal surface favours initiation of myelin deposition (Coman et al., 2005).

In recent years, evidence has accumulated supporting a role of Neuregulins (NRGs) in myelination. NRGs are a large family of proteins related to epidermal growth factors that occur in multiple isoforms, of which some are membrane bound and others are soluble (Nave and Salzer, 2006). Studies show that the membrane-bound neuregulin-1 (NRG1) type III on the axonal surface is required for myelination by SCs in the PNS, and that the level of NRG1 type III defines not only whether or not an axon will be myelinated but also the thickness of the sheath (Michailov et al., 2004; Taveggia et al., 2005). Although NRG1 has been shown to have trophic and mitogenic effects in oligodendrocyte development (Barres and Raff, 1999; Demerens et al., 1996), whether NRG1 might signal to oligodendrocytes from CNS axons in a similar way to that found in the PNS remains an open issue (Nave and Salzer, 2006).

One signal that seems to be required to trigger myelination in the CNS is electrical activity from neurons. The influence of neuronal electrical activity has been shown to be critical for the proliferation of oligodendrocyte progenitors (Barres and Raff, 1993). In addition, different studies performed on the optic nerve suggest that impulse activity can influence myelination. For instance, to examine the role of neuronal activity on myelination, Demerens and co-workers have used neurotoxins to either block or stimulate electrical activity in axons of myelinating cultures. Blockade of electrical activity greatly inhibited myelination without affecting viability of oligodendrocytes or neurons (Demerens et al., 1996).

It has been proposed that electrical activity of neurons might promote myelination by controlling the secretion of pro-myelinating factors and by changing the expression profile of axonal proteins (Coman et al., 2005). However, the effect of impulse activity may be independently regulated in the PNS and CNS. For instance, Adenosine triphosphate (ATP) has been identified as one of the pro-myelinating factors, which, during electrical activity, is released extra-synaptically and act on purinergic receptors expressed at the surface of oligodendrocyte precursors (Stevens et al., 2002). However, the action potential-mediated release of ATP has the opposite effect in the PNS, by delaying the terminal differentiation of SCs (Stevens and Fields, 2000).

Finally, the integrity of myelin also depends on the maintenance of a permanent relationship with an axon, since axotomy has been shown to result in downregulation of

myelin-related genes and de-differentiation of the previously differentiated glial cell (Scherer and Salzer, 2001).

1.2 Neuron-glia interactions and the organization of myelinated axons

1.2.1 Local influences of myelin on the axonal cytoskeleton and biology of neurons

The interactions between the axon and the myelinating glial cell are likely to be bidirectional. Both in the PNS and in the CNS, several studies have shown that myelination leads to local changes in the organization and composition of the axonal cytoskeleton (Witt and Brady, 2000).

The role of myelin on neuronal structure and function has been mostly inferred from mutations in genes that encode myelin proteins. Studies of *Trembler* mice, which have a missense mutation in the *Peripheral Myelin Protein-22* (*PMP22*) gene and consequently do not form compact myelin in the PNS, have shown that demyelinated axons have a reduced calibre compared to wild-type (Witt and Brady, 2000). De Waegh and colleagues showed that neurofilaments were less phosphorylated in axon segments surrounded by grafted *Trembler* SCs than in axons with wild-type compact myelin (de Waegh et al., 1992). They hypothesized that the phosphorylation state of NFs could regulate axon calibre by modifying the charge on NFs side arms, thus affecting interfilament spacing. In other words, the more neighbouring NFs are phosphorylated the more they repel each other and the less densely packed they become, and viceversa.

Similar to the PNS, the non-myelinated CNS axons of *Shiverer* mutants, which lack the myelin basic protein (MPB), a major constituent of mature myelin, mirror the effects of the demyelination seen in *Trembler* mice. There were also local changes in the rates of slow axonal transport and microtubule density (Brady et al., 1999).

Subsequent studies in myelinating cultures have supported the idea that myelinating glia directly regulate neurofilament density in the absence of other supporting cells (Starr et al., 1996). Moreover, in large fibers, normally the axon diameter at nodes of Ranvier and axon initial segments can be reduced to as little as 20% of the diameter of the internode (Salzer, 1997). This decreased axon calibre reflects, in part, a higher packing density of neurofilaments which are less heavily phosphorylated and are transported more slowly (de Waegh et al., 1992; Mata et al., 1992; Sanchez et al., 1996). Thus, myelinating glia appear to play an active role in shaping the axonal cytoskeleton. Yin and co-workers have proposed that Myelin Associated Glycoprotein (MAG) might be the signal that modulates the calibre of myelinated axons (Yin et al., 1998). MAG, a minor constituent of myelin in the PNS and CNS, belongs to the I-type lectin subgroup of the immunoglobulin (Ig) gene superfamily. It is enriched in the periaxonal membrane of myelinating cells and has been implicated in the formation and maintenance of myelin. Moreover, the extracellular structure of MAG is believed to predispose the molecule for interaction with an axonal ligand (Schachner and Bartsch, 2000).

In their study of MAG deficient mice, Yin and colleagues demonstrated that, in the absence of MAG, although myelin compaction occurs normally, axons display reduced calibres, decreased neurofilament spacing and phosphorylation. These changes are correlated with axonal atrophy and degeneration in the absence of inflammation or other overt phenotype. Furthermore, such changes are not observed in unmyelinated fibers of MAG-deficient mice (Yin et al., 1998).

Therefore, MAG remains a strong candidate for mediating communication between the glial cells and the axons. It cannot be excluded that MAG might play a less direct role, perhaps by facilitating another signalling pathway while maintaining spatial proximity between the axon and the myelinating glia (Witt and Brady, 2000). In this regard, MAG has been shown to bind to the Nogo-66 receptor, a glycosyl phosphatidylinositol (GPI)-anchored multi-subunit neuronal receptor belonging to the

reticulon family of transmembrane proteins, which is involved in mediating myelin-dependent restriction of axon outgrowth (Barton et al., 2003).

1.2.2 Molecular composition of functional domains along myelinated axons

Myelin-forming glial cells are programmed not only to protect axons and shape the axonal cytoskeleton but also to organise the axonal membrane so that it becomes competent for the saltatory mode of action potential conduction. The contact between a myelinating glial cell and the axon results in a striking reorganization of the axonal membrane into distinct longitudinal functional domains. Each of these domains contains a unique set of proteins that assemble into macromolecular complexes and confer axons with a highly polarised structure. The establishment and integrity of these domains is essential for ensuring efficient propagation of nerve impulse, an observation that is underscored by the analysis of various mutant mice in which one or more of these domains have been disrupted (Salzer, 2003). These domains include the axon initial segments and nodes of Ranvier, the paranodes and the juxtaparanodes (Figure 4).

What follows is a description of the well-established molecular components of nodes and AIS, paranodes and juxtaparanodes. In all these domains, a unique composition of CAMs exist as multiprotein complexes, some of which are linked to ion channels via scaffolding molecules in the cytoplasm.

THE INITIAL SEGMENTS AND NODES OF RANVIER

As mentioned earlier, the axon initial segments and the nodes of Ranvier are the sites of initiation and propagation of action potentials respectively. Given their functional similarity, it is not surprising that these domains have a similar, though not identical, molecular composition (Figure 4b and Figure 5). The axonal membrane of both domains contains a high concentration of Nav channels ($>1200/\mu m^2$), that are responsible for inward current flow (Peles and Salzer, 2000).

Nav channels are members of multigene families and comprise multimeric complexes, consisting of a pore-forming α- subunit, i.e. the ion channel itself, and one or more auxiliary β-subunits (Ratcliffe et al., 2001). The latter are members of the

immunoglobulin (Ig) superfamily of cell adhesion molecules and are thought to regulate channel behaviour, surface expression and binding to other nodal components (Isom, 2001; Yu and Catterall, 2003). The α- subunit Nav 1.6 is the predominant subtype of Nav channels present at adult nodes of Ranvier, both in the PNS and the CNS (Boiko et al., 2001; Caldwell et al., 2000). Conversely, adult AIS co-express Nav1.6 and Nav1.2 (Boiko et al., 2003).

The mammalian Nav channel subtypes and their tissue distribution are summarised in Table 1.

Na$_v$ α-subunit subtype	Former name	Distribution
Na$_v$1.1	Rat I	CNS, sensory neurons
Na$_v$1.2	Rat II	CNS, sensory neurons
Na$_v$1.3	Rat III	CNS, embryonic sensory neurons
Na$_v$1.4	μ1	Skeletal muscle
Na$_v$1.5	H1	Cardiac muscle, immature and denervated skeletal muscle
Na$_v$1.6	NaCh6	CNS, sensory neurons, nodes of Ranvier in both CNS and PNS
Na$_v$1.7	PN1	Sensory neurons, sympathetic neurons, Schwann cells
Na$_v$1.8	SNS/PN3	Sensory neurons
Na$_v$1.9	SNS2/NaN	Sensory neurons

TABLE 1. The mammalian voltage-gated sodium (Nav) channel subtypes and their tissue distribution (Ekberg and Adams, 2006).
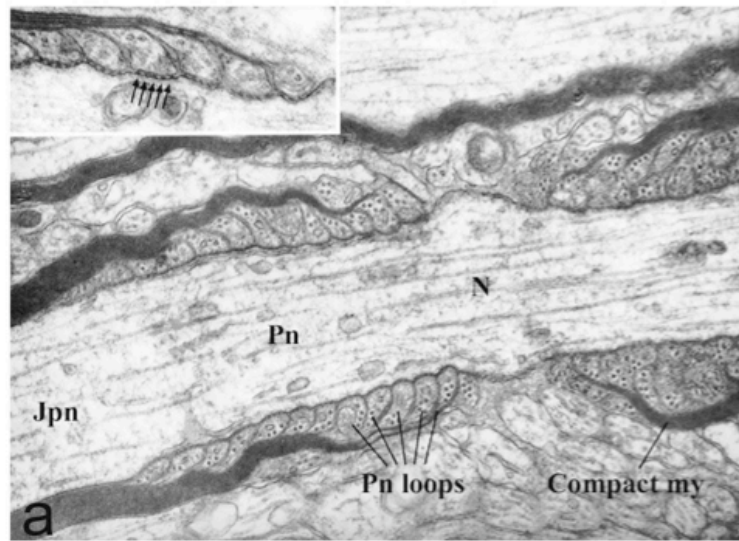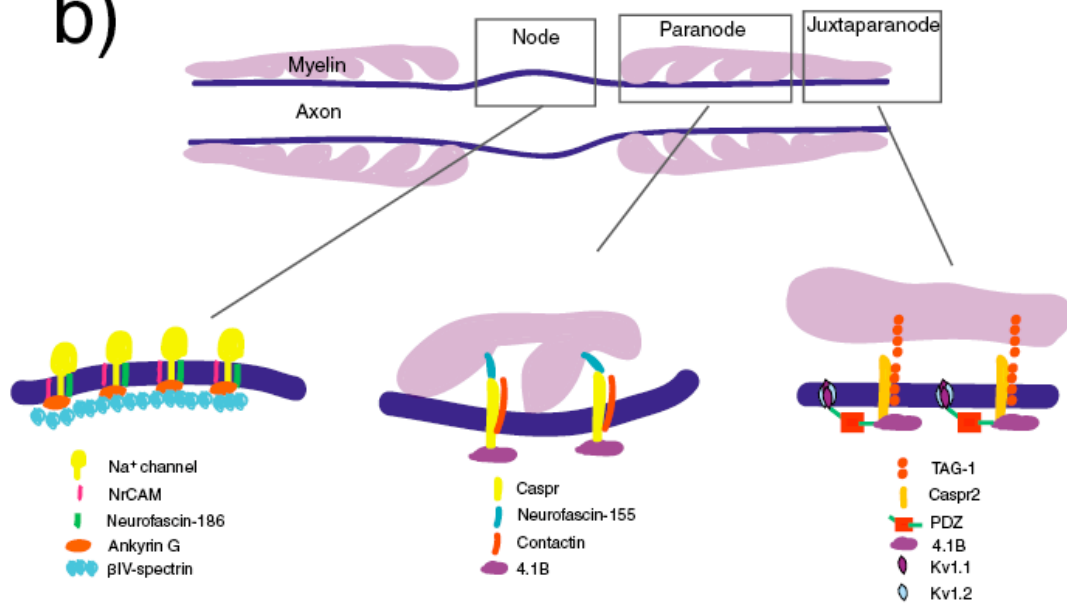
FIGURE 4. Domains of Myelinated Axons

a) Electron micrograph of a longitudinal section of adult murine sciatic nerve, showing the nodal region (N), the paranode (Pn) and the juxtaparanode (Jpn). The inset displays a high magnification of the paranodal axoglial junctions, which are visible as electron dense transverse bands resembling the septate junctions found in invertebrates (Source: Pedraza et al., 2001). **b)** Schematic representation of the node of Ranvier, the paranodes and the juxtaparanodes together with their molecular composition (Source: Simons et al., 2006).
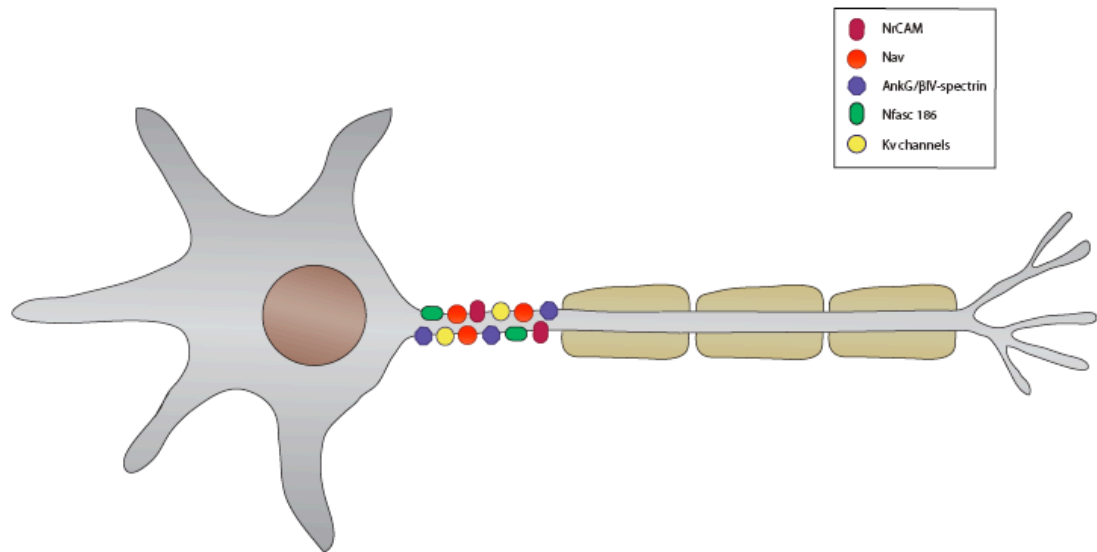
FIGURE 5. Schematic Representation of the Molecular Constituents at AIS
The molecular composition at AIS is very similar to that found at the nodes of Ranvier. It includes a high concentration of voltage-gated sodium and potassium channels, cell-adhesion molecules, such as NrCAM and the neuronal isoform of Neurofascin, Nfasc186. It also contains the cytoskeletal proteins Ankyrin G and βIV Spectrin.

Nav channels are differentially expressed during development. In the CNS, Nav 1.2 is initially localised to newly forming nodes but it is later replaced by Nav1.6. *In vitro* studies suggest that this sequential clustering is differentially controlled and that myelination is necessary for Nav1.6 clustering (Kaplan et al., 2001). Similarly, in the PNS, Nav1.2 is initially detected at newly forming nodes and lost subsequently (Boiko et al., 2001). However, Nav1.6 is also present at all newly forming nodes and stably remains localised at these sites (Schafer et al., 2006). The physiological significance of the transition from one Nav channel subtype to another or their co-expression at these domains is not yet clear (Salzer, 2003).

Nav channels are part of a protein complex that participates in both intracellular and extracellular interactions. Nodes of Ranvier and AIS are enriched with cell adhesion molecules (CAMs), including the neuron-glia related CAM (NrCAM) and the 186 kD isoform of Neurofascin (Nfasc186), which belong to the L1 family of CAMs. They both interact with the extracellular Ig-like domain of the β1 subunit of Nav channels (McEwen and Isom, 2004; Ratcliffe et al., 2001) and were originally isolated on the

basis of their binding to the cytoskeletal adaptor protein Ankyrin G, via a conserved twelve-amino-acid sequence found in their cytoplasmic domain (Bennett and Lambert, 1999; Davis et al., 1996; Davis et al., 1993). Ankyrin G binds this motif only when it is dephosphorylated, suggesting that unidentified tyrosine kinases and phosphatases might regulate this interaction (Garver et al., 1997; Tuvia et al., 1997).

Ankyrin G is one of three ankyrin genes, each implicated in membrane cytoskeleton targeting, organization and stabilization. Two brain specific isoforms of Ankyrin G of 480 kD and 270 kD are localized at nodes of Ranvier and axon initial segments (Kordeli et al., 1995). In addition to binding to CAMs, Ankyrin G has been shown to interact with α- and β- subunits of Nav channels (Lemaillet et al., 2003; McEwen et al., 2004). The β1-subunit recruits Ankyrin G to the plasma membrane (Malhotra et al., 2000; Ratcliffe et al., 2001), whereas binding to the α-subunit through a conserved nine-amino-acid motif is required to cluster Nav channels, at least at AIS (Garrido et al., 2003b).

Thus, Nav channels interact with NrCAM and Nfasc186 via two distinct mechanisms: a direct *cis* interaction with the β1 subunit, and indirectly via interaction with Ankyrin G to which both CAMs bind.

Ankyrin G also binds to the cytoskeletal protein βIV Spectrin, and both are required for stable coexpression at peripheral nodes of Ranvier and AIS (Jenkins and Bennett, 2001; Komada and Soriano, 2002). βIV Spectrin is a member of the β-spectrin family of submembranous scaffolding proteins that provides a link between membrane proteins and the actin cytoskeleton (Berghs et al., 2000). Two different splice variants are coexpressed at AIS and nodes of Ranvier: the first is a longer Σ1 splice variant which includes 17 spectrin repeats, an N-terminal actin binding domain and a C-terminal domain, and it is the predominant version found at these domains. The second protein is a shorter Σ6 splice variant consisting of approximately the last half of the Σ1 variant (Berghs et al., 2000; Komada and Soriano, 2002). The relative contributions of these two splice variants are not completely understood, although genetic studies suggest that they might be differentially involved in localisation and stability of membrane proteins at AIS and nodes of Ranvier (Lacas-Gervais et al., 2004; Uemoto et al., 2006).

Other nodal components include the glycosyl phosphatidylinositol (GPI)-anchored protein of the immunoglobulin superfamily, Contactin, which is stably expressed in

CNS nodes but just transiently present at low amounts early in PNS node formation (Kazarinova-Noyes et al., 2001; Rios et al., 2000). Contactin has been shown to associate with Nav channels and to enhance channel surface expression (Kazarinova-Noyes et al., 2001; McEwen et al., 2004).

Nav are not the only ion channels present at the nodes and AIS. A subset of adult CNS nodes contains the voltage-gated potassium channel (Kv) 3.1b of the K^+ channel superfamily (Devaux et al., 2003). Moreover, the delayed rectifier Kv1.1 and Kv1,2 are transiently expressed during development at PNS nodes, whereas in the CNS they are found at some initial segments but not at their corresponding nodes (Salzer, 2003). In addition, KCNQ2 and KCNQ3 subunits of Kv7 channels have been found to be functional components of AIS and nodes, colocalising with Ankyrin G and Nav channels throughout the CNS and PNS (Devaux et al., 2004; Pan et al., 2006). Kv, 1.1, 1.2, 3.1 and KCNQ channels may maintain the resting potential by facilitating action potential repolarisation, in order to reduce excitability and sustain high-frequency firing. Their heterogeneous distribution might reflect the differential requirements displayed by different nerve fibers as well as by nodes and AIS (Lai and Jan, 2006).

Thus, it is clear that nodes and AIS appear to form a meshwork of interacting components in which transmembrane proteins are associated with both each other and intracellular adaptor proteins. These multimolecular complexes are further stabilized by binding to extracellular matrix (ECM) components, which include the hyaluronan-binding proteoglycan Tenascin C and NG2 proteoglycan in the PNS, and Tenascin R, Phosphacan and the versican-binding protein Bral1 in the CNS (Oohashi et al., 2002; Poliak and Peles, 2003).

The nodal gap of PNS nodes is filled with Schwann cell microvilli which project from the outer collar of adjacent SCs plasma membrane, interdigitate and come in close proximity with the nodal axolemma, perpendicularly to the node (Salzer, 1997). They are enriched, among other proteins, in the Ezrin-Radixin-Moesin (ERM) family of actin binding proteins (Melendez-Vasquez et al., 2001) which has been recently shown to interact with the 155 kD isoform of Neurofascin (Nfasc155) also present in microvilli (Gunn-Moore et al., 2006). In addition, a new protein, Gliomedin (see section 1.2.3), which belongs to the olfactomedin protein family, was recently identified as a novel component of PNS nodes and as a Schwann cell ligand for Nfasc186 and NrCAM

(Eshed et al., 2005). In contrast to the PNS, CNS nodes may or may not be contacted by perinodal astrocytes (Poliak and Peles, 2003) and putative ligands to CAMs present at central nodes have not been identified yet.

PARANODES

Adjacent to the node, the compact myelin sheath opens up to form cytosplasmic-filled loops that spiral around and closely appose the axon at either side of the node, i.e. paranodes (Figure 4a-b). The paranodal loops are helically arranged and provide cytoplasmic continuity from the innermost to the outermost layers of the myelin sheath (Ellisman et al.,2001). Molecular interchange occurs across the loops themselves, the external environment and the axon. The junctions between the loops contain members of the Connexin family of gap-junction proteins and of the calcium-dependent cell-cell adhesion glycoproteins, such as E-cadherins, which form intercellular channels (Altevogt et al., 2002; Fannon et al., 1995).

The outermost loops are attached to the underlying axons via axoglial junctions which, in longitudinal sections, are visible as electron dense intercellular bands, resembling the septate junctions (SJs) found in invertebrates (Pedraza et al., 2001) (Figure 4aAQ-inset). Axoglial junctions are the sites of closest contact between the glial membrane and the axolemma, and have been proposed to serve several functions, including: first, to form a partial diffusion barrier into the periaxonal space; second, to demarcate axonal domains by limiting lateral diffusion of molecules and therefore separate the electrical activity at the node from the internodal region and, finally, to facilitate bidirectional signalling between axons and myelinating glial cells (Brophy, 2001; Denisenko-Nehrbass et al., 2002; Dupree et al., 1999; Trapp and Kidd, 2000).

At the paranodes, CAMs mediate the interaction of glial loops with the axonal membrane. The axolemma contains a *cis* complex of two cell-recognition molecules, namely Contactin-associated protein (Caspr) (Peles et al., 1997), also known as Paranodin (Menegoz et al., 1997), and Contactin (Rios et al., 2000).

Caspr is a Type I transmembrane protein belonging to a subgroup of the Neurexin superfamily, termed NCP (Neurexin IV, Caspr, Paranodin) (Bellen et al., 1998) whose extracellular region consists of several domains that are implicated in protein-protein interaction, including a discoidin and fibrinogen-like domain, epidermal growth factor

motifs and regions with homology to the G domain of Laminin A (Menegoz et al., 1997). Caspr has been shown to interact with Contactin, through a region that encompasses Ig-like domains, an association which is required for efficient transport of Caspr from the endoplasmic reticulum to the plasma membrane (Faivre-Sarrailh et al., 2000; Peles et al., 1997), as well as the cell surface transport of Contactin (Gollan et al., 2003).

More specifically, Contactin exists in two different glycoforms, of which only a high-molecular weight (HMw), endoglycosidase H (EndoH) resistant form, can reach the plasma membrane independently of Caspr, whereas a low-molecular weight (LMw)-Contactin isoform requires association with Caspr for transport to the cell surface, suggesting that Caspr regulates the level of glycosylation of Contactin (Gollan et al., 2003; Rios et al., 2000). This role is further supported by the observation that, during development, there is a gradual increase of Caspr expression correlating with a transition from HMw- to LMw-Contactin detection (Einheber et al., 1997). Accordingly, deletion of Caspr in mice by gene targeting results in a shift from expression of LMw- to HMw-Contactin isoform (Gollan et al., 2003), which remains preferentially expressed at nodes rather than paranodes of CNS axons (Bhat et al., 2001)

The essential role of this complex in axoglial junction formation has been demonstrated by defects in the paranodes of mice deficient in either protein, although compact myelin forms normally in these mice (Bhat et al., 2001; Boyle et al., 2001).

The localisation of Caspr at the paranodes in myelinating co-cultures is perturbed by addition of a soluble RPTPβ protein, a receptor tyrosine phosphatase, which binds Contactin but is not located at the nodal axolemma, suggesting that the paranodal localization of Caspr-Contactin complex is mediated by a glial ligand (Rios et al., 2000).

The most probable glial ligand to the Caspr-Contactin complex is the glial isoform of Neurofascin, Nfasc155, the only known glial component of the paranodal junction. The extracellular domain of Nfasc155 has been shown to bind to transfected cells expressing the Caspr-Contactin complex and to co-immunoprecipitate with the complex from brain lysates (Charles et al., 2002). These results suggest that the Caspr-Contactin complex interacts in *trans* with Nfasc155 forming a tripartite protein complex.

However, other *in vitro* data suggest that the *cis*-interaction between Caspr and Contactin actually inhibits binding of the LMw-Contactin to Nfasc155, supporting the hypothesis that two separate populations of Contactin exist at paranodes and that Caspr might control the ability of this cell-adhesion molecule to interact with other ligands (Gollan et al., 2003). In addition, these results possibly indicate that other components might mediate the interaction of Nfasc155, Caspr and Contactin at the axoglial junction.

The intracellular region of Caspr has also been shown to bind to protein 4.1B, a member of the 4.1 family of proteins with actin-spectrin-binding domains, which could immobilize the Caspr /Contactin complex to the plasma membrane, thus providing a link between the intercellular complex and the cytoskeleton (Denisenko-Nehrbass et al., 2003). This idea is consistent with the observation that protein 4.1B is mislocalised along peripheral myelinated fibers of Contactin-null mice, which lack paranodal Caspr, and its expression correlates with that of Caspr (Poliak et al., 2001). Furthermore, in mutants lacking the cytoplasmic tail of Caspr, the Caspr-Contactin complex is not maintained at the paranodes, suggesting that the Caspr-protein 4.1B interaction is essential to stabilise the complex by anchoring it to the axonal cytoskeleton (Gollan et al., 2002).

Recently, additional paranodal proteins have been identified by mass spectrometry and are likely to be associated with the paranodal cytoskeleton in both CNS and PNS. They include Ankyrin B, αII Spectrin and βII Spectrin (Ogawa et al., 2006) and, although their role remains to be fully characterised, these proteins indicate that the paranodal cytoskeleton might be important for formation and maintenance of axon-glial interactions (Ogawa et al., 2006). In addition, Ankyrin G has been found to be transiently expressed at paranodes in myelinated fibers of the CNS at early stages of myelination (Jenkins and Bennett, 2002). However, it is not known whether Ankyrin G is present in the glial paranodal loops or in the axon.

JUXTAPARANODES

The juxtaparanodal domains lie just adjacent to the paranodes, under the compact myelin sheath. They are enriched in two delayed rectifier K^+ channels of the *Shaker* family, heteromultimers of α subunits Kv1.1,1.2, 1.4 and their cytoplasmic β2 subunit (Wang et al., 1993). These are slow activating and inactivating channels which are thought to maintain the internodal resting potential by preventing hyperexcitation and by providing a pathway for K^+ ion movement from the axoplasm to the periaxonal space (Rasband, 2004).

A complex of adhesion molecules anchor these channels to the juxtaparanodes. Specifically, Kv1.1 and Kv1.2 are associated with Caspr2, a neuronal protein with sequence similarity to Caspr expressed at the paranodes, but containing a consensus binding sequence for PDZ (PSD-95/DLG/ZO-1) domains at its carboxyl terminus (Poliak et al., 1999).

Another PDZ domain protein, PSD-95 (postsynaptic density protein of 95 kD) has been found at juxtaparanodes to colocalise with Kvβ2 (Baba et al., 1999) but it does not to interact directly with Caspr2, since Kv1.1 and Kv1.2 still accumulate in the juxtaparanodes of mice deficient in PSD-95 (Poliak et al., 1999; Rasband et al., 2002). The putative PDZ binding protein mediating Caspr2 association to Kv channels has not been identified yet.

Similarly to Caspr at paranodes, Caspr2 binds protein 4.1B, which is also found at juxtaparanodes, suggesting that 4.1B anchors these axonal proteins to the actin-based cytoskeleton in both of these domains (Denisenko-Nehrbass et al., 2003).

At the time of its identification, Caspr2 was proposed to be involved in Kv channel localization through interaction with an unidentified glial partner. This hypothesis was based on the observation that both dysmyelination and demyelination result in loss of clustering of Kv1 channels (Rasband et al., 1998; Wang et al., 1993). The binding partner was later identified as the transient axonal glycoprotein-1 (TAG-1), a GPI-anchored CAM related to Contactin, that is expressed by both neurons and myelinating glia (Furley et al., 1990; Traka et al., 2002).

Studies show that TAG-1 on the glial membrane binds homophilically to a *cis* complex of Caspr2 and TAG-1 present on the axon, forming a scaffold that is necessary to maintain Kv channels at the juxtaparanodes. Moreover, the key role of the reciprocal

interaction of TAG-1 and Caspr2 in juxtaparanode formation is supported by the fact that in mice deficient in either TAG-1 or Caspr2 the entire juxtaparanodal complex is dispersed along axons (Poliak et al., 2003).

Finally, the juxtaparanodal glial membrane contains Connexin 29 (Cx29), a gap junction protein that has been shown to colocalise with Kv1 channels in all myelinated fibers of the PNS and in small diameter fibers of the CNS. Cx29 has been proposed to form functional hemichannels, possibly involved in K^+ ion clearance in the periaxonal space (Altevogt et al., 2002).

1.2.3 Developmental organization of domains in myelinated axons

Myelination is developmentally regulated in a spatio-temporal fashion. In both the PNS and CNS, myelinated fibers display a highly defined clustering of proteins whereas non-myelinated or unsheathed fibers show a diffuse pattern of distribution of proteins which organize into domains upon myelination (Salzer, 2003). Moreover, myelination regulates the kind of ion channels that are expressed by axons, most notably Nav channel isotypes. During development and remyelination, Nav1.2 is expressed at both unmyelinated regions and at newly formed nodes (Boiko et al., 2001; Dupree et al., 2005). However, mature nodes express Nav1.6 and, in the absence of compact myelin, like in the *Shiverer* mouse, this Nav isotype transition does not occur (Boiko et al., 2001).

An important question is: What are the mechanisms controlling domain assembly and maintenance? Other related questions include: is clustering of proteins at nodes and AIS determined by the glial cells or intrinsically specified by the axon? What is the order of domain assembly and do these domains form independently? Are there differences between the PNS and the CNS in the mechanisms that drive domain assembly?

Using genetic and molecular tools, most of our current knowledge of how functional domains organise along myelinated fibers has been provided by studies of the initial events of assembly of these domains. In the past few years, rapid progress has been made in elucidating how the loss of individual components affect domain organization and function, and these will be discussed below. Special emphasis will be given to those contributions that have improved our understanding of the mechanisms of assembly of

nodes of Ranvier and AIS, and of the role of paranodal axoglial junctions in the formation and/or maintenance of the nodal environs. Differences between the PNS and CNS will be highlighted.

MECHANISMS OF ASSEMBLY OF NODES OF RANVIER AND AIS: INTRINSIC AND EXTRINSIC DETERMINANTS

Formation of nodes of Ranvier, both in the PNS and CNS, depends on extrinsic factors, namely the presence of myelinating glia. Nav channel clusters can be detected in rat sciatic nerves as early as postnatal day (P) 1. These clusters first appear adjacent to the edges of myelinating Schwann cells as soon as these cells express MAG and become committed to myelination (Vabnick et al., 1996). Moreover, ERM-positive Schwann cell processes overlie and are associated closely with nascent nodes of Ranvier prior to the formation of compact myelin (Melendez-Vasquez et al., 2001).

In the CNS, Nav channels clusters are first detected in developing rat optic nerve at at the onset of myelination (at P9-10) and are found adjacent, but not overlapping with, Caspr-labelled axoglial junctions, which constantly precede the detection of Nav channels by about 2 days (Rasband et al., 1999a). This suggests that oligodendrocytes may cluster Nav channels by excluding them from sites of close axoglial contact (Rosenbluth et al., 2003). As myelination progresses, in both the PNS and CNS, Nav channel clusters move laterally and ultimately fuse to form a node (Melendez-Vasquez et al., 2001; Rasband et al., 1999a; Vabnick et al., 1996). Thus, glial cell processes appear to dictate the positioning of the nodes, which are continuously remodelled during development in concert with the longitudinal expansion of the myelin segments (Salzer, 2003).

In the PNS, Nav channels cluster only if SCs myelinate axons; neither simple contact nor SC conditioned media is sufficient to induce Nav channel clustering *in vitro* (Ching et al., 1999). In addition, results from experiments on sciatic nerves during both development (Vabnick et al., 1996) and remyelination (Dugandzija-Novakovic et al., 1995) have confirmed that Schwann cell contact and myelination are required for nodal Nav channel clustering.

A mechanism supporting the notion that neuron-glia interaction mediates Nav channels clustering was initially suggested by the observation that cell adhesion

molecules, namely Nfasc186 and NrCAM, are the first axonal molecules clustered at nascent PNS nodes, followed by Ankyrin G, βIV Spectrin and Nav channels (Custer et al., 2003; Lambert et al., 1997; Melendez-Vasquez et al., 2001; Schafer et al., 2006). A glial ligand for these CAMs has long been elusive until recently. Eshed and co-workers (2005) have shown that when Gliomedin is expressed in heterologous cells, NrCAM-Fc and Nfasc186-Fc fusion proteins bind to the surface of the transfected cells. Similarly, if Nfasc186 is expressed in heterologous cells, Gliomedin-Fc fusion protein binds to the surface. Moreover, when soluble Gliomedin is added to dorsal root ganglion (DRG) cultures, it is sufficient to induce clustering of Nav channels and Ankyrin G along axons. Conversely, when Nfasc186-Fc fusion protein is added to myelinating co-cultures, clustering of nodal proteins is inhibited, presumably by interfering with the Gliomedin-Nfasc186 interaction. Finally, ablation of Gliomedin expression by RNA interference (RNAi) results in failure of Nav channel clustering.

Therefore, Schwann cell-associated Gliomedin is likely to participate in node assembly, at least in the PNS, by virtue of its interaction with axonal CAMs, in particular Nfasc186. Conversely, NrCAM appears not to be critically important for node assembly since NrCAM-null mice have normal PNS nodes, despite a slight delay in Nav channel clustering (Custer et al., 2003).

The role of Ankyrin G at peripheral nodes of Ranvier has not been directly demonstrated in a mutant mouse. However, knockdown of Ankyrin G in myelinating co-cultures has been recently shown to result in loss of all components at the node, including Nfasc186, suggesting that reciprocal interactions between components of the nodal complex may promote long-term stable expression (Dzhashiashvili et al., 2007). In contrast, loss or mutation of βIV Spectrin results in a milder destabilization of the nodal membrane with reduced, albeit detectable, Nav channels and Ankyrin G immunoreactivity (Komada and Soriano, 2002; Lacas-Gervais et al., 2004; Yang et al., 2004).

Taken together, these studies lead to the conclusion that, in the PNS, the binding of the SC ligand Gliomedin to axonal CAMs is the first step in positioning the node followed by the assembly of Nav channels and cytoskeletal proteins, which have the role to stabilise the multimolecular complex.

In the CNS, several studies have also indicated that the initial clustering of nodal proteins is regulated by axon-oligodendrocyte interaction. Most notably, the requirement of glial cells for node of Ranvier formation has been demonstrated after ablation of oligodendrocytes in transgenic mice, which results in loss of nodal markers, such as Nav channels and Ankyrin G (Mathis et al., 2001). Furthermore, in retinal ganglion cells, Nav channels have been found clustered at nodes after the axons cross the *lamina cribrosa* and become myelinated, whereas they remain diffusely distributed in the corresponding unmyelinated segments (Boiko et al., 2001).

However, the mechanisms regulating the initial organization of nodal clusters remain controversial. On one hand, the need for a physical contact between the axon and the myelinating oligodendrocyte is supported by findings where paranodal interactions regulate Nav channels clustering independent of a compact myelin sheath (Rasband et al., 1999a; Rios et al., 2003). Furthermore, as already mentioned, paranodal junctions defined by the expression of Caspr and Nfasc155 appear to form before nodal components can be detected (Rasband et al., 1999a; Schafer et al., 2004).

On the other hand, Kaplan and collaborators demonstrated that a soluble factor released by oligodendrocytes might be sufficient to trigger nodal clustering suggesting that node formation might be independent of myelination (Kaplan et al., 1997). To support this idea, studies of myelin mutants, such as the *Myelin deficient* (*md*) rats and *Jimpy* mice, which have profound CNS dysmyelination associated with oligodendrocyte cell death, show that node-like clusters can still form, albeit in those axons that are at least partially surrounded by oligodendrocyte processes (Arroyo et al., 2002; Baba et al., 1999). Furthermore, using *in vivo* models of demyelination, Dupree and colleagues have provided evidence that, in the absence of myelin, oligodendrocytes can protect against the rapid loss of Nav clusters, and that this effect might be independent of myelination (Dupree et al., 2005).

Hence, these studies suggest that the presence of oligodendrocytes and a short range interaction, but not myelination, are essential for initial clustering of Nav channels at nodes of Ranvier in the CNS. They also indicate that the mechanisms for clustering nodal proteins may differ between CNS and PNS, possibly due to the fact that oligodendrocytes do not have microvilli that extend into the nodal gap.

The sequence in which proteins accumulate at central nodes is also different from that found in the PNS and is less well defined. Ankyrin G, and not CAMs, appears at nascent nodes before Nav channels (Jenkins and Bennett, 2002; Rasband et al., 1999a) but, overall, its importance for CNS node formation has primarily been inferred from studies of assembly of AIS (see below).

Using adenovirus for transgene delivery into myelinated neurons, Yang and colleagues suggest that Ankyrin G might play a key role in the recruitment of βIV Spectrin and, possibly, of other components of the nodal complex (Yang et al., 2007), since Ankyrin G has the ability to retain Nav and Kv channels at nodes (Pan et al., 2006). Moreover, *Quivering* (*Qv*) mice, which have mutations affecting the C-terminal region of the βIV Spectrin splice variants, display widened CNS nodes. However, Ankyrin G and Nav channels are still targeted and clustered at these sites, albeit with increasingly less immunoreactivity over time (Pan et al., 2006; Yang et al., 2004; Yang et al., 2007).

Thus, at central nodes, indirect evidence indicates that extrinsic glial-derived signals regulate the initial clustering of Ankyrin G and the subsequent accumulation of other nodal components. Whereas Ankyrin G might be essential for node formation, βIV Spectrin appears to play more of an important role in node stability.

In contrast to nodes of Ranvier, AIS assemble by an intrinsic mechanism that is independent of glial cells. Both *in vitro* and *in vivo,* AIS have been observed to assemble independently of the presence of myelinating glia (Alessandri-Haber et al., 1999; Boiko et al., 2001; Dzhashiashvili et al., 2007; Mathis et al., 2001; Rasband et al., 1999a; Zhang and Bennett, 1998).

The axon initial segment may be intrinsically specified owing to its invariant position and its role as a "gatekeeper" of electrical signalling since it acts as a barrier against the lateral diffusion of proteins between the axon and the somato-dendritic compartments (Boiko and Winckler, 2003). This barrier function has been associated to the ankyrin-spectrin cytoskeleton (Boiko et al., 2007). In particular, Ankyrin G has been shown to target and link Nav and KNCQ channels to the underlying cytoskeleton (Devaux et al., 2004; Garrido et al., 2003a; Lemaillet et al., 2003; Pan et al., 2006). Moreover, localisation and/or retention of both Nfasc186 and NrCAM at AIS depends on the interaction with Ankyrin G since mutation of a single tyrosine in their common Ankyrin

G- binding intracellular motif abrogates the clustering of both proteins at this domain (Lemaillet et al., 2003; Zhang et al., 1998).

During development, both Ankyrin G and βIV Spectrin have been observed to accumulate at initial segments prior to the localisation of CAMs (Jenkins and Bennett, 2001), whose role in AIS assembly and /or maintenance has not been directly addressed yet. Nevertheless, short hairpin RNA (shRNA)- mediated knockdown of Nfasc186 does not inhibit Ankyrin G and Nav channel accumulation at AIS in cultured hippocampal neurons, suggesting that, in contrast to PNS node assembly, similar mechanisms operate at AIS and CNS nodes, whereby cytoskeletal proteins direct the assembly of complexes found at these sites (Dzhashiashvili et al., 2007).

In support of this idea, the importance of Ankyrin G for AIS assembly has been demonstrated directly in a mutant mouse lacking Ankyrin G at Purkinje neuron initial segments (Zhou et al., 1998). In these mice, Nav channels, Nfasc186, KNCQ2 and βIV Spectrin all fail to accumulate, suggesting that Ankyrin G might be the principal organizer of the membrane proteins located at AIS (Pan et al., 2006; Jenkins and Bennett, 2001).

However, in mice lacking βIV Spectrin, neither Ankyrin G nor Nav channels cluster at AIS, indicating that βIV Spectrin is also indispensable for organising AIS (Komada and Soriano, 2002). Nevertheless, recent evidence suggests that, early in AIS formation, βIV Spectrin recruitment depends on Ankyrin G, since dominant-negative expression of Ankyrin G in neurons results in loss of βIV Spectrin from AIS, without disrupting Nav channels or endogenous Ankyrin G clustering (Yang et al., 2007).

A possible explanation of these contrasting results is that early time points of AIS assembly were not investigated in βIV Spectrin-null mice. Therefore, it is likely that AIS formed properly in these mice early in development, but that with increasing age the absence of βIV Spectrin destabilised the membrane domain, resulting in the loss of the other AIS components. Consistent with this interpretation, analysis of central nodes and AIS of *Qv* mice suggest that proteins gradually disperse over time, further supporting a role for βIV Spectrin in stabilising rather than in assembling these domains (Yang et al., 2004; Yang et al., 2007).

Based on the experimental evidence so far, we can conclude that, in contrast to nodes of Ranvier, assembly of AIS is governed by intrinsic mechanisms and that the

cytoskeletal protein Ankyrin G might be the critical organizer of this domain, since its accumulation precedes that of other AIS components and its deletion prevents assembly of the domain altogether. However, stabilization of the molecular complex at AIS also requires βIV Spectrin. Nevertheless, Xu and Shrager used RNAi to knockdown Nav channel expression in spinal motor neurons and found that Ankyrin G, Nfasc186 and NrCAM failed to accumulate at AIS (Xu and Shrager, 2005). These results suggest that formation of the initial segment requires at least both Ankyrin G and Nav channels and that it may not be appropriate to think of one protein as the master organizer, but rather that a variety of protein-protein interactions are necessary for formation and/or stabilization of this functional domain.

***ROLE OF PARANODAL AXOGLIAL JUNCTIONS IN DOMAIN ASSEMBLY
AND/OR MAINTENANCE***

Do nodes of Ranvier assemble independently of other domains? In particular, what is
the role of paranodal axoglial junctions in organising and stabilising proteins near and at
the nodes of Ranvier?

Numerous studies show that one of the first correlates of axonal dysfunction resulting
from dysmyelination or demyelination is the disruption of axoglial junctions (Scherer
and Arroyo, 2002). For instance *md* rats fail to form septate-like junctions and do not
accumulate Caspr, Contactin and Nfasc155 at paranodes (Scherer and Arroyo, 2002).
Therefore, molecules expressed at the paranodal axoglial junctions have been
considered to be good candidates to mediate interactions between glial cells and axons
and, in line with an hypothesised role of the septate-like junctions as molecular sieves
(Pedraza et al., 2001), to be ideally suited to direct node assembly by selectively
segregating proteins in their respective domains.

Mice with mutations in genes that encode paranodal components have provided useful
insights into the role of the paranodes in the formation and function of adjacent
domains. Genetic ablation of Caspr and Contactin results in loss of septate-like
junctions and mislocalisation of Kv channels to paranodes, which is accompanied by
reduction in nerve conduction velocity and amplitude (Bhat et al., 2001; Boyle et al.,
2001). A similar phenotype is observed in MAG- deficient mice and other paranodal
mutants, such as mice lacking the enzymes that synthesise two major myelin
galactolipids, Galactocerebroside and Sulfatide [UDP-galactose:ceramide
galactosyltransferase-null (CGT-null) and cerebroside sulfotransferase-null (CST-null)]
(Dupree et al., 1999; Ishibashi et al., 2002; Marcus et al., 2002). These galactolipids are
enriched in myelin and are believed to play a role in the trafficking of proteins to
detergent–insoluble raft-like microdomains, such as the paranodes (Dupree et al., 1999).

In all these mutants, Caspr and Contactin are absent from the paranodes. In addition,
whereas during development of wild-type peripheral nerves, Caspr2 and Kv1.2 are
initially detected at the paranodes before relocating to the adjacent juxtaparanodal
region, this transition is not observed in *CGT* mice, where Caspr2 and Kv1.2 remain
paranodal (Poliak et al., 2001).

In the CNS, Kv channels are normally detected at juxtaparanodes at late stages in myelination (Rasband and Shrager, 2000). However, in the absence of well-formed axoglial junctions, Kv channels are mislocalised to paranodes and progressively lost, remaining diffusely distributed throughout the axolemma (Ishibashi et al., 2002; Rasband et al., 1999a; Rasband and Shrager, 2000; Rios et al., 2003).

Thus, these studies show that the formation of septate-like junctions is essential to act as a paracellular barrier to sequester and maintain Kv channels and other components at juxtaparanodes. But what about their role in node assembly?

As mentioned earlier, at least in the CNS, the use of paranodal markers, such as Caspr and glial Neurofascin, to determine early events in node formation initially favoured a model in which paranodal contacts occur prior to Nav channel clustering (Rasband et al., 1999; Schafer et al., 2004). Additionally, in the hypomyelinating mouse mutant *Shiverer,* normal-appearing clusters were only observed adjacent to intact axoglial contacts, as defined by Caspr immunoreactivity, suggesting a necessary role for such contacts in protein clustering at the nodes (Rasband et al., 1999a).

However, this model has been questioned because all the aforementioned paranodal mutants have relatively normal nodal clusters in both PNS and CNS, albeit CNS nodes appear wider and disperse over time (Dupree et al., 1999; Bhat et al., 2001; Boyle et al., 2001; Rios et al., 2003). In this regard, it is important to note that, in contrast to the CNS where many paranodal loops are everted, most paranodal loops in the PNS of those mutants remain in close association with the axon, although axoglial junctions or transverse bands are not formed (Dupree et al., 1999; Marcus et al., 2002; Rios et al., 2003). This is possibly due to the presence of a basal lamina and of microvilli, which might provide structural stability to the node and explain why the disruption of nodes is more severe in the CNS than in the PNS.

Nonetheless, paranodal transverse bands are required for the maintenance of Nav1.6 and, possibly, other components at the node (Rasband et al., 2003; Suzuki et al., 2004). Furthermore, they are necessary for the developmental switch from the Nav 1.2 to the Nav 1.6 channel subtype, which is found at mature nodes (Boiko et al., 2001: Rios et al., 2003; Suzuki et al., 2004).

Thus, nodes are able to assemble independently of paranodal axoglial junctions both in the PNS and in the CNS. Conversely, formation of septate-like junctions is essential

for the delineation of axonal domains and their maintenance, in accordance with their ascribed function as a barrier to the mobility of juxtaparanodal and nodal constituents (Pedraza et al., 2001). Moreover, axoglial junction integrity may affect aspects of nodal function and maturation.

Finally, paranodal axoglial junctions also regulate the organization of the underlying cytoskeleton, which in turn stabilises the paranodal complexes (Ogawa et al., 2006). Consistent with this idea, Caspr mutant mice display severe cytoskeletal disorganization and axon degeneration (Garcia-Fresco et al., 2006).

In conclusion, although there might be different mechanisms regulating the developmental organization of domains along myelinated fibers in the CNS compared to PNS, three main common themes have begun to emerge: 1) myelinating glia initiate clustering of molecules associated with nodes of Ranvier; 2) cell-adhesion molecules play key roles in organizing membrane domains near and at the node of Ranvier; and 3) a specialised cytoskeletal scaffold is essential to maintain transmembrane proteins at each of these domains (Schafer and Rasband, 2006) .

1.3 The Neurofascins

It has become increasingly clear that cell-adhesion molecules play an essential role in myelination and in directing assembly of axonal domains along myelinated fibers. Among these are the Neurofascins, transmembrane glycoproteins first identified in the chicken brain (Rathjen et al., 1987), which are members of the L1 subgroup of the Ig superfamily of nervous system CAMs, including vertebrate L1, NrCAM, NgCAM, F3/Contactin-like GPI-linked molecules, and Neuroglian in *Drosophila* (Walsh and Doherty, 1997). All these molecules are widely expressed during the development of the nervous system and participate in multiple activities that involve cell-cell recognition, including cell adhesion and motility, neurite outgrowth, axon fasciculation, synaptogenesis and intracellular signalling (Fields and Itoh, 1996; Walsh and Doherty, 1997). Moreover, they can engage in complex molecular interactions, homophilically and heterophilically, both in *trans* and in *cis* with other related molecules and to themselves, as well as with ECM components (Brummendorf and Rathjen, 1996; Hortsch, 1996; Pruss et al., 2004).

No known human disease has been directly mapped to mutations in the *Neurofascin* (*Nfasc*) gene, although mutations in the L1 gene underlie the highly variable recessive neurological disease described as X-linked hydrocephalus, MASA syndrome (mental retardation, aphasia, shuffling gait, adducted thumbs) or spastic paraplegia type 1 (SPG1), all characterised by varying degrees of brain malformations, which include hypoplasia of the cortico-spinal tract and underdeveloped corpus callosum (Brummendorf et al., 1998)

In the mouse, the gene stretches approximately 72 kilobases (kb) along Chromosome I and comprises 33 exons. Approximately fifty possible messenger RNAs (mRNAs) have been identified in vertebrates as a result of variant splicing (Hassel et al., 1997), which might modulate ligand binding and be developmentally regulated, thus providing multiple possible functions for different molecular compartments at particular stages in development (Koticha et al., 2005; Pruss et al., 2006; Volkmer et al., 1998).

Two of the best characterised gene products are a 186kD and a 155kD isoform, which are differentially expressed in neurons and in myelinating glia respectively (Collinson et al., 1998; Davis et al., 1996; Pruss et al., 2006; Tait et al., 2000). Nfasc186 was initially

identified, among other possible neuronal isoforms, as being highly enriched in neuronal cell bodies and fiber tracts early in embryonic development, supporting a role in migration, axon growth and guidance (Rathjen et al., 1987) Moreover, *in vitro* antibody perturbation assays suggested a role in axon fasciculation and neurite extension on other axonal surfaces expressing NrCAM, axonin-1 and Contactin (Volkmer et al., 1996; Volkmer et al., 1998). Subsequently, Nfasc186 was recognised as the predominant isoform expressed at nodes of Ranvier and axon initial segments in both the PNS and CNS (Davis et al., 1996; Lustig et al., 2001). As already mentioned, Nfasc186 is recognised as one of the early nodal components (Lambert et al., 1997) and there is indirect evidence that it might be a critical molecule in driving assembly of the nodal complex at peripheral nodes of Ranvier (Eshed et al., 2005; Koticha et al., 2006; Lambert et al., 1997). Nfasc186 has also been shown to cluster at AIS early in development, albeit following accumulation of Ankyrin G, Nav channels and βIV Spectrin (Jenkins and Bennett, 2002; Kordeli et al., 1995; Xu and Shrager, 2005).

By *in situ hybridisation,* a glial isoform of Neurofascin was initially detected in the white matter tract of the spinal cord, where its spatial and temporal distribution corresponded to the ventral to dorsal order in which spinal tracts are myelinated (Moscoso and Sanes, 1995). Similarly, in the cerebellum, the pattern of labelling corresponded to that of the Proteolipid Protein (PLP) mRNA, a known marker of oligodendrocyte differentiation, and displayed a transient peak of expression corresponding to early stages in myelination (Collinson et al., 1998). Subsequently, the generation of isoform specific probes for *in situ hybridisation* and antibodies for immunocytochemistry confirmed that the glial isoform of Neurofascin is Nfasc155 and that, after a transient peak of diffuse expression in oligodendrocyte cell bodies and processes ensheathing axons, the protein becomes highly concentrated at paranodes (Chang et al., 2000; Tait et al., 2000). Moreover, immunoelectron microscopy confirmed that Nfasc155 was a glial component of the paranodal axoglial junction which was further supported by the demonstration of a biochemical interaction between the extracellular domain of Nfasc155 and the axonal Caspr-Contactin complex (Tait et al., 2000; Charles et al., 2002) (Figure 6).

These observations supported a possible role for Nfasc155 in mediating axon-glia recognition and paranodal formation. Indeed, Nfasc155 specific antibodies and soluble

extracellular domain fused to the Fc region of human IgG inhibited myelination in myelinating co-cultures, possibly by interfering with the adhesive properties between the axon and the glial cell (Charles et al., 2002).
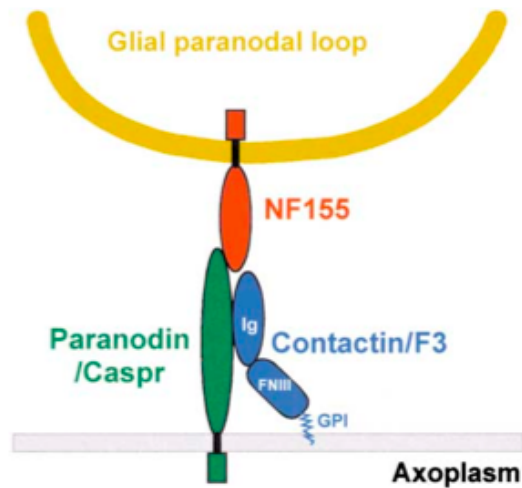
FIGURE 6. Model of Nfasc155 Interaction with the Paranodin/Caspr-Contactin Complex at the Axoglial Junction (Charles et al., 2002).

With regard to their domain structure, both Neurofascin isoforms share common features of the Ig superfamily. From the N-terminus to the C-terminus, both proteins contain six extracellular Ig domains followed by four fibronectin type three (FNIII) repeats, a transmembrane domain and a cytoplasmic region (110 amino acids). However, Nfasc 155 contains a unique FNIII repeat (C) with an arginine, glycine, aspartic acid (RGD) motif, whereas Nfasc186 has a mucin-like proline-, alanine-, threonine-rich (PAT) domain and an extra FNIII repeat (E) (Davis et al., 1996) (Figure 7).

Their cytoplasmic domain contains an Ankyrin G binding domain with a conserved peptide motif, namely the FIGQY sequence, which is in common with other L1 family members and is susceptible to phosphorylation (Jenkins et al., 2001). *In vitro,* Ankyrin G binding is favoured when this motif is dephosphorylated (Garver et al., 1997), whereas phosphorylation decreases Neurofascin-mediated intercellular adhesion (Tuvia

33

et al., 1997). *In vivo,* phosphorylated Neurofascin has been observed in paranodes of adult sciatic nerves (Jenkins et al., 2001), in developing optic nerve (Tait et al., 2000) and in regions of neuronal migration of vertebrate central nervous system, including the embryonic cortex, the neonatal cerebellum and the adult rostral migratory system (Jenkins et al., 2001).
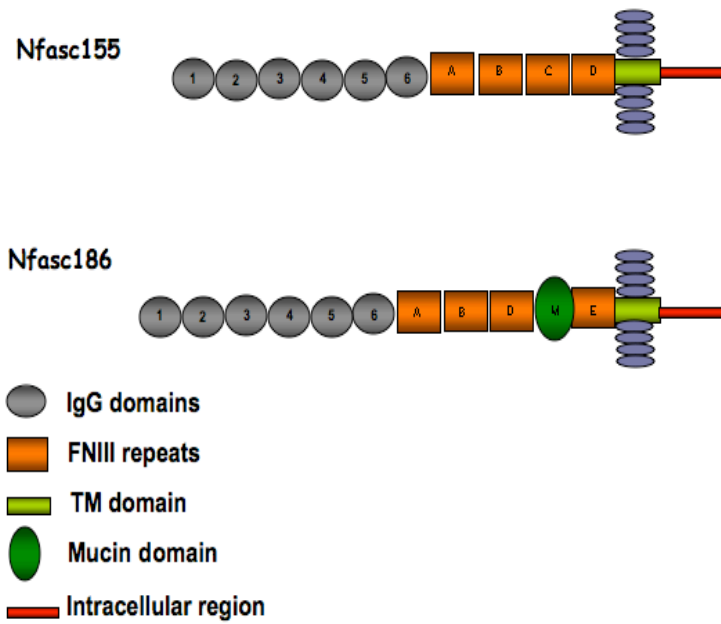
FIGURE 7. Domain Organization of Glial Nfasc155 and Neuronal Nfasc186 (TM=transmembrane)

These observations suggest that at site of cell-cell contact, local dephosphorylation of Neurofascins could play a role in the morphogenesis and stabilization of functional microdomains through its binding to cytoskeletal proteins, such as Ankyrin G (Jenkins and Bennett, 2002). Conversely, phosphorylation might be physiologically important for cell migration and neurite extension early in the development of the nervous system (Kizhatil et al., 2002).

The extreme cytoplasmic tail of Nfasc186 and Nfasc155 also contains a PDZ-binding sequence, which can interact with the PDZ domain of Syntenin-1 by yeast two-hybrid screening (Koroll et al., 2001).

In the ectodomain, the Ig-1 and the second FNIII domain have been shown to mediate a *cis* interaction with the extracellular Ig-like domain of the β1 subunit of Nav channels, and since β1 subunits colocalise with Neurofascin at nodes of Ranvier, this association is believed to occur with Nfasc186 rather than Nfasc155 (Ratcliffe et al., 2001).

Targeting of Nfasc186 to nodes of Ranvier and AIS has been recently investigated by nucleofecting neurons with various cDNA encoding epitope-tagged Nfasc186. Dzhashiashvili and colleagues (2007) were able to show that the ectodomain of Nfasc186 is necessary for its targeting to peripheral nodes of Ranvier, and that this targeting is mediated by the Ig domains rather than either the FNIII repeats or the mucin-like domain. Moreover, by use of a combination of transfection and knockdown experiments, the authors provide compelling evidence that targeting of Nfasc186 to peripheral nodes of Ranvier is required to recruit Ankyrin G and Nav channels.

Conversely, targeting of Nfasc186 to AIS of cultured hippocampal neurons and to proximal segments (PS) of dorsal root ganglia requires interactions of the cytoplasmic domain with Ankyrin G, since constructs in which the ankyrin binding domain was deleted failed to localise at these sites (Dzhashiashvili et al., 2007). These results are consistent with a previous study in which a mutation of the ankyrin binding sequence of Nfasc186 impaired its accumulation at AIS (Lemaillet et al., 2003).

In contrast to nodes, short hairpin RNA (shRNA) treatment of Nfasc186 does not inhibit Ankyrin G and Nav channel accumulation at AIS and PS of neurons, indicating that Nfasc186 is dispensable for AIS/PS formation (Dzhashiashvili et al., 2007). In this regard, one of the proposed roles of Nfasc186 is to direct presynaptic input of

GABAergic interneurons to the AIS of CNS neurons, where its positioning is controlled by Ankyrin G (Ango et al., 2004).

Altogether, these results show that AIS and peripheral nodes of Ranvier assemble by very different mechanisms, and since Nfasc186 is targeted to CNS nodes with a delay, akin to that observed at AIS, they suggest that targeting to nodes may also differ between CNS and PNS (Dzhashiashvili et al., 2007).

A specific role for the unique FNIII repeat of Nfasc155 in paranode formation has not been investigated yet, although it has been suggested that the RGD motif might mediate initial axoglial contacts (Koticha et al., 2005). However, the entire extracellular domain of Nfasc155 is sufficient to target it to paranodes, since transgenic expression of the truncated protein is correctly delivered to the glial plasma membranes in both the PNS and the CNS (Sherman et al., 2005). In addition, the extracellular domain is sufficient to co-imnunoprecipitate the Caspr-Contactin complex from brain lysates, suggesting that its ectodomain mediates axoglial junction formation (Charles et al., 2002). It has been shown that a soluble Nfasc155-Fc can bind directly to cells expressing the HMw isoform of Contactin and not the associated Caspr-LMw Contactin complex (Gollan et al., 2003). This leaves open the question regarding the nature of NFasc155/HMw-Contactin interaction, as well as of the molecules required to bridge between these proteins at the axoglial junction.

In addition, Nfasc155 has been shown to be present in low-density, detergent insoluble membrane fractions, also known as "lipid-rafts", and to acquire these biochemical properties as paranodes form, suggesting that both *trans* interactions with Caspr- Contactin and *cis* interactions with galactolipids might be important for formation and stabilization of the paranodal junctions (Schafer et al., 2004).

The extreme C-terminus of the cytoplasmic tail of Nfasc155 interacts with the FERM (4.1-ezrin-radixin-moesin) domain of the actin-binding protein Ezrin in the nodal microvilli of Schwann cells, suggesting a second mechanism, in addition to the binding via Ankyrin G, by which Neurofascin can be linked to the actin cytoskeleton (Gunn-Moore et al., 2006). Conversely, no intracellular binding partners of Nasc155 present at paranodes have been identified yet.

1.3.1 The *Neurofascin-null* mice: insights into the role of the Neurofascins in establishing axonal domains.

The role of the Neurofascins in assembly of the node and paranode in the PNS has been tested directly using mice with a targeted deletion of the *Neurofascin* gene. Sherman and collaborators (Sherman et al., 2005) generated Neurofascin-null mice by homologous recombination in embryonic stem (ES) cells, which produced mice lacking both neuronal Nfasc186 and glial Nfasc155 (Figure 8). Neurofascin-null mice died suddenly at 6-7 days after birth and therefore were analysed before they displayed any obvious clinical phenotype.

In the PNS of $Nfasc^{-/-}$ mice, myelin amount and structure appeared grossly normal (Figure 9A). However, the conduction velocity was dramatically reduced in the sciatic nerves of mutant animals when compared to wild-type littermates.

Electron microscopy of the paranodes in longitudinal sections of peripheral nerves showed that, compared to wild-type, the septate-like junctions were no longer present and that there was an increased gap between the base of the paranodal loops and the axolemma (Figure 9C). Moreover, immunofluorescence data showed that Caspr and Contactin were not clustered at the paranodes of these mutants, but rather diffusely distributed along the axon. In addition, $Nfasc^{-/-}$ mice failed to cluster NrCAM, Nav channels, Ankyrin G and βIV Spectrin at nodes of Ranvier, albeit the amount of all these nodal and paranodal proteins was unaffected (Figure 9B).
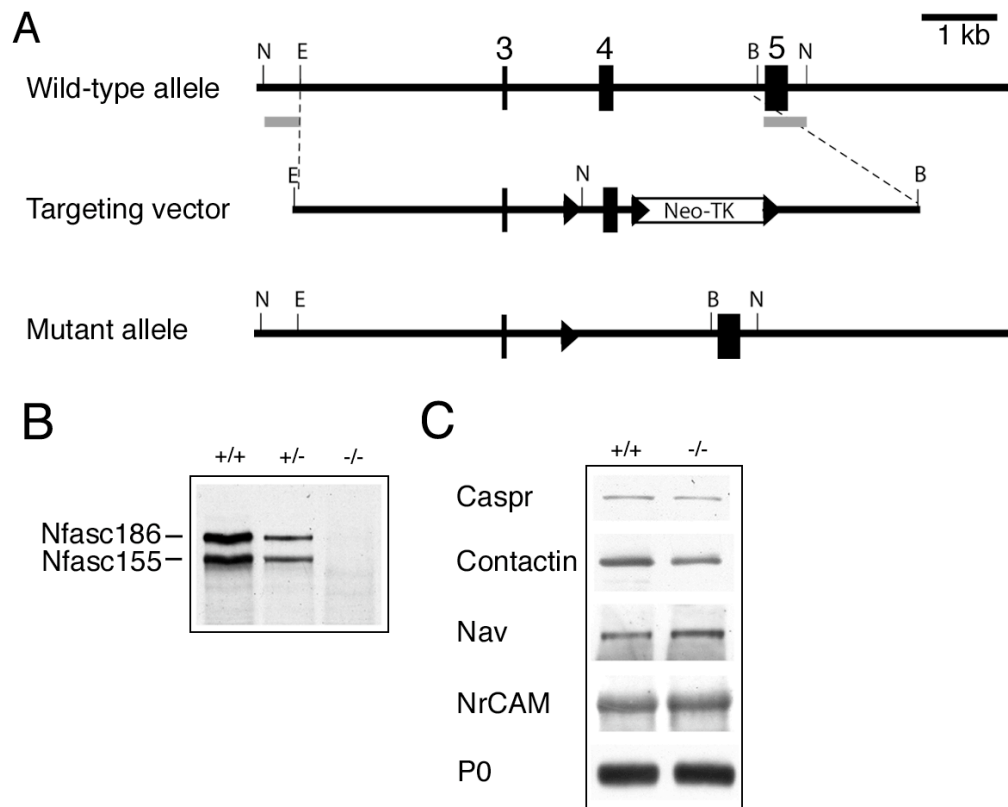
FIGURE 8. Generation of Neurofascin-null mice

A) Schematic diagram of the wild-type *Neurofascin* gene, the targeting vector and the mutant allele after *Cre*-mediated excision. The targeting construct was designed to delete exon 4 resulting in a in-frame stop codon in exon 5.

B) Western blot analysis of sciatic nerve homogenates from wild-type, heterozygous and Neurofascin-null mice, confirming the complete ablation of Nfasc186 and Nfasc155 in the mutant.

C) Western blot analysis showing that the absence of the Neurofascins does not affect the amount of paranodal (Caspr, Contactin), nodal (Nav channels, NrCAM) and myelin (P0) components in the peripheral of mutant mice. (Source: adapted from Sherman et al., 2005)
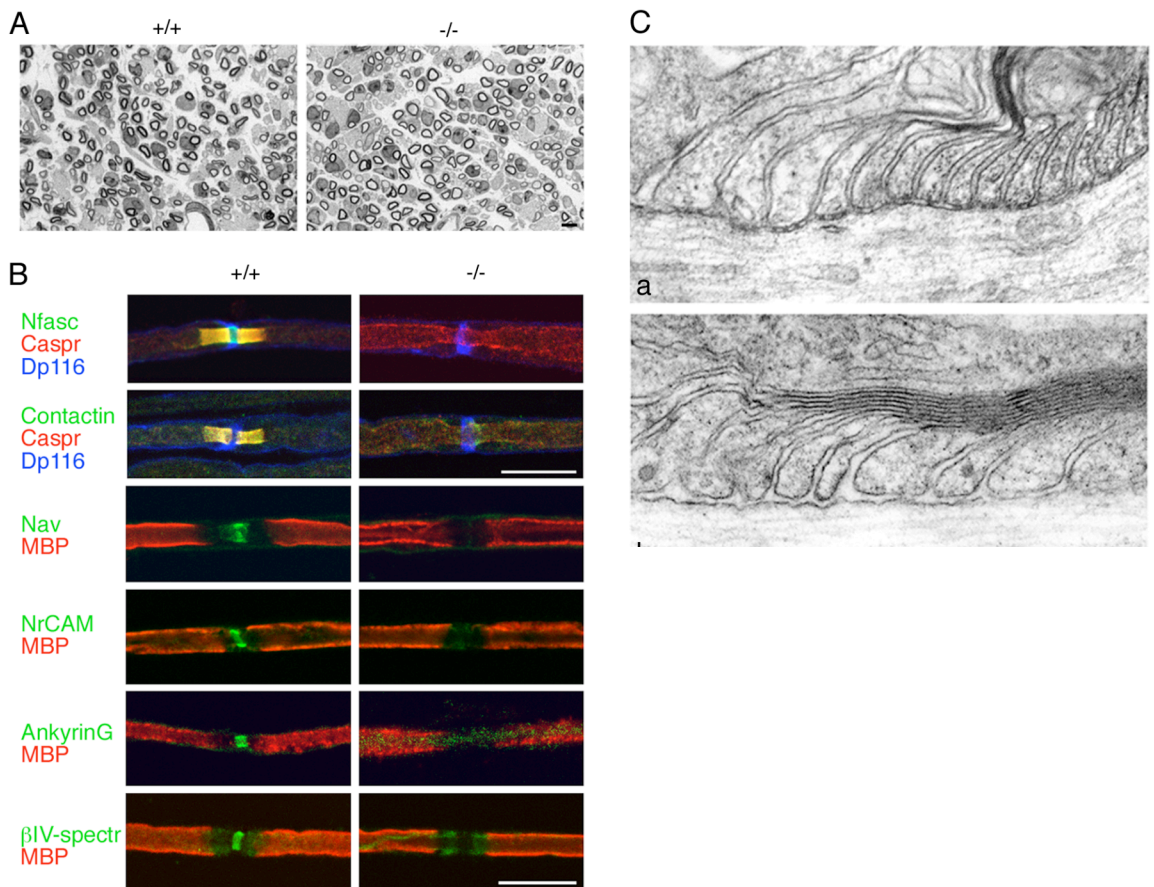
FIGURE 9. Disruption of the Paranodes and Nodes in the PNS of *Neurofascin* Mutant
Mice

A) Light microscopy shows no difference in the number or thickness of myelin sheath in transversal
sections of sciatic nerves from wild-type and $Nfasc^{-/-}$ mice at P6. **B)** Immunofluorescence analysis of
teased fibers reveals that Caspr and Contactin are no longer detected at paranodes and that all nodal
components, NrCAM, Nav channels, Ankyrin G and βIV Spectrin do not cluster at nodes of the mutants.
An isoform of Dystrophin (Dp116) concentrated at Schwann cell microvilli was used to independently
localize the nodes in the absence of other markers. **C)** Electron microscopy of the paranodes shows that
septate-like junctions are clearly visible in wild-type (a) but are absent in Neurofascin-null (b) mice
leaving a gap between the axolemma and the paranodal loops (Source: Sherman et al., 2005).

These results strongly suggested that the primary role of Nfasc155 and Nfasc186 was to ensure that their respective paranodal and nodal complexes were appropriately assembled. However, it was not possible to determine their unique contributions in establishing these domains. To distinguish between their respective roles, Sherman and collaborators expressed an epitope-tagged transgene, comprising the extracellular and transmembrane domain of Nfasc155, in glial cells of Neurofascin-null mice. In these mice, the paranodal complex was rescued, as evidenced by Caspr and Contactin immunoreactivity; however, the nodal complex, comprising Nav channels, NrCAM, Ankyrin G and βIV Spectrin, remained mislocalised (Sherman et al., 2005) (Figure 10).

Together these data provide the first direct evidence that Nfasc155 is an essential component of the Caspr-Contactin adhesion complex and that localization of the Caspr-Contactin complex depends on the presence of Nfasc155 at paranodes. Conversely, Nfasc155 can be targeted to the paranode in the absence of either Caspr or Contactin (Bhat et al., 2001; Boyle et al, 2001). In addition, similar to *Caspr* and *Contactin* mutants, Neurofascin-null mice lack septate-like junctions, suggesting that all three CAMs are necessary for axoglial junction formation.

These results also strongly corroborate previous indirect findings suggesting that Nfasc186 is required for the assembly of the nodal complex, at least in the PNS. They also show that, although both Nfasc186 and NrCAM bind Ankyrin G and have been shown to colocalise early in node of Ranvier formation (Lambert et al., 1997), recruitment of NrCAM to nodes depends on Nfasc186 and NrCAM cannot compensate for the loss of Nfasc186.

Finally, these results are consistent with the idea that an intact axoglial junction is not required for assembly of peripheral nodes, since rescuing the paranodal axoglial junction is not sufficient to cluster the nodal complex, whose disruption in *Nfasc*$^{-/-}$ mice is due to the absence of Nfasc186.
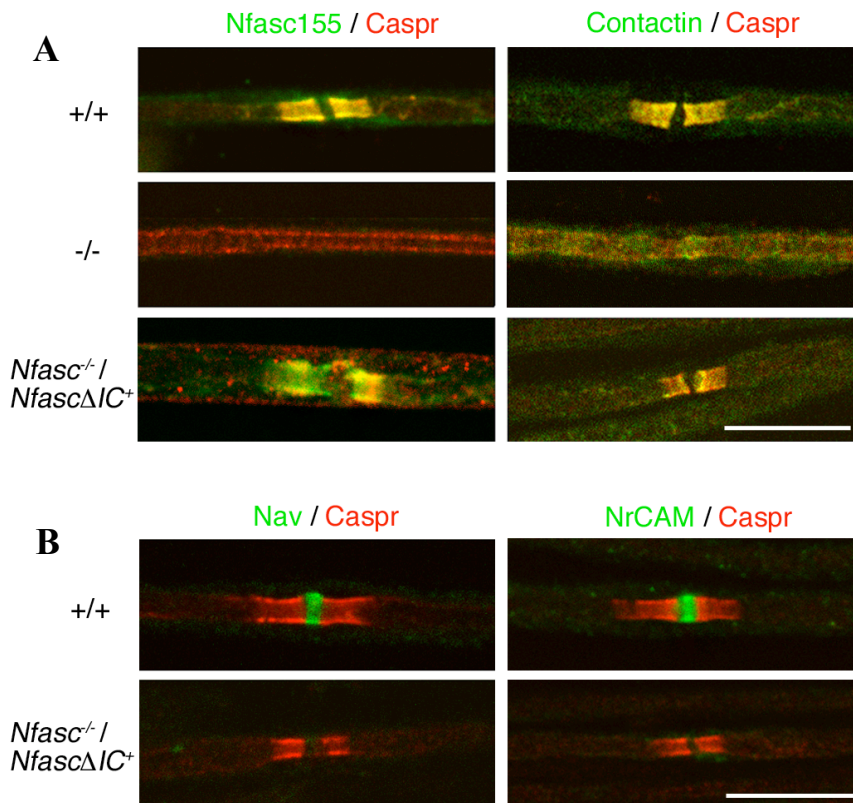
FIGURE 10. Reformation of the Paranodal Adhesion Complex Does Not Rescue the Node of Ranvier in the PNS.
A) Immunostaining of teased fibers shows that when the truncated form of Nfasc155, Nfasc155ΔIC, is expressed on a Neurofascin-null background, the paranodal adhesion complex of Caspr and Contactin is reconstituted. **B)** Despite formation of the paranodal complex, the nodal components, Nav channels and NrCAM, are not rescued (Source: Sherman et al., 2005).

If Nfasc186 is the key molecule in the process of node formation, what targets Nfasc186 at discrete clusters along PNS axons? As mentioned earlier, Gliomedin expressed on SC microvilli is ideally suited to restrict the localisation of Nfasc186 by virtue of their reciprocal interaction, which might cause Nfasc186 to accumulate at the distal ends of myelinating SCs (Eshed et al., 2005).

Based on several lines of evidence, a model can be drawn on how the Neurofascins might establish axonal domains as a result of axoglial interactions during myelination in the PNS (Eshed et al., 2005; Sherman et al., 2005; Yang et al, 2007): at the node, accumulation of Gliomedin at the edges of SCs and interaction with Nfasc186 recruits NrCAM, both of which can function as a docking site for Ankyrin G. Subsequently, Ankyrin G serves as a scaffold for the retention of Nav channels and ßIV Spectrin. At the paranode, Nfasc155 is delivered independently of Caspr and Contactin, but it is required for the localization of the Caspr-Contactin complex, suggesting that it might also be a pioneer molecule at paranodes.

Nodes and paranodes appear to assemble independently of each other, although intact paranodal axoglial junctions are likely to influence aspects of nodal maturation and might serve to further stabilise the nodal complex (Figure 11).
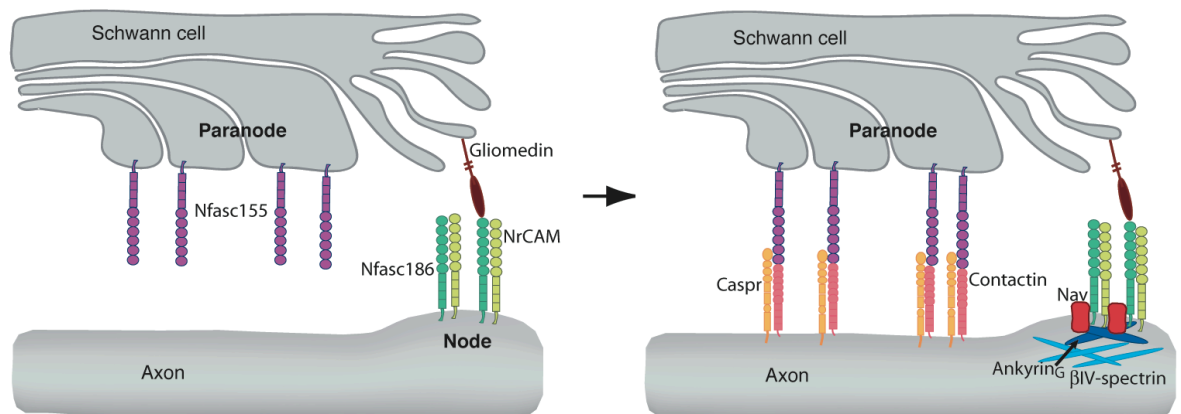
FIGURE 11. Model of the Potential Role of the Neurofascins in Establishing Axonal Domains in the PNS.

The assembly of node and paranode requires Nfasc186 and Nfasc155 respectively. Gliomedin-dependent accumulation of Nfasc186 at nascent nodes recruits NrCAM and subsequently the nodal complex is assembled. At the paranode, accumulation of Nfasc155 is necessary for localising Caspr and Contactin and axoglial junction formation (Source: Sherman et al., 2005).

1.4 Purpose of the project

From the analysis of the direct role of the Neurofascins in the assembly of peripheral nodes and the model depicted above, a few questions necessarily follow: are similar mechanisms used to cluster multi-protein complexes at axonal domains in the CNS as in the PNS? Is Nfasc186 essential in CNS node formation? And, since paranodal axoglial junctions, as defined by Nfasc155 and Caspr-Contactin immunoreactivity, appear to form in the CNS before nodal components are detected (Schafer et al., 2004), does Nfasc155 play a facilitating role in node assembly?

The answer to these questions requires the analysis of myelinated axons in the CNS of the *Nfasc* mutants, which constitutes the main objective of this work. In addition, this work aims to provide direct evidence and corroborate previous findings suggesting that central nodes and AIS assemble by different mechanisms from PNS nodes as well as from each other.

Finally, to understand the distinctive role of each isoform in node assembly, this work will make use of transgenic mice in which either Nfasc155 or Nfasc186 are reintroduced on a null background.

2. MATERIALS AND METHODS

2.1 Construct preparation for transgenesis

2.1.1 FLAG tagged full length Nfasc186 cDNA

The full length *Nfasc186* cDNA (~3.8 kb) with 5'-Kozak consensus sequence (CTGAGG) was prepared by Dr Stewart Gillespie using RT-PCR from P7 cerebellum mRNA. The cDNA was then subcloned into the pSP72 vector (Promega) using the HindIII and EcoRI restriction sites in the multiple cloning site (MCS). The plasmid pSP72Nfasc186 was checked by sequencing (DNA Sequencing Service, Dundee University).

To fuse a FLAG tag (GGDYKDDDDK) to the 3' end of *Nfasc186* cDNA, a ~1.9 kb fragment was generated by a single step "patch" PCR (Squinto *et al.*, 1990) (Figure 12) using three oligonucleotide primers, as follows: 1) a forward primer annealing to sequences in exon 17 which are unique to Nfasc186 and located upstream of a unique BamHI restriction site (5'-TGATCAGGCCACTCCAACTAACCGTTTGG-3'); 2) one reverse patch primer (FLAG1) coding for complementary sequences to the last six codons at the 3' end of Nfasc186, upstream of the termination codon (TGA), followed by the full FLAG sequence. The primer included a Gly-Gly bridge sequence between the Nfasc186 and the FLAG sequences (5'-CTTGTCATCGTCATCCTTGTAGTCACCTCCGGCAAGGGAATAGATGGCA-3').
3) a second reverse patch primer (FLAG2) partially annealing to the FLAG sequence of FLAG1 primer followed by a tail sequence encoding a stop codon and a unique HindIII restriction site (5'-GGCCCAAGCTTTCACTTGTCATCGTCATCCTT-3').

A primer ratio was chosen so that PCR amplification using the 5' and FLAG1 primers ceased after a few cycles and amplification between 5' and FLAG2 primers could initiate and give a high yield of the final PCR product.

Approximately 20 ng of cDNA template were used in a total 50 µl PCR reaction containing Pfu polymerase buffer, 0.2 mM dNTPs, 0.2 µM forward primer, 0.002 µM reverse primer FLAG1, 0.2 µM reverse primer FLAG2 and Pfu polymerase (1U, Stratagene). The PCR conditions were: 1 cycle of 94°C denaturation for 1 min, 5 cycles of 94°C denaturation for 30 s, 55°C annealing for 30 s, and 72°C extension for 4 min. These conditions favoured the amplification using the 5' and FLAG1 primers, after which conditions were modified to allow the 5' and FLAG2 primer pair to amplify the

product resulting from the first amplification. These conditions consisted of 25 cycles of 94°C denaturing for 30 s, 60°C annealing for 30 s and 72°C for 4 min. The last cycle consisted of 72°C extension for 4 min.

The PCR product was purified using the QIAquick PCR purification kit (QIAGEN).

Both pSP72Nfasc186 and the purified FLAG tagged Nfasc186 fragment (~1.8kb) were digested with BamHI and HindIII. The bands of expected size were excised from a 1% agarose gel, extracted using the Qiaex II gel extraction kit (Qiagen) and quantified on a 1% agarose gel against a High Mass Ladder (Invitrogen).

The FLAG tagged 3'-Nfasc186 fragment (360 ng) was then subcloned into pSP72Nfasc186 (100 ng), using BamHI and HindIII restriction sites (Figure 13). The ligation was performed using 1 U of T4 DNA Ligase, Quick Ligase Buffer (New England BioLabs) at room temperature for 10 min. Competent XL1-blue cells were transformed (Sanbrook and Russell, 2001) and plated on Luria-Bertani medium (LB) agar (Melford) containing 0.1 mg/ml Carbenicillin. Randomly selected colonies were screened for insertion by colony PCR (see details below), using a forward primer in the Nfasc186 mucin-like domain sequence downstream of the BamHI site (5'-CTCCAACTGCAGCTC-3') and the FLAG2 reverse primer, generating a ~ 1 kb product.

Two positive clones were grown overnight in 5 ml LB, 1mg/ml Carbenicillin and purified by SDS/alkaline lysis using a plasmid DNA purification kit (Nucleospin, Macherey-Nagel). Plasmids were then sent for sequencing to check for errors (DNA Sequencing Service, Dundee University).
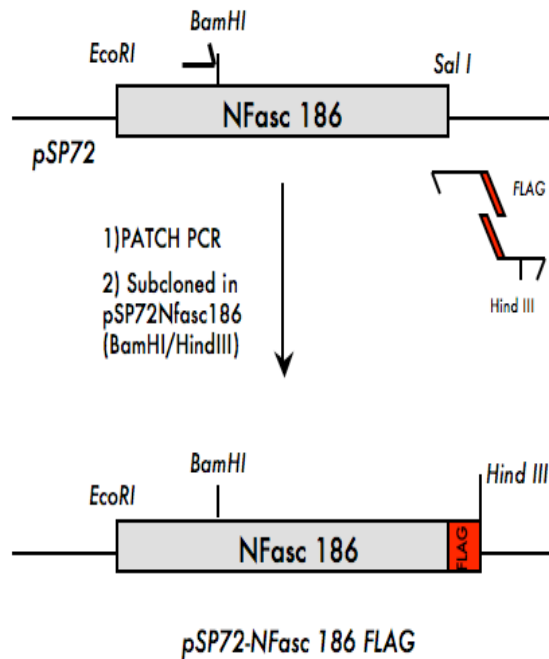
FIGURE 12. "Patch" PCR Synthesis of the FLAG Tag to the 3' end of Nfasc186.
Diagram showing the position of the 5'- and 3'- primers for the PCR reaction and the subcloning of the
product into pSP72Nfasc186 to generate the pSP72Nfasc186Flag construct.

In preparation for insertion of Nfasc186FLAG sequence into other vectors, the
plasmid pSP72Nfasc186FLAG (10 µg) was digested with EcoRI and HindIII.

For insertion into the pGCHNFL-As vector, the Nfasc186FLAG construct needed to
be flanked by ClaI restriction sites. After digestion with EcoRI and HindIII, the insert
was cloned into EcoRI/HindIII digested pBS-SK vector and released by digestion with
EcoRI and SalI This allowed to pick up a ClaI site at the 3' end of the insert. Subcloning
into pSP72 vector using EcoRI and SalI restriction sites permitted to flank the
Nfasc186FLAG insert by ClaI sites. Restriction digest with ClaI on miniprep DNA
(Sanbrook and Russell, 2001) revealed that the insert was present and plasmid DNA
was further purified using Nucleospin columns. For cloning into the pGCHNFL-As,
Nfasc186 FLAG was released using a ClaI digest. After gel electrophoresis, a 3.8 kb
band was excised, Qiaex purified and quantified as previously described.
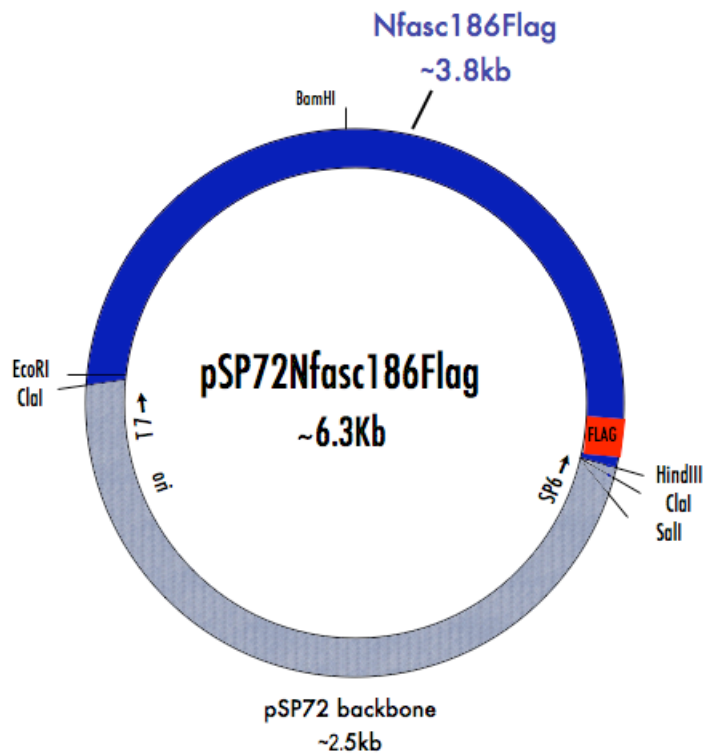
FIGURE 13. The pSP72Nfasc186Flag Plasmid
Diagram showing the full length Nfasc186 cDNA with a FLAG tag at the 3' end subcloned into the
pSP72 plasmid. Restriction digest with ClaI permitted its subcloning into the pGCHNFL-As vector.

2.1.2 pNFL-Nfasc186Flag construct

The pGCHNF-L vector was a kind gift from Dr Diane E. Merry (Thomas Jefferson University, Philadelphia). It contains the basal promoter region of the human Neurofilament light chain gene (hNF-L), the hNF-L gene (4 exons), a 1.5 kb fragment from the mouse β-globin gene including splice donor and acceptor signals, a polyadenylation signal, and BlueScript SK- sequences (Abel et al., 2001; Charron et al., 1995).

A preliminary step required modifying the vector in order to be able to remove the prokaryotic sequences once Nfasc186FLAG had been inserted. This modification consisted in substituting a KpnI restriction site with an AscI site, using AscI phosphorylated linkers (New England BioLabs). Briefly, pGCHNF-L was linearised by

48

digestion with KpnI and blunt ends generated by incubation with T4 Polymerase and 0.1 mM dNTPs at 37°C for 5 min, followed by incubation at 75°C for 20 min to stop the reaction. 30 Picomoles of AscI linkers were ligated per μg of vector. After transformation, the incorporation of the linker and the release of the BlueScript backbone were assessed by single and double restriction digests with AscI and Not1. Purification of the resulting pGCHNFL-As plasmid was performed using the Nucleospin Plasmid DNA purification kit.

In preparation for insert ligation, the pGCHNFL-As plasmid was digested with ClaI and dephosphorylated using the calf intestinal alkaline phosphatase kit (CIAP, Gibco BRL) at 50°C for 1 hour.

Ligation of Nfasc186Flag (20 ng) into pGCHNFL-As (50 ng) was performed at room temperature for 6 hours. XL1-Blue competent cells were transformed and minipreps were performed by SDS/alkaline lysis (Sambrook and Russell, 2001) on 5 ml overnight cultures from individual colonies. Insertion and orientation of the insert were checked by ClaI and XbaI restriction digests respectively. One positive clone was selected and the purified plasmid DNA was sequenced, using primers at the 5' and 3' ends of Nfasc186Flag.

DNA was prepared from a 100 ml overnight culture using the Qiagen midi-prep kit. For preparation of DNA for microinjections, 50-70 μg of plasmid was digested with AscI and NotI to release the BlueScript backbone (Figure 14).
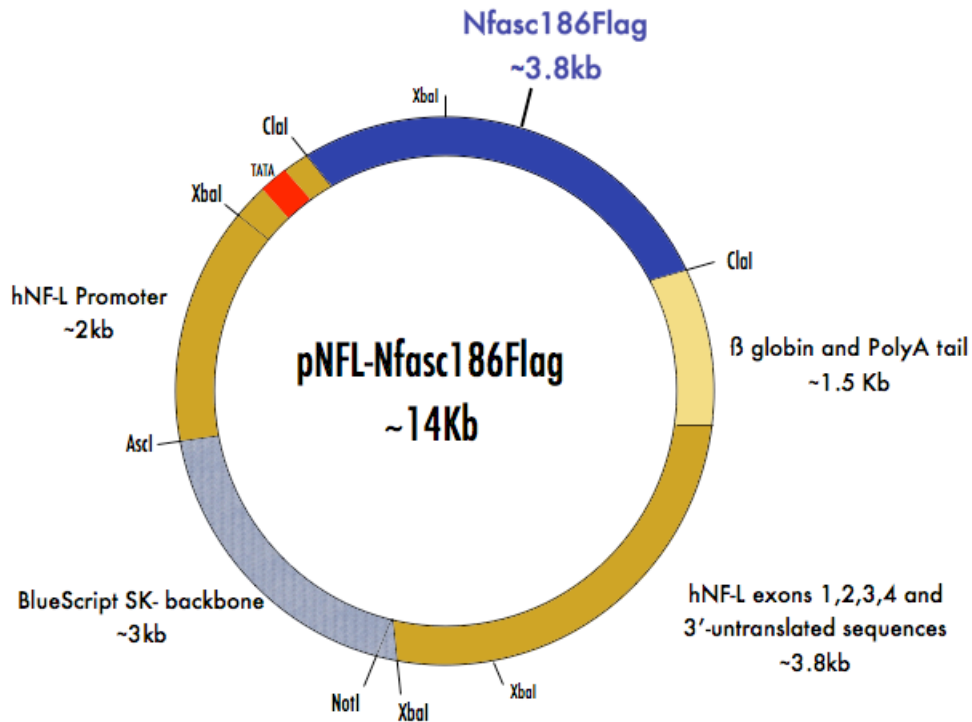
FIGURE 14. The pNFL-Nfasc186Flag Plasmid
Diagram showing Nfasc186FLAG subcloned into ClaI-digested pGCHNFL-As plasmid. For microinjection, a restriction digest with AscI and NotI released the BlueScript backbone.

2.1.3 DNA purification for injection

Dr Diane Sherman purified DNA for microinjection. Briefly, prokaryotic sequences were removed by restriction digest of 50 µg of plasmid followed by 0.8% low melting point agarose gel electrophoresis. The transgene was excised and the agarose was digested with Gelase (Epicentre Biotechnologies) according to the manufacturer's instructions. The DNA was then purified on an Elutip-D column (Whatman), followed by ethanol precipitation and resuspension in injection buffer (0.1 mM EDTA, pH 8.0, 10 mM Tris HCl, pH 7.5). The DNA was dialysed against injection buffer and concentration calculated. Finally, the purified DNA was diluted with injection buffer to obtain a final concentration of 2.5 µg/ml.

2.2 Animals and genotype screening

All animal procedures reported in this work were performed according to Home Office regulations.

2.2.1 *Nfasc*^{-/-} mice

$Nfasc^{-/-}$ mice were generated by homologous recombination in ES cells as previously described (Sherman *et al*, 2005). Briefly, the targeting construct was designed to generate S129 ES cells clones with a deletion of exon 4 (3 kb), which introduces a frame shift resulting in a stop codon in exon 5. One clone with the desired modification (2D7) was then injected into C57Bl/6-derived blastocysts, transferred into pseudo-pregnant mothers to generate chimeras. $Nfasc^{+/-}$ mice were backcrossed to a C57BL/6 background for at least six generation before experimental analysis.

Since $Nfasc^{-/-}$ mice die by postnatal day (P) 7, litters were harvested at P6 and identified by genotyping using tail biopsy.

2.2.2 *NrCAM*^{-/-} mice

NrCAM-null mice were generated by homologous recombination in ES cells in the laboratory of Prof. F.G. Rathjen, at the Max-Delbrück Center for Molecular Medicine, Berlin. Whole brains from *NrCAM* wild-type and mutant mice at P6 were kindly provided for analysis following fixation in 4% PFA as described in section 2.4.1.

2.2.3 Transgenic mice

Nfasc^{-/-}*/NfascΔIC transgenic mice.*
Transgenic mice expressing a truncated form of Nfasc155 on a null background were generated by standard pronuclear injection, as previously described (Sherman et al.,

2005). In brief, the transgenic construct consisted of the pPLP-SV40/bluescript vector carrying the PLP promoter and cDNA encoding all the extracellular domain of Nfasc155, the transmembrane domain and the first 13 amino acids of the intracellular tail (110 amino acids total) with a FLAG tag sequence fused to its 3' end. The PLP promoter ensured robust expression of the transgene in both oligodendrocytes and Schwann cells in one transgenic line, which was selected for backcrossing to a C57BL/6 background for at least 6 generations, followed by interbreeding with $Nfasc^{+/-}$ to generate $Nfasc^{-/-}/Nfasc155\Delta IC$ mice.

NFL-Nfasc186 transgenic mice

Transgenic mice expressing FLAG-tagged full length Nfasc186 driven by the Neurofilament light chain (NF-L) neuronal promoter were generated by pronuclear microinjection and embryo transfers (Hogan et al., 1994), which were performed by Heather Anderson and Professor Peter J. Brophy. Briefly, fertilised oocytes were obtained from superovulated C57BL6/CBA F1 hybrid female mice mated with F1 hybrid males. Once injected, fertilised eggs at the one or two-cell division stage were transferred into pseudo-pregnant MF1 foster mothers. Ear biopsies were taken at approximately P21. Transgenic founders were identified by PCR (see details below), back-crossed to a C57BL6 background and interbred with $Nfasc^{+/-}$ to generate $Nfasc^{-/-}/Nfasc186$ mice.

2.2.4 Ear and tail biopsies

Ear biopsies and approximately 5 mm tail clips were digested overnight at 55ºC in 50 and 150 µl lysis buffer respectively. Lysis buffer contained 50 mM TRIS, 50 mM EDTA pH 8.0, 0.25% SDS and 4 µl Proteinase K (1mg/ml) (Roche).

   After digestion, unpurified DNA was vortexed, spun briefly and diluted 1:10 in double distilled (MilliQ) water. For PCR, 2 µl from ear and 1µl from tail digests were added to the PCR reaction.

2.2.5 PCR

PCR reactions were performed in a total 25 µl consisting of 1 X Go Taq Buffer, 1.5 mM MgCl$_2$, 0.2 mM dNTPs, 0.5 µM of primers and 1 U of Go Taq polymerase (Promega) in MilliQ water. Positive and negative controls were always included alongside the test samples.

PCR products were resolved on 1% agarose gel in TAE buffer containing 0.5 µg/ml ethidium bromide and visualised by UV transillumination (Uvitec, Cambridge).

COLONY PCR

Colonies grown on agar plates were randomly picked and resuspended in 5 µl LB. For PCR, 2 ul were added to the PCR reaction.

The PCR conditions were: 1 cycle 94°C denaturing for 2 min, 57°C annealing for 30 s and 72°C extension for either 1 min or 30 s according to the size of the product. This was followed by 30 cycles of 94°C for 40 s, 57°C for 30 s and 72°C for either 1 min or 30 s. The final step consisted of 94°C for 40 s, 57°C for 30 s and 72°C for 2 min.

GENOTYPING OF ANIMALS

To identify Neurofascin-null mice, the primers were designed to flank exon 4. The forward primer NFFW1 (5'-GTGCTGATCCAGCCTAAAGC-3') and the reverse primer NFRV1 (5'-TCAGCTGTTTTGAGCCACAC-3') generated approximately 1.1 kb and a 700 bp products in wild type and null mice respectively (Figure 15). The PCR conditions were: 1 cycle of 94°C denaturation for 1.5 min, 55°C annealing for 30 s, and 72°C extension for 3.5 min. This was followed by 38 cycles of 94°C for 30 s, 55°C for 30 s, and 72°C extension for 1 min 10 s. Finally, the last cycle consisted of 94°C for 40 s, 55°C for 30 s and 72°C for 6 min.
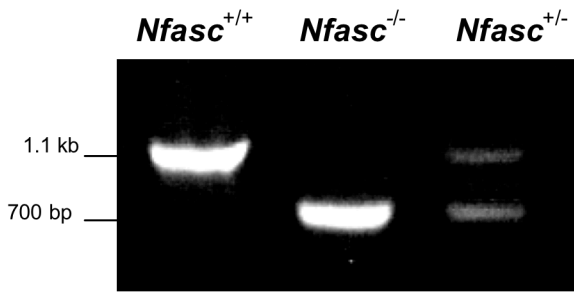
FIGURE 15. PCR products generated by genotyping wild-type, *Nfasc* mutant and heterozygous mice.

To identify *Nfasc155ΔIC* mice, a forward primer in the Fibronectin III C domain specific for Nfasc155 was used (5'-ACAAGCTGGAGATGGTGG-3'). The reverse primer FLAGSalR1 was designed to anneal to the FLAG tag sequence (5'-TGACTCGAGGTCGACGTGAACAGTAGCAGTAGGAAG-3'). The transgene was identified by the generation of a 500 bp PCR product (Figure 16).

The PCR conditions included 1 cycle of 94°C denaturation for 2 min, 56°C annealing for 30 s, 72°C extension for 40 s, followed by 33 cycles of 94°C for 40 s, 56°C for 30 s, and 72°C for 40 s. The last cycle consisted of 94°C for 40 s, 56°C for 30 s, and 72°C for 1 min.
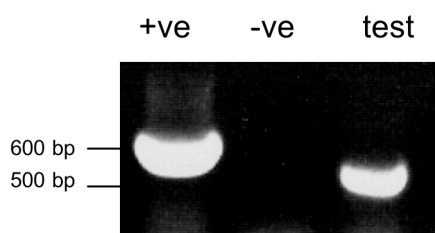
FIGURE 16. PCR product generated by genotyping *Nfasc155ΔIC* transgenic mice.
cDNA of full length Nfasc155 was used as a positive control (+ve) which generated a 600 bp PCR product. No template was used as a negative control (-ve). Genomic DNA from *Nfasc155ΔIC* transgenic mice (test) generated a PCR product of 500 bp.

Identification of transgenic mice expressing the full length Nfasc186 was performed by use of a forward primer located in the Fibronectin IIIE domain specific for *Nfasc186* (5'-GTGGTTGAGTACATCGACAG-3') and a reverse primer annealing to the FLAG tag sequence (5'-GGCCCAAGCTTTCACTTGTCATCGTCATCCTT-3'). The transgene generated a PCR product of approximately 600 bp (Figure 17). The PCR conditions consisted of 1 cycle of 94°C denaturation for 2 min, 56°C annealing for 30 s, 72°C extension for 40 s, followed by 33 cycles of 94°C for 40 s, 56°C for 30 s, and 72°C for 40 s. The final cycle consisted of 94°C for 40 sec, 56°C for 30 sec, and 72°C for 1 min.
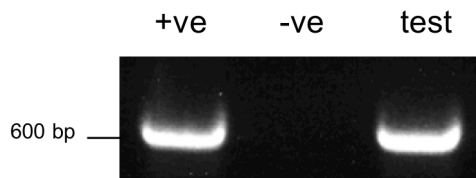
FIGURE 17. PCR product generated by genotyping *NFL-Nfasc186* transgenic mice
cDNA (pNFL-Nfasc186Flag) was used as positive control (+ve) and no template was used as a negative control (-ve). Genomic DNA from NFL-Nfasc186Flag transgenic mice (test) generated a PCR product of 600 bp.

2.3 Organotypic cerebellar culture

This protocol is a modified version of that designed by Dusart and colleagues (Dusart et al., 1997).

Organotypic cultures were obtained from newborn mouse cerebella. The mice were later genotyped using DNA purified from tails. After decapitation, brains were dissected into ice-cold Hanks' Balanced Salt Solution (HBSS; Sigma) and meninges carefully removed. Connectivity of cerebellum to midbrain and brainstem was preserved, whereas the forebrain was discarded. Cerebella parasaggital slices (250 μm) were cut on a McIlwain tissue chopper and separated gently in sterile-filtered culture medium composed of 50% Minimum Essential Medium Eagle (MEM, Sigma), 25% Earle's Balanced Salt Solution (Sigma), 25% heat-inactivated horse serum (Sigma), glucose (6.5 mg/ml), L-glutamine (2 mM) (Sigma), penicillin-streptomycin solution (100

μg/ml) (Sigma), and Amphotericin B solution (Sigma). The slices were then transferred to the membrane of 30 mm Millipore culture inserts (0.4 μm pore size) (Millicell, Millipore, Bedford, MA, USA), which were placed in six-well plates containing pre-warmed culture medium (1ml/well). Cultures were maintained in a 37°C incubator with a 5% carbon dioxide-enriched humidified atmosphere. Culture medium without Amphotericin B was replaced on the day after slice preparation and changed every 2 days.

2.4 Indirect Immunofluorescence

2.4.1 Tissue fixation and preparation for immunostaining

Adult, 4-week old, P6 and P4 mice were anesthetised with an intraperitoneal injection of pentobarbital (0.2 mg/g body weight) and perfused through the left ventricle with 4% paraformaldehyde in 0.1 M phosphate buffer (PB), pH 7.4. Generally, whole brains, cervical spinal cords (C2-C7), optic nerve and sciatic nerves were harvested and postfixed in the same fixative for 30 minutes at room temperature, with the exception of brains from young and adult mice, which were postfixed for at least 3 h.

CRYOSECTIONS

In preparation for immunostaining, specimens were washed 3 X 10 min in 0.1 M PB and cryoprotected in 30% sucrose in PB at 4°C overnight. Tissue samples were oriented appropriately in O.C.T. embedding matrix compound (CellPath Ltd) and frozen with isopentane cooled in liquid nitrogen. The blocks were then stored at -80°C until use. Consecutive 10 μm parasaggital brain sections, transverse and longitudinal sections of cervical spinal cords were cut using a Leica CM 3050 S cryostat and collected on 3-aminopropyltriethoxysilane (TESPA)-coated glass slides. Sections were dried and stored at -20ºC until use.

TEASED FIBER PREPARATION

After fixation, sciatic nerves and cervical spinal cords were washed in PBS 3 X 10 min and placed in a 35 mm Petri dish.

The perineurium from sciatic nerves was removed and fiber bundles gently separated, using a pair of acupuncture needles, in a drop of PBS on TESPA-coated slides.

Cervical spinal cords were placed in the Petri dish with the ventral side facing up and the ventral funiculi *or* columns, i.e. the white matter tracts flanking the ventral median fissure, were carefully pealed away using fine forceps. Small fragments of tissue were then placed in a drop of PBS on TESPA-coated slides. Using acupuncture needles, single fibers were gently separated from the bulk of the tissue.

Slides with teased fibers were dried for immunostaining or stored at -20°C until use.

ORGANOTYPIC CEREBELLAR SLICES

Parasaggital cerebellar slices (250 μm) cultured for 9 DIV (days *in vitro*) and 15 DIV were fixed by immersion in 4% paraformaldehyde in 0.1 M PB for 1 h at room temperature, followed by 3 X 15 min washes in PBS. Using a scalpel, pieces of the membrane containing single or multiple slices were cut out and all subsequent steps were performed in the wells of 6-well tissue culture plates.

2.4.2 Immunostaining and image acquisition

Fixed tissue cryostat sections, teased fibers and organotypic cerebellar slices were blocked in 5% fish gelatine, 0.1% Triton in PBS for 1 h at room temperature in humidified chambers. Primary antibodies were diluted in the same buffer overnight at room temperature. After several washes with 0.1% Triton in PBS (30 min), the appropriate fluorescent-conjugated secondary antibodies were applied in blocking buffer for 1 h 15 min at room temperature. For immunofluorescence staining of organotypic cerebellar slices, prolonged washes in 0.1% Triton in PBS (4 h) were followed by incubation in the secondary antibodies overnight at 4ºC.

Excess of secondary antibodies was removed by washing several times in PBS (30 min), with the exception of cerebellar culture slices which were washed with 0.1% Triton overnight at 4ºC, followed by a final wash in PBS. Slides were then coverslipped using an antifade-mounting medium (Vectashield, Vector Laboratories).

For dilutions of primary and secondary antibodies refer to Table 2 and Table 3 in section 2.7, "Antibodies used for immunolabelling".

An Olympus BX60 microscope equipped with a Hamatsu ORCA-ER digital camera and OpenLab software (version 5.0) was used to capture images for morphometric analysis.

All images displayed were acquired using a Leica TCL-SL confocal microscope and proprietary software. FITC, TRITC and Alexa Fluor-647 fluorophores were excited with an Argon (488 nm), HeNe (543 nm) and Red Diode (637 nm) laser respectively, and rendered using Adobe Photoshop (version 7.0).

2.5 Electron microscopy

Nfasc$^{-/-}$ mice and wild-type littermates were terminally anesthetised and transcardially perfused with 3% paraformaldehyde, 3% glutaraldehyde in 0.1 M sodium cacodylate buffer, pH 7.3. Cervical spinal cords (C2-C7) and optic nerves were dissected. More specifically, the ventral *funiculi* of the spinal cord (C2-C5) were pealed away as previously described, and the caudal portion was cut in partial diagonal with respect to the midline. This was done so that the tissue could be orientated subsequently for transverse sections from the rostral end. Similarly, the optic chiasm was kept intact to identify the orientation for preparing optic nerve transverse sections of the region immediately posterior to the nerve's emergence from the rear of the orbit.

After whole body perfusion, the harvested tissue was immersed in the same fixative for 4 h at room temperature, followed by 3 X 5 min washes with 0.1 M cacodylate buffer. The tissue was then postfixed in 1% osmium tetroxide (OsO_4), 0.1 M cacodylate buffer for 1.5 h at room temperature, followed by dehydration in graded ethanols (50%, 70%, 90% and 100% for 10 min each) and propylene oxide. The tissue was subsequently embedded in Araldite in either longitudinal or transverse orientation, and polymerised at 60ºC for 48 h.

Semithin sections, 1 μm thick, were cut on a Reichert OMU4 ultramicrotome (Leica Microsystems Ltd), stained with 10% Toluidine Blue and viewed under a light microscope to select suitable areas for morphometry.

Ultrathin sections, 70 nm thick, were stained in Uranyl Acetate and Lead Citrate and examined with a Phillips CM12 transmission electron microscope. Areas of interests were photographed on electron image film.

2.6 Western Blotting.

2.6.1 Protein extraction

Five frozen cervical spinal cords obtained from P4, P6 wild-type and *Nfasc*$^{-/-}$ mice were homogenised in 200 μl Phosphate buffer saline (PBS), Complete protease inhibitor cocktail (Roche), 1 mM PMSF and kept on ice. An equal volume of homogenising buffer (200 μl) with 2% sodium dodecyl sulfate (SDS) was added and the homogenates were either boiled for 10 min or warmed at 55ºC for 5 min, followed by centrifugation (14,000 G) at room temperature. The supernatant was then recovered and stored at -40ºC until use. Protein concentration was estimated using the BCA (Bicinchoninic acid) assay (Pierce). Approximately 15 μg and 20 μg of total protein from wild-type and *Nfasc*$^{-/-}$ homogenates respectively were separated on either 6% or 15% SDS-PAGE in 1X sample buffer (20% glycerol, 130 mM Tris pH 6.8, 8% SDS, bromophenol blue) containing 100 mM dithiothreitol (DTT).

2.6.2 Immunoblotting

Gels were transferred to nitrocellulose membrane in buffer containing 25 mM Tris HCl pH 8.3, 250 mM glycine and 20% methanol for 2 h at 400 mA. The membrane was blocked overnight at 4ºC in 5% skimmed milk, 0.1% Tween 20 in PBS.

For the detection of proteins, the membrane was incubated with primary antibodies, diluted as specified in Table 2 and 3 (refer to section 2.7, "Antibodies used for immunolabelling") in blocking buffer containing 0.2% gelatine, 0.1% Tween 20 in PBS for 1 h at room temperature. After several washes with blocking buffer, the membrane was incubated with species-specific HRP-labelled secondary antibody for 45 min at room temperature. The excess of secondary antibody was removed by 6 washes of 5

min each in PBS and detected using the enhanced chemiluminescence (ECL) method (Amersham).

2.7 Antibodies used for immunolabelling

The following tables display the antibodies used for indirect immunofluorescence (IF) and Western blotting (WB), indicating the dilutions at which they were used.

TABLE 2. Primary antibodies

Antibody name	Species	Source	Dilution
Anti β Actin (2-15)	Rabbit	P.J. Brophy	1:10000 (WB)
Anti βIII Tubulin	Mouse, monoclonal IgG_{2b}	Sigma	1:500 (WB)
Anti βIV Spectrin	Chicken, IgY	P. Soriano	1:200 (IF)
Anti βIV Spectrin	Rabbit	P.J. Brophy	1:200 (IF)
Anti Ankyrin G	Mouse, monoclonal IgG_1	Calbiochem	1:50 (IF)
Anti Ankyrin G	rabbit	V. Bennett	1:1000 (IF)
Anti APC (Ab-7)-CC1	Mouse, monoclonal IgG_{2b}	Oncogene	1:100 (IF)

TABLE 2. Primary Antibodies (CONTINUED)

Antibody name	Species	Source	Dilution
Anti Calbindin D-28K	Mouse, monoclonal IgG$_1$	Sigma	1:1000 (IF)
Anti Calbindin D-28K	Rabbit	Swant	1:5000 (IF)
Anti CASPR	Guinea pig	D.Colman	1:200 (IF)
Anti CASPR	Mouse, monoclonal IgM	M. Rasband	1:50 (IF-WB)
Anti CASPR	Rabbit	D.Colman	1:5000 (IF)
Anti Contactin	Rabbit	S. Harroch	1:200 (IF)
Anti FLAG M2	Mouse, monoclonal IgG$_1$	Sigma	1:400 (IF)
Anti-FLAG	Goat	Santa Cruz	1:100 (IF)
Anti GFAP (GA5)	Mouse, monoclonal IgG$_1$	Boehringer	1:100 (IF)
Anti L-MAG	Rabbit	P.J. Brophy	1:2000 (IF) 1:4000 (WB)
Anti MAG (972)	Mouse, monoclonal IgG$_1$	P.J. Brophy	1:400 (IF)
Anti-MBP	Chicken, IgY	Chemicon	1:25 (IF)
Anti MBP (peptide 7)	Rabbit	P.J. Brophy	1:2000 (IF) 1:5000 (WB)
Anti NFC2 (Pan Neurofascin)	Rabbit	P.J. Brophy	1:1000 (IF) 1:2000 (WB)
Anti NFF3 (Nfasc155)	Rabbit	P.J. Brophy	1:1000 (IF) 1:2000 (WB)
Anti NF-H 200kD	Mouse, monoclonal IgG$_1$	Sigma	1:200 (IF)
Anti NF-M, NF-L (R39)	Rabbit	Dahl	1:4000 (WB)
Anti NF-M RMO55	Mouse, monoclonal	V.Lee	1:500 (WB)
Anti NF-M RMO26	Mouse, monoclonal	V. Lee	1:1000 (WB)
Anti NF-M	Mouse, monoclonal IgG$_1$	Sigma	1:2000 (WB)
Anti NrCAM (1)	Rabbit	P.J. Brophy	1:200 (IF)
Anti OSP/Claudin 11	Mouse, monoclonal IgG2a	A. Gow	1:100
Anti OSP/Claudin 11	Rabbit	Zymed	1:50 (IF) 1:500 (WB)
Anti Pan Nav channels	Mouse, monoclonal IgG$_1$	Sigma	1:100
Anti PLP (107)	Rabbit	D. Colman	1:1000 (WB)

TABLE 3. Secondary antibodies

Antibody name	Species	Source	Dilution
Alexa Fluor-568-conjugated anti mouse IgG2b	Goat	Molecular Probes	1: 1000
Alexa Fluor-647-conjugated anti mouse IgG1	Goat	Molecular Probes	1:200
Alexa Fluor-647-conjugated anti rabbit IgG	Donkey	Molecular Probes	1:300
FITC-conjugated anti chicken IgY	Donkey	Jakson	1:50
FITC-conjugated anti mouse IgM	Goat	Southern Biotec	1;100
FITC-conjugated anti rabbit IgG	Goat	Cappel	1:200
FITC-conjugated anti-goat IgG	Donkey	Jackson	1:100
FITC-conjugated anti rabbit IgG	Donkey	Jackson	1:100
HRP-conjugated anti mouse IgG	Sheep	Diagnostic Scotland	1:2000
HRP-conjugated anti rabbit IgG	Donkey	Diagnostic Scotland	1:2000
TRITC-conjugated anti mouse IgG1	Goat	Southern Biotec	1:200
TRITC-conjugated anti mouse IgG2a	Goat	Jackson	1:100
TRITC-conjugated anti guinea pig IgG	Donkey	Jackson	1:150
TRITC-conjugated anti rabbit IgG	Donkey	Jackson	1:100

2.7 Morphometry and statistical analysis

2.7.1 Quantification of oligodendrocytes

To visualise oligodendrocyte cell bodies by immunofluorescence, the CC-1 antibody, also known as APC (Oncogene), was used. This antibody labels the oligodendrocyte cell body but not myelin sheaths, thus facilitating cell counting.

Five sections from each animal were selected at random and 4 non-overlapping images from each section were captured using a 10x objective lens. All CC1+ cells meeting the criteria mentioned above were counted and the area for each image outlined using Improvision OpenLab software (version 5.0). For each animal, the total number of oligodendrocytes and the area (mm^2) for each section were calculated and averaged.

An unpaired student *t*-test ($\alpha = 0.1$; two-tailed P value) was used to compare means of total number of oligodendrocytes per cross-sectional area between wild-type and *Nfasc*$^{-/-}$ mice. The test was performed using GraphPad software (on line: http://graphpad.com/quickcalcs/index.cfm) and the graph produced using Microsoft Excel (version 11.2.3). Data are expressed as means ± SEM (standard error of the mean).

2.7.2 Quantification of optic nerve axons

The number of axons in the optic nerve of 3 *Nfasc$^{-/-}$* mice and matched controls was assessed by light (LM) and transmission electron microscopy (TEM). Semithin and ultrathin sections of optic nerve immediately posterior to the rear of the orbit were cut perpendicular to the long axis and stained as previously described. To measure the area of the optic nerve, images from semithin sections were captured a low magnification (20x). The area of optic nerves was averaged by outlining the outer border three times on each of three consecutive sections from each animal (OpenLab software).

In order to estimate the total number of axons, the mean axonal density was initially calculated. Five random electron micrographs of optic nerve sections for each animal were taken at high magnification (65,000x). A counting frame of approximately 148 μm^2 on scanned images was traced and used to count axons (using OpenLab software) according to unbiased rules. Axons profiles that were not round or oval in shape and that did not contain neurofilaments were excluded from the count.

For each animal, the total number of axons was estimated by multiplying the mean axonal density by the area of the optic nerve cross section.

To evaluate the results, an unpaired student t-test (α= 0.1;two-tailed P value) was performed. Data are displayed as means ± SEM using Microsoft Excel.

2.7.3 Measurement of inter-heminodal gaps

Teased *ventral funiculi* from P6 *Nfasc$^{-/-}$* , age-matched controls and P4 wild-type mice (3 animals each) were stained using MAG and neurofilament heavy chain (NF-H; 200 kD) antibodies, as previously described. Separate images (40x) were obtained of the staining patterns in the red (TRITC) and green (FITC) channels respectively, and subsequently merged. Lengths (μm) of inter-heminodal gaps, i.e. the length of NF-H+ axons flanked by MAG+ processes of myelinating oligodendrocytes, were measured using OpenLab software. A total of 120 random, non-overlapping measurements (μm) were taken per condition and binned into 20 μm increments and a frequency distribution was calculated using Microsoft Excel.

The significance of the difference between mean values was evaluated by a one-way analysis of variance (ANOVA) followed by a Tukey HSD multi comparison test (VassarStats, on line: http://faculty.vassar.edu/lowry/VassarStats.html).

2.7.4 Quantification of nodes with Nav channel immunoreactivity

To compare the percentage of nodes displaying Na_v channel immunoreactivity between P6 wild-type, *Nfasc⁻/⁻* , *Nfasc⁻/⁻/NfascΔIC* and *Nfasc⁻/⁻/Nfasc186* (3 animals each), frozen longitudinal sections or teased fibers of the ventral columns of cervical spinal cords were triple-labelled with either Claudin 11, Caspr and Nav channel or Claudin 11, Flag and Nav antibodies, as previously described. Claudin 11 was used as an independent marker of paranodes when Caspr immunoreactivity was absent. Confocal images of 75 nodal regions per condition were taken. Immunoreactivity for Nav channel either flanked by Caspr or colocalising with Flag was scored. Means of percentage of Nav channel immunoreactivity and SEM were calculated using Excel.

3. RESULTS/DISCUSSION

3.1 CNS phenotype of Neurofascin-null mice: the nodal environ

Sherman and collaborators have shown that in the PNS of Neurofascin-null mice, nodes and paranodes fail to assemble in myelinated fibers (Sherman et al., 2005). This work follows up their investigation to determine whether the Neurofascins play a similar role in domain assembly of myelinated fibers in the CNS.

3.1.1 Nfasc$^{-/-}$ mice display severe neurological defects and die prematurely

Homozygous Neurofascin-null mice develop normally and are indistinguishable from their littermates until 4 days after birth. At postnatal day (P) 5, they appear smaller in size compared to their littermates, and by P6 they clearly show signs of malnutrition, dehydration and hindlimb paralysis. They die suddenly between P6 and P7 (Figure 18).

FIGURE 18. Phenotype of *Nfasc$^{-/-}$* mice
A Neurofascin-null mouse at P6 is shown on the left. Compared to its littermate on the right, the mutant is smaller is body size. Moreover, its hindlimbs are paralysed as indicated by their full extension on a flat surface.

The reason why Neurofascin-null mice die so prematurely is not known. It has been suggested that their sudden death coincides with the period when the transition to saltatory conduction is occurring in myelinated tracts of the CNS and PNS (Sherman et al., 2005). Since, in the mouse, myelination starts in the first week of life and proceeds caudo-rostrally in the brain and rostro-caudally in the spinal cord (Foran and Peterson, 1992), one can speculate that the inability of myelinated fibers in the brain stem to efficiently conduct nerve impulse may interfere with vital functions, such as feeding and breathing. Alternatively, since it has been proposed that the neuronal isoform Nfasc186, may be involved in axon growth, guidance and migration in embryonic development (Rathjen et al., 1987), structural defects in CNS cytoarchitecture and axon pathfinding may account for lethality.

To examine the cause of death, an autopsy was performed on Neurofascin-null pups by Dr. David Brownstein at the Research Animal Pathology Core Facility, Queen's Medical Research Institute in Edinburgh. At P6, the brain and spinal cord of Neurofascin-null mice appeared grossly normal, although reduced in size in accordance with an overall reduced body size compared to littermates. Severe depletion of lipid stores, milk absent from stomach and small intestine, fatty atrophic liver and dehydration were findings consistent with malnutrition as a possible cause of death, as well as failure to nurse as the proximate cause.

In support of these findings, when littermates were removed from the cage to give Neurofascin-null pups an increased opportunity to feed, they still failed to nurse, suggesting that it was their inability to suck rather than their hindlimb paralysis or maternal care the cause of death. Interestingly, Dr Brownstein found stool in the distal colon and rectum of Neurofascin-null mice indicating previous nursing, consistent with the observation of normal development earlier on. No forced feeding was attempted to determine whether these mice could survive longer. At all ages, heterozygous appeared normal.

3.1.2 The Neurofascins are required for assembly of nodes and paranodes in myelinated fibers of the CNS

To test the role of the Neurofascins in the assembly of functional domains along myelinated fibers of the CNS, whole litters were obtained at P6 and the identity of Neurofascin-null mice was subsequently confirmed by genotyping. For all analyses, cervical spinal cords were harvested since a survey by immunostaining revealed that myelination was more advanced in this tissue at this early stage in development. Moreover, the ventral funiculi or columns, i.e. ascending and descending fiber tracts in the ventral spinal cord, contain large axons (Arroyo et al., 2002) and thus facilitated teased fiber preparation.

Immunofluorescence revealed that Caspr, Contactin and Ankyrin G, which is transiently expressed at CNS paranodes in the first week of the murine postnatal life (Jenkins and Bennett, 2002), were no longer localised to paranodes in the *Nfasc$^{-/-}$* mouse. Similarly, in the absence of Neurofascins, nodal components including Nav channels, Contactin, βIV Spectrin and Ankyrin G were not clustered (Figure 19A).

The antibody Claudin 11, also known as Oligodendrocyte Specific Protein (OSP), was used as an independent marker for paranodes. Claudin 11 is a transmembrane protein and the third most abundant protein in CNS myelin, after myelin basic protein (MBP) and Proteolipid protein (PLP); it belongs to the Claudin family of tight junction proteins (Bronstein et al., 1996; Gow et al., 1999). Since Claudin 11 has been found to accumulate at paranodes (Gow et al., 1999), the antibody was particularly useful to identify paranodes in the absence of other nodal and paranodal markers. Nevertheless, it is important to note that symmetrically Claudin 11-labelled paranodes were much more difficult to detect in the mutant mouse than in the wild-type control. This observation was subsequently addressed by analysis of the difference in the amount of myelin proteins between wild-type and mutants (see section 3.1.4).

In wild-type nerves, 100% of all nodal gaps of less than 5 μm in length had Nav channels. Interestingly, a small percentage of nodes in mutant nerves (16% ± 6.1%, mean ± SEM, 75 measurements per animal, n=3) also displayed immunoreactivity to Nav channel antibody (see Figure 32C). This observation suggests that Nav channels can still be targeted to the node but that either their delivery is inefficient or their stability is affected. Moreover, both focal and elongated clusters immunoreactive to

Ankyrin G, βIV Spectrin and Nav channels were occasionally noted, though they were not flanked by Claudin-11 positive paranodes, suggesting that their location along the nerve was probably ectopic (data not shown).

The amount of Caspr in cervical spinal cord lysates was assessed by immunoblotting and was found to be equivalent between wild-type and mutant mice (Figure 19B), suggesting that this protein is still produced but remains diffusely distributed along the fiber. A similar assessment of the amount of the other major paranodal component, Contactin, was not performed since it is also present at central nodes and in oligodendrocytes (Koch et al., 1997). Similarly, the amount of the nodal components Nav channels, Ankyrin G and βIV Spectrin could not be assessed since the same molecules are present at AIS, and therefore could potentially confound the results. Nevertheless, one can assume that since immunoreactivity to nodal components was still observed, the proteins were still produced but, similarly to what happens in the PNS (Sherman et al., 2005), failed to localise.

Thus, the disruption of the paranodal and nodal proteins observed in the PNS (Sherman et al., 2005) was also observable in the CNS. Moreover, the disruption of paranodes, as evidenced by the absence of Caspr and Contactin, was further analysed at the electron microscopy level. In longitudinal sections of ventral funiculi of the cervical spinal cord, septate-like junctions are no longer present in mutant paranodes, and there is a larger gap clearly visible between the base of the paranodal loops and the axolemma in the mutant mice compared to wild-type (Figure 19C).

Therefore, in the absence of Nfasc155, axoglial junctions do not form and this phenotype is similar to that found in *Caspr* and *Contactin* mutants (Bhat et al., 2001; Boyle et al., 2001; Rios et al., 2003). In these mutants, Nfasc155 could still be detected at paranodes, suggesting that a *trans* interaction with the Caspr-Contactin complex is not required for targeting Nfasc155. Conversely, in the absence of Nfasc155, both Caspr and Contactin fail to cluster at paranodes, suggesting that axoglial junction formation requires a tripartite complex forming between Caspr-Contactin on the axolemma and Nfasc155 on the glial paranodal loops. It is possible that, since association of Caspr and Contactin in *cis* is necessary for their mutual delivery to the axonal membrane (Faivre-Sarrailh et al., 2000; Peles et al., 1997), their binding to Nfasc155 might be required for their targeting to the paranodes.

Furthermore, in *Caspr* and *Contactin* mutants, *Shaker*-like Kv channels, which are normally found at juxtaparanodes, were still enriched on both sides of the node, but they were abnormally located at paranodes, directly in contact with nodal Nav channels (Bhat et al., 2001; Boyle et al., 2001). Mislocalisation of Kv channels could not be assessed in the *Nfasc* mutant, since at P6 these proteins are not clustered yet (data not shown), which confirms previous reports showing that clustering of juxtaparanodal components correlate with late stages in myelination (Baba et al., 1999; Poliak et al., 1999; Poliak et al., 2001; Rasband and Shrager, 2000; Rasband et al., 1999b; Vabnick et al., 1996).
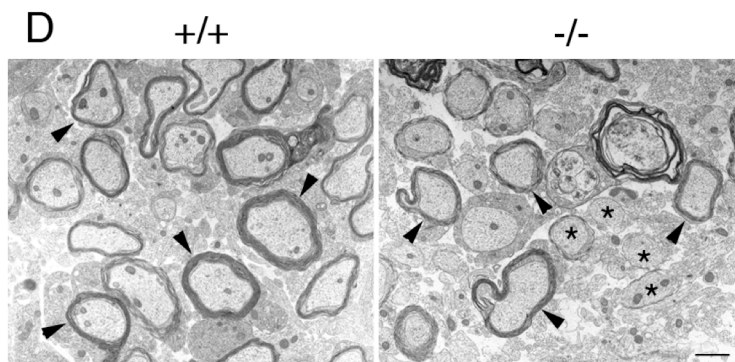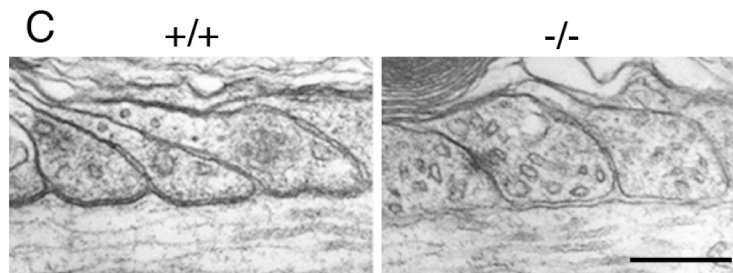
FIGURE 19 (Overleaf). Disruption of CNS Paranodes and Nodes in *Nfasc*^{-/-} Mice.

A) Immunofluorescence analysis of teased ventral funiculi of the cervical spinal cord from wild-type and Neurofascin-null animals at P6 shows that, in the absence of the Neurofascins, Caspr, Contactin and the transient localisation of Ankyrin G are no longer detected at paranodes. In addition, the nodal components Nav channels (Nav), Contactin, ßIV-Spectrin (βIV-Spec) and Ankyrin G are absent. Of note is that the Contactin antibody strongly stains nodes of Ranvier and to a lesser extent paranodes in the wild-type, possibly due to the penetration of this particular antibody. Immunostaining using a pan-Neurofascin (Pan-Nfasc) antibody shows that Nfasc186 at the node and Nfasc155 at the paranode are present in wild-type but absent in the mutant. Claudin 11 was used to localise the paranodes of CNS myelin. Scale bar, 5 μm. See separate channels in supplementary Figure S1, Section 6.

B) Western blot analysis of cervical spinal cord lysates from 6-d old wild-type and Neurofascin-null mice shows that, when loadings are normalised against the 160 kD neurofilament isoform (NF-M), the total amount of the paranodal component Caspr is similar in wild-type and mutant mice.

C) Electron microscopy of the paranodes in ventral funiculi of wild-type and mutant mice shows that, in Neurofascin-null mice, electron dense transverse bands are no longer present, leaving a gap between the base of the paranodal loops and the axolemma. Scale bar, 0.2 μm.

D) Electron microscopy of transverse sections from cervical spinal cord of wild-type and mutant mice shows that axons are ensheathed in both animals (arrowheads). At this early stage, myelin appears loose and uncompacted. Nevertheless, unmyelinated profiles (asterisks) were more often observed in the mutant compared to wild-type. Scale bar, 1 μm.

A

Nfasc$^{+/+}$ Nfasc$^{-/-}$

Claudin 11
Pan Nfasc

Claudin 11
Caspr
Nav

Claudin 11
Contactin

Claudin 11
βIV Spectrin

Claudin 11
Ankyrin G

B

+/+   -/-

Caspr

NF-M

C   +/+   -/-

D   +/+   -/-
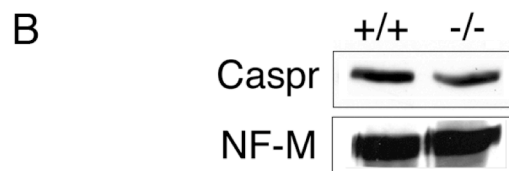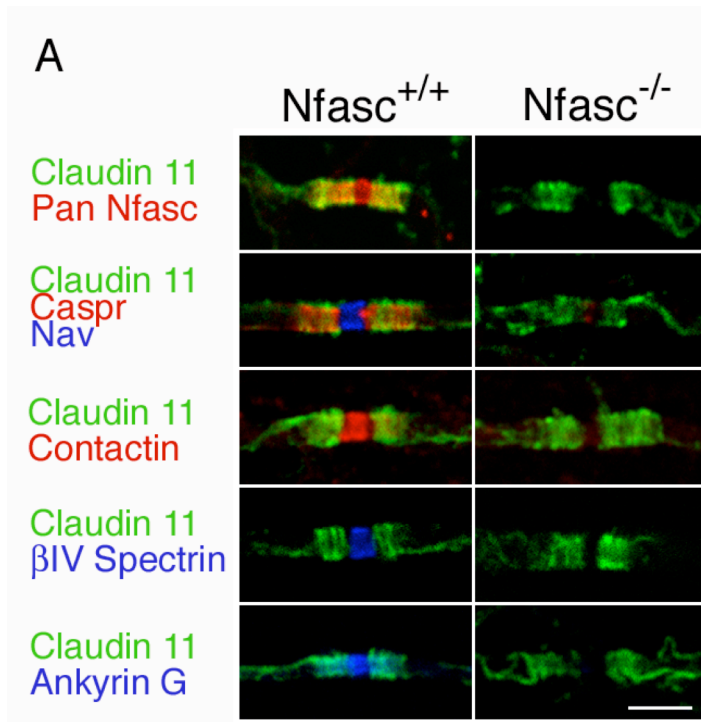
3.1.3 NrCAM is not found at central nodes

As mentioned previously, in the PNS, NrCAM is among the first molecules detected at peripheral nodes of Ranvier early in development (Lambert et al., 1997; Sherman et al., 2005) and is among those molecules that are disrupted at peripheral nodes in the Neurofascin-null mouse (Sherman et al., 2005). Given the similar molecular composition of peripheral and central nodes, there was no apparent reason to believe that NrCAM could not be equally disrupted in CNS nodes of the Neurofascin-null mouse.

Although much evidence is found relatively to the presence of NrCAM at nodes in the PNS (Custer et al., 2003) and AIS in the CNS (Jenkins and Bennett, 2001), its presence at CNS nodes has always been inferred from those studies. Indeed, in the course of analysis of domain assembly in wild-type myelinated fibers, NrCAM was never detected at CNS nodes by immunofluorescence both early in development and in the adult, as shown in Figure 20.
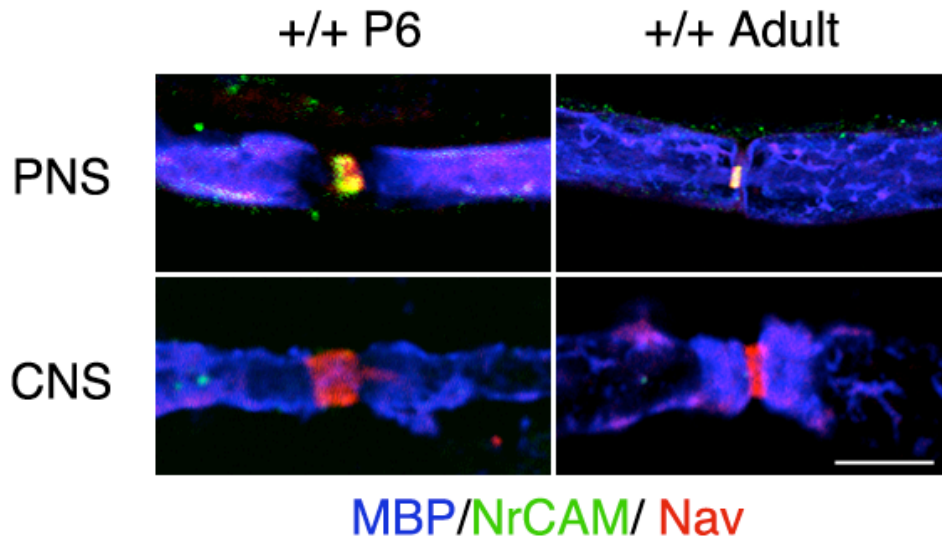
FIGURE 20. NrCAM is Not Found at Central Nodes.
Teased sciatic nerves (PNS) and ventral funiculi of cervical spinal cord from wild-type mice at postnatal day 6 (P6) and at 3 months of age were immunolabelled with MBP, NrCAM and Nav channels. NrCAM colocalises with Nav channels at nodes of myelinated peripheral nerves, whereas it is not present in central nodes. Scale bar, 5 μm.

NrCAM at peripheral nodes has been shown to be dispensable, since in its absence nodes still assemble, although with a slight delay (Custer et al., 2003). However, in the absence of Nfasc186, NrCAM is not targeted at peripheral nodes, suggesting that Nfasc186 is required for targeting NrCAM at these sites (Sherman et al., 2005).

The reason why central nodes do not have NrCAM is currently unknown. One can only speculate that, given their structural similarity, in the course of evolution, Nfasc186 might have taken over a possible redundant function performed by NrCAM.

A new and updated diagram of the molecular composition of nodes of Ranvier in the CNS is shown in Figure 21.
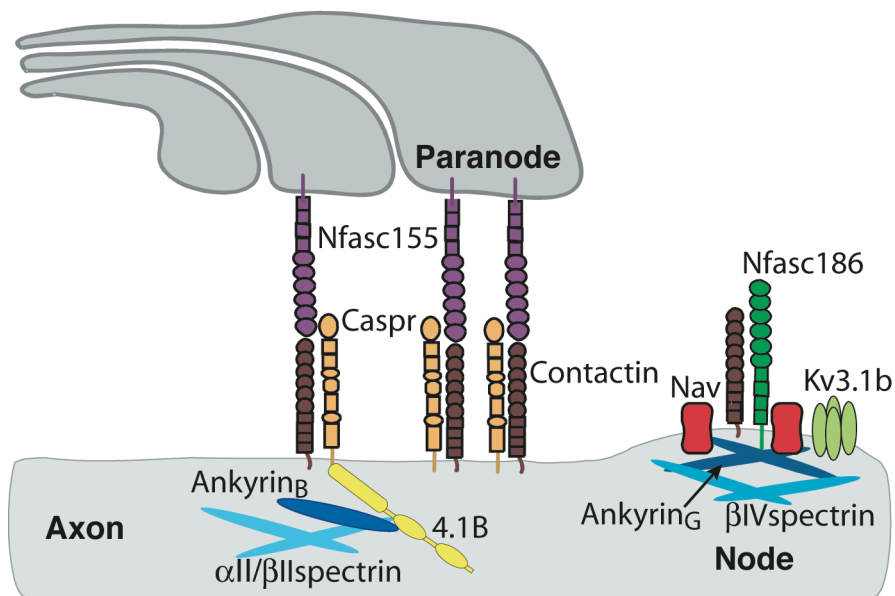
FIGURE 21. The Molecular Composition of Nodes and Paranodes in the CNS.

3.1.4 Myelination is reduced in the Neurofascin-null mice

Sherman and collaborators showed that, in peripheral nerves of Neurofascin-null mice, the amount of myelin appeared to be equivalent to that of wild-type as judged by Western blotting for the major myelin protein P0. Moreover, light microscopy revealed that the myelin sheath was normal in both animals (Sherman et al., 2005).

To determine whether the same observation applies to the CNS, transverse sections of ventral funiculi in cervical spinal cords from P6 *Nfasc*$^{-/-}$ mice and wild-type littermates were analysed by electron microscopy. The latter revealed that, at this early stage in development, both myelinated and unmyelinated axons were present in both animals, but possibly with an increased incidence of unmyelinated profiles in the mutant (Figure 19D).

The total amount of myelin proteins was further assessed by Western blotting, which revealed that Myelin Basic Protein (MBP), MAG, Proteolipid Protein (PLP) and Claudin 11 were all significantly reduced in Nfasc mutant spinal cord compared to wild-type control, when both were normalised against βIII Tubulin, a neuronal marker (Figure 22 and Figure 25).

FIGURE 22. Myelin Proteins Are Reduced in the *Neurofascin* Mutant

Western blot analysis of cervical spinal cord lysates from P6 wild type and *Nfasc*$^{-/-}$ mice shows that there is a dramatic reduction in the amount of myelin proteins in the mutant compared to control. ßIII Tubulin was used as a loading control (MAG: myelin associated glycoprotein; PLP: proteolipid protein).

These findings were clearly in contrast to those found in the PNS. Further, the reduction in myelin raised the question of whether axonal neurofilament phosphorylation could also be affected, since myelination regulates axon calibre which in turn depends on neurofilament phosphorylation (de Waegh et al., 1992).

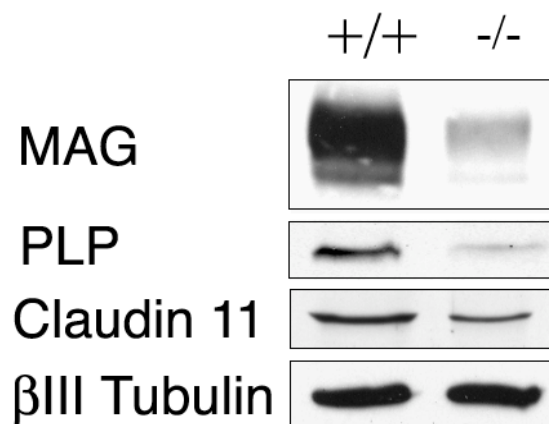Western blotting of cervical spinal cord lysates from wild-type and Neurofascin-null mice was performed using an antibody that recognizes a phosphorylation-dependent NF-M epitope (RMO55/P++) and an antibody recognising a phosphorylation-independent epitope in the NF-M core (RMO26/P-ind) (Black and Lee, 1988). The latter was used to standardize the relative amount of neuronal protein. The results revealed that the overall phosphorylation of neurofilaments was not affected in the mutant compared to wild-type (Figure 23). It also suggested that the fibers in the mutant were all at least partially ensheathed.
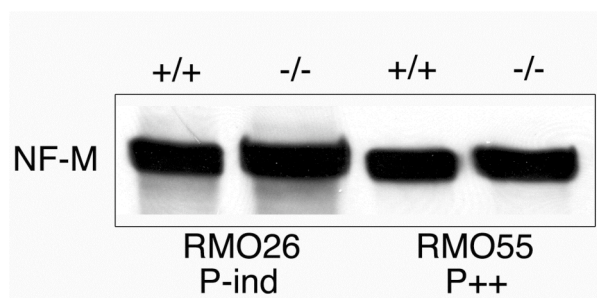
FIGURE 23. Neurofilament Phosphorylation Is Unaffected in the *Neurofascin* Mutant
Western blot analysis of cervical spinal cords homogenates from 6-d old wild-type (+/+) and Neurofascin-null (-/-) animals shows that the level of neurofilament phosphorylation, as judged by immunoreactivity to RMO55, is equivalent in both conditions, when the total amount of neuronal protein is standardised against RMO26.

To account for the reduction of CNS myelin in the Neurofascin-null mice, two possibilities were explored: 1) Neurofascin-null mice have a reduced number of axons and therefore a reduced number of myelinated fibers; 2) oligodendrocytes are fewer in number and consequently myelinated fibers are reduced.

To investigate whether the absence of Nfasc186 might affect axon number in the CNS, axon counting was performed on transverse sections of optic nerves from wild-

type and mutants. This tissue was chosen because it is a whole nerve and axons runs parallel to the longitudinal axis, therefore facilitating quantification in transverse sections (Figure 24a). Using a combination of light and electron microscopy, estimates of the total number of axons per area of the optic nerve cross sections were obtained (see Chapter 2, Materials and Methods for details) and were found not to be significantly different between wild-type and mutant animals, suggesting that axonal loss could not account for the reduced amount of myelin (Figure 24c).

To investigate whether absence of Nfasc155 could affect oligodendrocyte number and subsequently the amount of myelin, oligodendrocyte cell bodies were immunolabelled with the CC1 antibody (Figure 24b) and counted in transverse sections of cervical spinal cord from wild-type and mutants. Oligodendrocyte number per cross sectional area did not differ between wild type and Neurofascin-null mice (Figure 24d).

Thus, in the CNS of Neurofascin-null mice an overall reduction in myelin does not affect the level of neurofilament phosphorylation along nerve fibers and cannot be explained by either axon loss or reduced amount of oligodendrocytes.

FIGURE 24 (Overleaf). Quantification of Axon and Oligodendrocyte Number in the *Neurofascin* Mutant

a) Electron microscopy of transverse sections of optic nerve from 6-d old wild-type and *Nfasc*$^{-/-}$ mice showing unmyelinated axon profiles that are round or oval in shape. In both images, oligodendrocyte processes extending from the cell soma (asterisks) are also clearly visible. Scale bar, 1 μm. **b)** Transverse sections of cervical spinal cord from 6-d old wild-type and *Nfasc*$^{-/-}$ mice were immunolabelled with the CC-1 antibody, a marker of oligodendrocyte cell bodies. Images of the area surrounding the ventral midline of the spinal cord show that CC1-positive oligodendrocytes are found to be highly concentrated in the medial longitudinal and ventral funiculi. However, they are also sparsely present in the gray matter. Scale bar, 100 μm. **c)** Quantification of the total number of axons in cross sections of optic nerves shows that there is no significant difference in axon number between 6-d old wild-type (72,710 ± 11,398) and mutant animals (65,066 ± 3,541) (means ± SEM, *p*, not significant; unpaired *t*-test, two-tailed; minimum 5 ROI, 3 animals per condition). **d)** Quantification of the total number of oligodendrocytes in cross sections of cervical spinal cords shows that oligodendrocyte number is not significantly different between 6-d old wild-type (201 ± 5) and *Neurofascin-null* mice (213 ± 9)(means ± SEM, *p*, not significant, unpaired student *t*-test, two-tailed; minimum 5 spinal cord sections, 3 animals per condition)

a) Optic nerve +/+ -/-

b) Spinal cord +/+ -/-
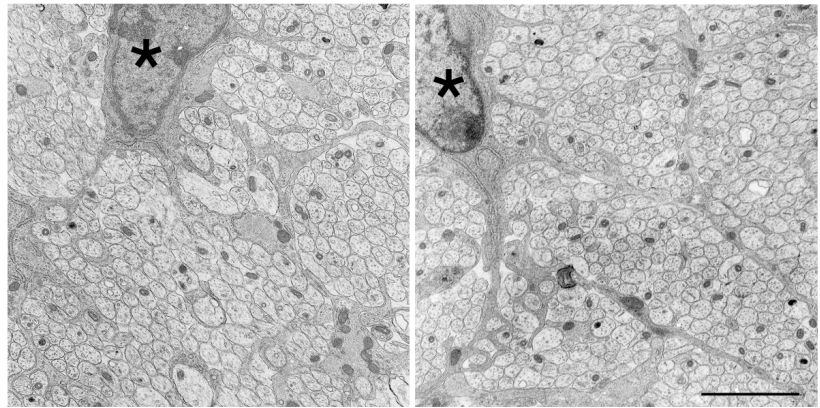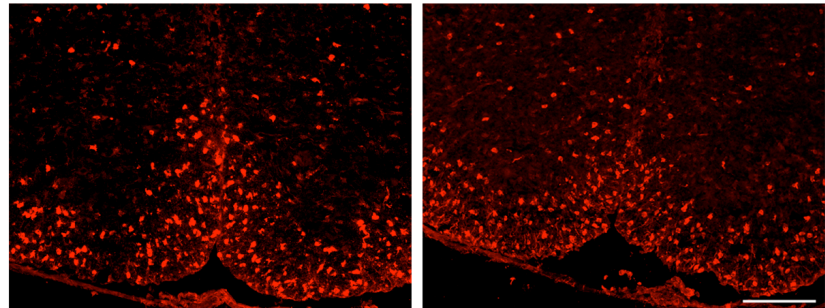
CC-1

c)
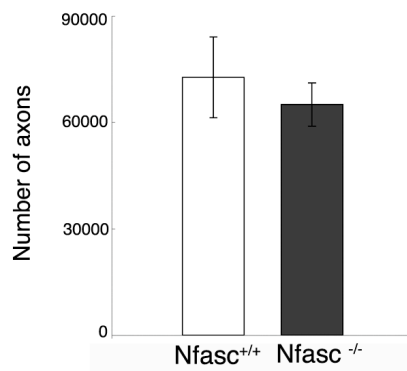
d)
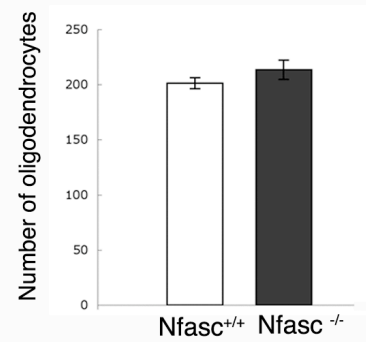
Hence, to account for the reduction in myelin proteins, a third possibility was considered, namely, that although myelination was occurring in mutant nerves (Figure 19D), ensheathment of axons was less extensive in the mutant compared to wild-type.

3.1.5 Inter-heminodal gaps are increased in the *Nfasc* mutant mice

The preparation of teased ventral funiculi facilitated a comparison of the myelination state of single fibers from P6 wild-type and Neurofascin-null mice. When immunolabelled with MAG and the 200 kD-Neurofilament heavy chain (NF-H) antibodies, it became obvious that in the mutant a greater proportion of NF-positive axons had segments that were devoid of myelin. In addition, although oligodendrocytes could migrate along axons, as judged by MAG immunoreactivity, the distance between converging processes (i.e. inter-heminodal gap) was increased in the mutant compared to the wild-type. This observation raised the possibility that mutant oligodendrocyte processes had a reduced ability to extend along axons and since, in the Neurofascin-null mouse, adjacent symmetrical Claudin 11-positive zones were still detected, suggestive of paranode formation, the incidence of unmyelinated segments could have represented a delay in development.

To support this hypothesis, preliminary developmental analysis was performed by Western blotting to compare the amount of myelin protein in cervical spinal cord homogenates from wild-type at earlier ages, at P6 and from *Nfasc* mutants (Figure 25).

The result shows that the amount of MBP is greatly reduced in the wild-type at P4 compared to P6, but it is similar between wild-type at P4 and the *Nfasc* mutant. This finding prompted a direct qualitative and quantitative comparison between the three conditions.
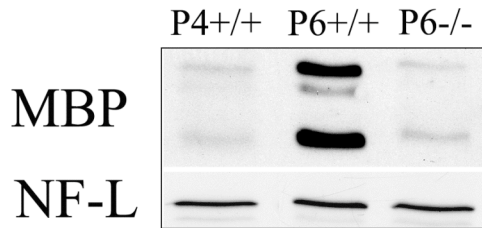
FIGURE 25. The Amount of Myelin Basic Protein in the *Neurofascin* Mutant Is Similar to that Found at an Earlier Stage in Wild-type Development
Western blotting of the relative amount of Myelin Basic Protein (MBP) in cervical spinal cord homogenates from 4-d old, 6-d old wild-type and *Nfasc*$^{-/-}$ animals shows a similar significantly reduced amount of MBP in wild-type at P4 and Nfasc$^{-/-}$ mice compared to wild-type at P6. The total amount of neuronal protein was normalised against the 68 kD neurofilament-light chain (NF-L),

Teased ventral funiculi of cervical spinal cords were triple-labelled with Caspr, NF-H and MAG, and analysed by immunofluorescence. Qualitatively, the incidence of inter-heminodal gaps appeared reduced in the wild-type at P6 compared to wild-type at P4 and to the Neurofascin-null mice. Moreover, in the wild-type at P4, the tips of myelinating processes were strongly stained for Caspr and Nfasc155, even when these converging processes were > 14 µm apart (Figure 26A), indicating that both proteins are colocalised at the edges of advancing myelinating processes.

To quantify these differences, the length of inter-heminodal gaps was obtained by measuring the distance between the tips of MAG-positive converging processes along axons immunolabelled with NF-H. The inter-heminodal gaps were similarly increased, both in frequency and in length, in the *Nfasc* mutant and wild-type at P4, compared to wild-type at P6, suggesting that the migration of converging processes was delayed in the mutant compared to wild-type of the same age, but was similar to that achieved at P4 (Figure 26B).

The number of nodes that were less than 5 µm in length was also calculated and represented 76% of the total in wild-type compared to 17% in the Neurofascin-null mouse (data not shown), which further illustrates the relative inefficiency of migration of oligodendrocyte processes in the mutant. However, as already described, this inefficiency could not be due to a reduced amount of oligodendrocytes in the mutant spinal cord.

The mean inter-heminodal gap was calculated and there was no significant difference between wild-type fibers at P4 compared to mutant fibers at P6. Nonetheless, the mean inter-heminodal gap in both was significantly larger than in wild-type nerves at P6 (Figure 26C).

Thus, these results suggest that inter-heminodal gaps represent a normal feature of early stages in myelination. Oligodendrocytes wrap axons and extend their processes longitudinally until the ends of the internodes abut a node of Ranvier. Instances of short (<5 μm) gaps, indicative of early node formation, were found at P4 in the wild-type spinal cord, but were less numerous than at P6. Similarly, larger gaps were found in both conditions. At the leading edges of wild-type myelinating processes, focal clusters of Caspr were also observed.

Caspr immunoreactivity had already been observed at the edges of MAG-labelled processes in the rat optic nerve as early as P7, and when two zones of Caspr were seen in close proximity, focal Nav channel immunoreactivity was invariably found in the gap between them (Rasband and Shrager, 2000). However, this study shows that axonal Caspr also always co-localised with glial Nfasc155 as early as P4.

In accordance with its role in promoting cell-cell adhesion (Koticha et al., 2005) and based on previous studies showing that soluble Nfasc155 can inhibit myelination in myelinating co-cultures (Charles et al., 2002), one can speculate that Nfasc155 might facilitate the advancing of the leading myelinating processes by signalling oligodendrocytes to extend longitudinally. Furthermore, the fact that Nfasc155 and Caspr were both found to be concentrated at the tips of oligodendrocyte processes and that in the absence of Nfasc155 (and Nfasc186) process extension was retarded, strongly supports the view that the axoglial adhesion complex might be required for the efficient migration of the myelinating processes.

Therefore, in the absence of Nfasc155 (and Nfasc186), an increased incidence of unmyelinated segments is indicative of a delay in myelination comparable to that observed at an earlier stage of development in wild-type CNS.
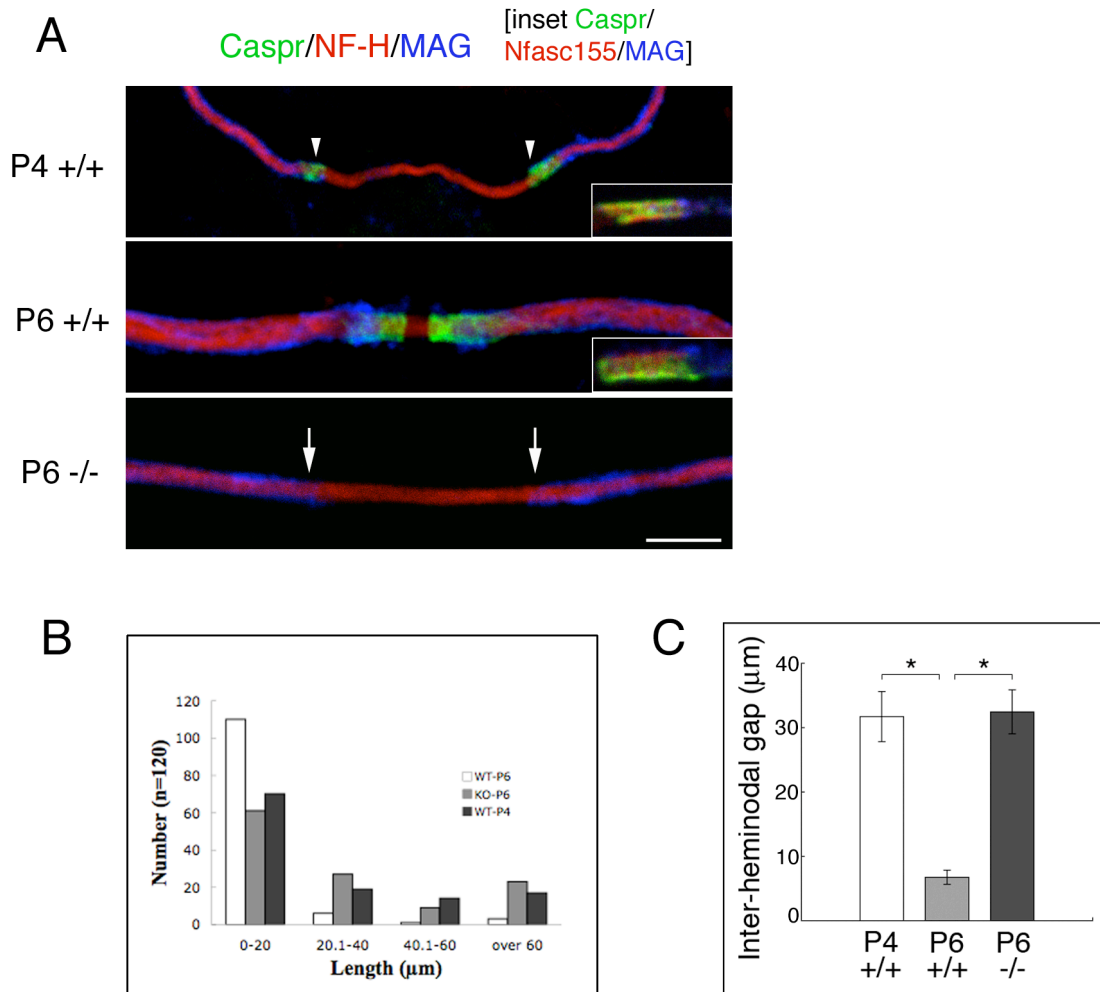
FIGURE 26. Inter-heminodal Gaps Are Increased in the Absence of the Neurofascins

A) Teased ventral funiculi of cervical spinal cord were immunostained for the myelin protein MAG, the axonal marker NF-H, Caspr and Nfasc155. Immunofluorescence analysis shows that Caspr is concentrated at the tips of oligodendrocyte processes (inverted arrows) and that the latter converge from P4 to P6 during wild-type development. The inset figures show co-localization of the Caspr/Nfasc155 adhesion complex at the process extremities. In the absence of the Neurofascins, Caspr is no longer detected at the tips of migrating processes. Scale bar, 10 μm.

B) Inter-heminodal lengths (μm) were quantified in wild-type at P4, P6 and in the *Nfasc* mutant. The total number of measurements for each condition (minimum 3 animals each) was binned into 20 μm increments and the data graphed. A greater percentage (91%) of inter-heminodal gaps at P6 were within 20 μm in length compared to *Nfasc* mutant (51%) and wild-type at P4 (58%). However, the frequency of increasingly longer inter-heminodal gaps was comparatively similar between wild-type at P4 and *Nfasc* mutant, but greater than that of wild-type at P6.

C) The mean inter-heminodal length was also found to be significantly different between wild-type at P6 (6.8 ± 1.1 μm) versus *Neurofascin-null* (32.5 ± 3.4 μm,) and wild-type at P4 (31.7 ± 3.9 μm) (means ± SEM; one-way ANOVA, $p < 0.0001$, minimum 40 measurements per mouse, 3 animals per condition).

SUMMARY SECTION 3.1

In this section, results on the analysis of the phenotype of Neurofascin-null mice in myelinated fibers of the CNS have been presented. Similarly to what has been previously observed in the PNS (Sherman et al., 2005), nodal and paranodal components are mislocalised and axoglial junctions do not form in the absence of the Neurofascins.

In contrast to the PNS, where ensheathment of axons is unaffected, the amount of myelin proteins in the CNS is greatly reduced in the mutant. This can be explained by the reduced ability of oligodendrocyte myelinating processes to extend along axons and the consequent increased incidence of unmyelinated segments comparable to earlier stages of development in wild-type CNS.

Co-localisation of Caspr on the axon and its glial partner Nfasc155 at the tips of wild-type myelinating processes, together with the increased inter-heminodal gaps observed in the mutant processes, suggest that the axoglial adhesion complex (Caspr-Nfasc155) might promote the migration of the myelinating processes along the axon.

3.2 CNS phenotype of *Neurofascin-null* mice: axon initial segments

As mentioned in the "Introduction" section, nodes of Ranvier and axon initial segments (AIS) share common functional and molecular characteristics. However, they do assemble by different mechanisms. Extrinsic signals from glial cells drive assembly of nodes whereas AIS are intrinsically specified (Hedstrom and Rasband, 2006). In the CNS, Ankyrin G has been observed to accumulate at nodes and AIS before other molecular components (Jenkins and Bennett, 2001, 2002) and its importance for AIS formation has been directly demonstrated by the analysis of a mutant mouse lacking Ankyrin G at Purkinje cells (PC) initial segments (Zhou et al., 1998). In these mice, Nav channels, Nfasc186 and βIV Spectrin fail to cluster at AIS (Jenkins and Bennett, 2001), suggesting that Ankyrin G is a protein central to either formation and/or maintenance of the AIS.

Consistent with this idea, Ankyrin G is required to link Nav and KCNQ channels to the underlying cytoskeleton through a common targeting motif (Garrido et al., 2003b; Lemaillet et al., 2003; Pan et al., 2006). The localisation of Nfasc186 and NrCAM has also been shown to depend on the interaction with Ankyrin G, since mutation of a single tyrosine in their common Ankyrin G-binding domain abrogates their ability to localise to the AIS (Zhang et al., 1998).

The functional importance of these two CAMs at AIS has not been addressed directly. One report suggests that Nfasc186 functions as a guidance molecule to target basket cells GABAergic synapses to the AIS of cerebellar Purkinje neurons, thus controlling their excitability (Ango et al., 2004). However, its localisation appears to be dispensable for AIS formation, since shRNA treatment of NFasc186 does not inhibit Ankyrin G and Nav channel accumulation at the AIS of hippocampal neurons (Dzhashiashvili et al., 2007).

To directly test the role of Nfasc186 and NrCAM in AIS domain assembly, Purkinje cells of the cerebellum from wild-type, Neurofascin-null and NrCAM-null mice at P6 were double-labelled with Calbindin (a calcium-binding protein strongly staining PC soma, proximal dentrites and initial segments) and antibodies against Nav channels, βIV Spectrin, Ankyrin G and NrCAM. Immunofluorescence results show that, in the

absence of Nfasc186, AIS components still assemble at AIS with the exception of NrCAM (Figure 27).
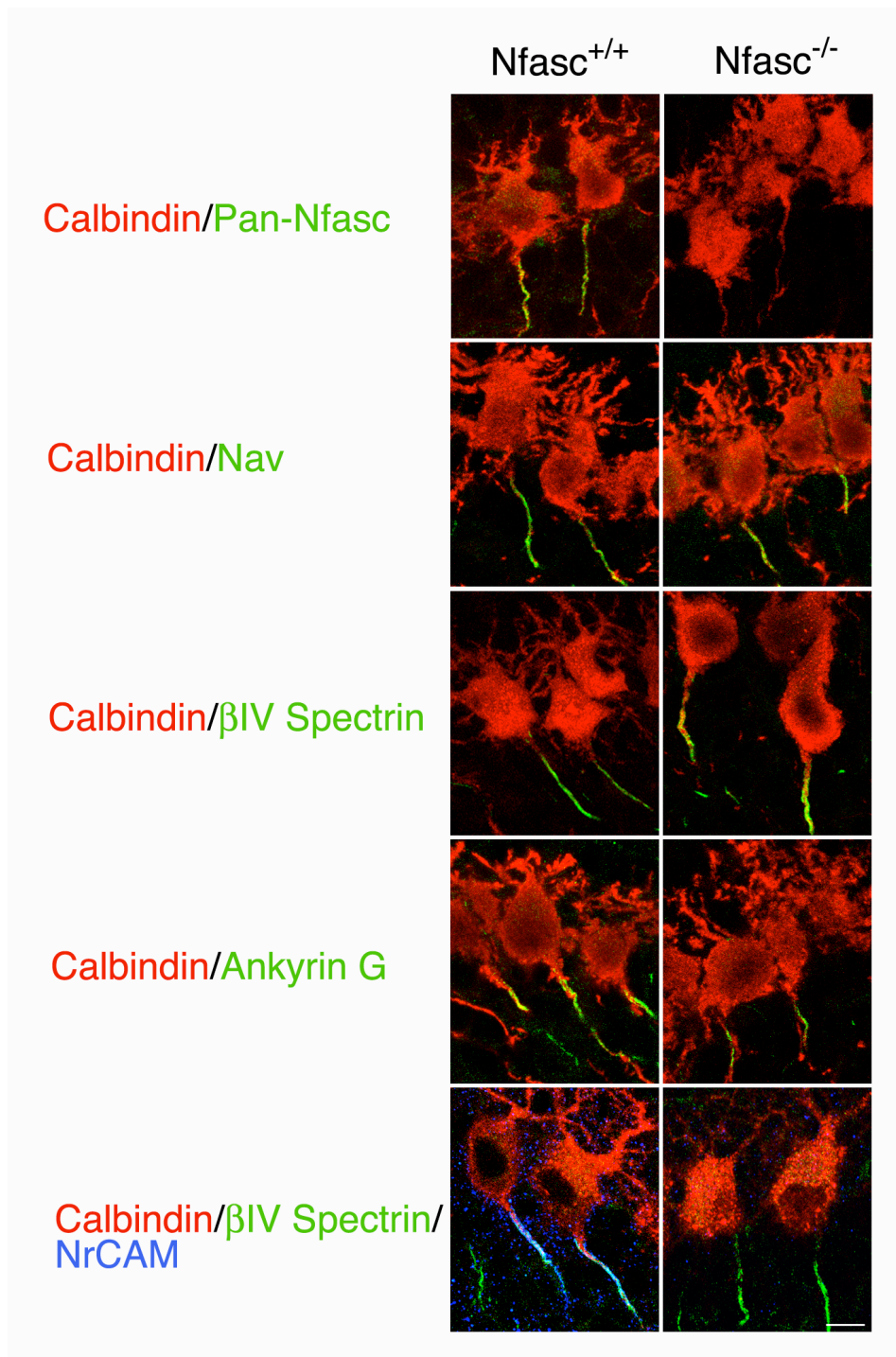
FIGURE 27.Nfasc186 is Not Required for Assembly of Proteins at AIS

Immunofluorescence images of Calbindin-positive Purkinje cells in sagittal sections of cerebella from P6 *Nfasc*^{-/-} and wild-type littermates show no qualitative difference between wild-type and *Nfasc* mutants in the expression of Nav channels (Nav), βIV Spectrin and Ankyrin G at AIS. However, NrCAM is no longer localised at AIS in the mutant, which were labelled with the anti βIV Spectrin antibody . Immunostaining with a pan Neurofascin antibody also shows that Nfasc186 is present in wild-type AIS but is absent in the mutant. Scale bar, 10 μm.

However, in the absence of NrCAM, Nfasc186 and other components do assemble normally (Figure 28), indicating that NrCAM requires Nfasc186 for its delivery to AIS whereas the reverse is not true.
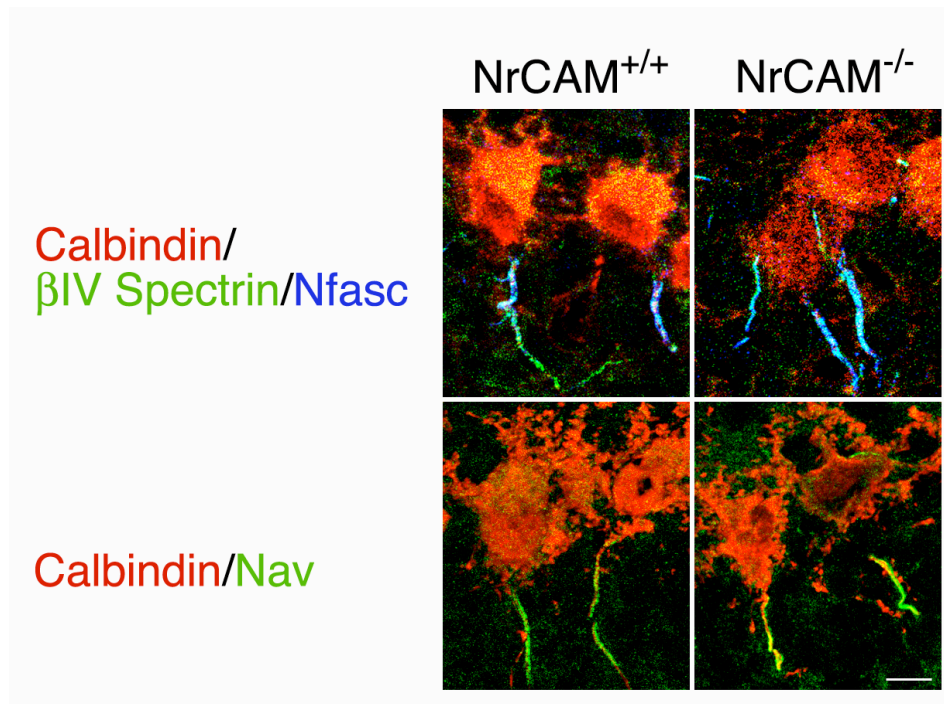
FIGURE 28. NrCAM is Not Required for Assembly of Proteins at AIS
Immunofluorescence of Calbindin-positive Purkinje cells in sagittal sections of cerebella from P6 wild-type and *NrCAM*^{-/-} mice shows no qualitative difference between wild-type and NrCAM mutants in the expression of Neurofascin (Nfasc), βIV Spectrin and Nav channels at AIS. Scale bar, 10 μm. See separate channels in supplementary Figure S2, Section 6.

Thus, NrCAM is dispensable for peripheral node (Custer et al., 2003) and central node assembly, whereas Nfasc186 is required to organise both peripheral (Sherman et al., 2005) and central nodes. However, neither NrCAM nor Nfasc186 are required to direct assembly of components at the AIS.

Since Nfasc186 can clearly compensate for the loss of NrCAM, then, what is the role of Nfasc186 at AIS? Since Neurofascin-null mice die at P7, to investigate whether, by virtue of its ability to bind Ankyrin G, Nfasc186 might be required for the maintenance of the multimolecular complex assembled at AIS, organotypic cerebellar cultures were

prepared from newborn mice that were subsequently identified as wild-type or Neurofascin-null by genotyping.

Slices of cerebella prepared from young rodents can be maintained in culture for a few weeks. Under optimal conditions (i.e. culture medium, stable substratum, sufficient oxygenation and incubation at a temperature of about 37ºC), nerve cells continue to develop organising the tissue in a fashion that closely resembles that observed *in situ* (Gahwiler et al., 1997).

In culture, the earliest time point at which all molecular components assembled at AIS of wild-type PC was after 9 days *in vitro*. The mutant PCs also displayed immunoreactivity for Nav, βIV Spectrin and Ankyrin G, with the exception of NrCAM (not shown), thus recapitulating what was observed at P6 *in vivo*. However, after 15 DIV, the AIS components were lost from the mutant AIS (Figure 29).
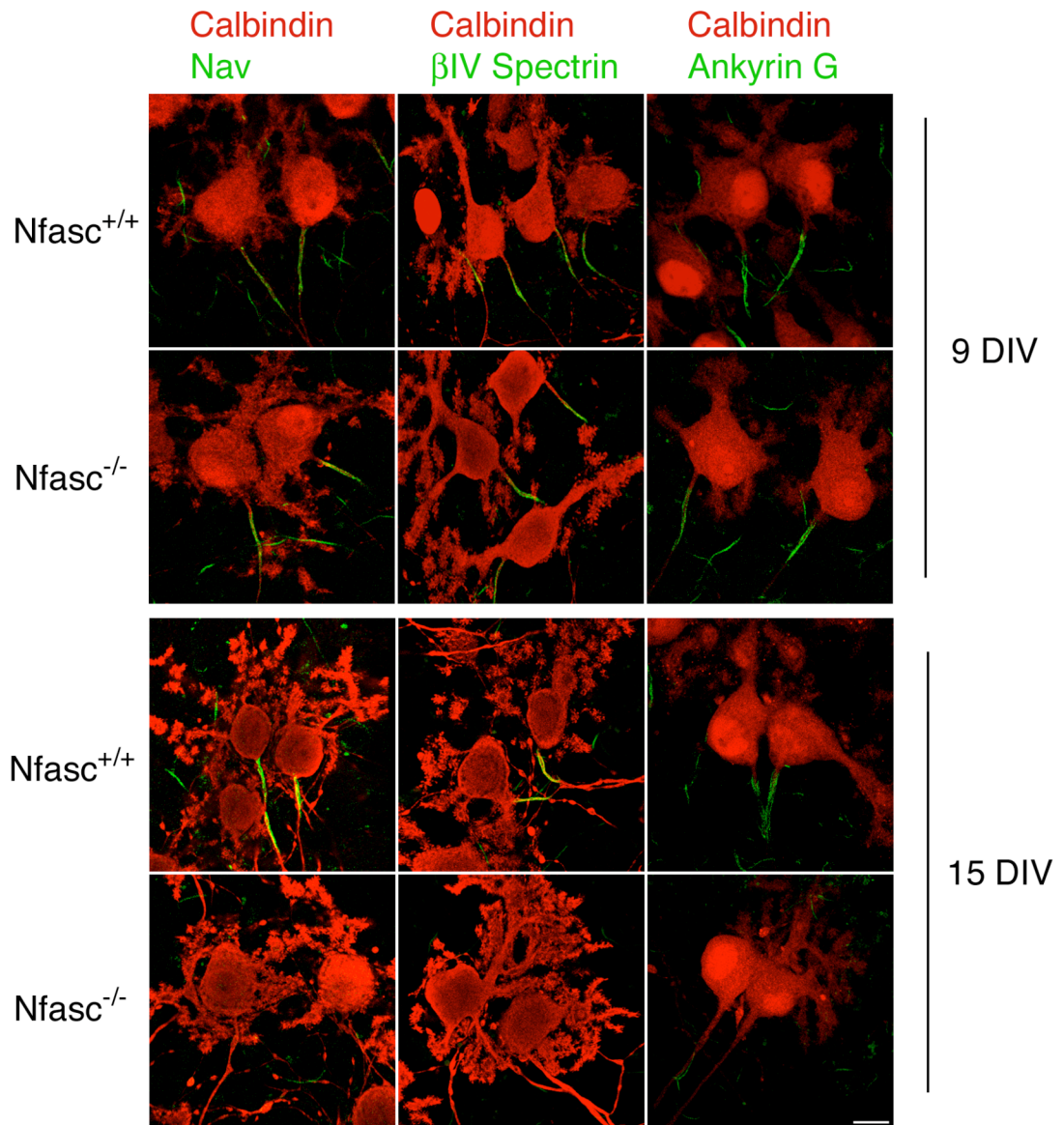
FIGURE 29. Nfasc186 is Required for Stabilising the Molecular Complex at AIS

Immunofluorescence of Purkinje cells from organotypic cerebellar cultures harvested from newborn *Nfasc*^{+/+} and *Nfasc* [-/-] animals shows that, at 9 DIV, the protein complement at AIS is present in both wild-type and mutant mice, replicating what is observed at P6 *in vivo*. However, at 15 DIV, Nav channels, ßIV Spectrin and Ankyrin G are no longer detected in slices harvested from Neurofascin-null mice. Scale bar, 10 µm.

See separate channels in supplementary Figure S3a (9DIV) and S3b (15DIV).

One can exclude that the disappearance of AIS components in the mutant PCs was due to tissue necrosis, since Calbindin staining of PC somas was equivalent to that of wild-type. This marker is commonly used to assess the survival and morphological changes that accompany PC development both *in vivo* and *in vitro* (Davids et al., 2002).

Thus, these results suggest that Nfasc186 is not required for the assembly but for the maintenance of the molecular complex at AIS. Although it is hard to draw definite conclusions from *in vitro* studies, these data provide the first insight into the role of Nfasc186 at AIS as a stabilizer rather than an organiser of this domain.

In polarised neurons, the targeting and assembly of microdomains (i.e. somato-dentritic and somato-axonal) is inevitably accompanied by the need to block diffusional mixing of proteins between these domains. It has been proposed that a membrane diffusion barrier is formed by accumulation of transmembrane proteins that are anchored to the actin cytoskeleton under the AIS membrane (Nakada et al., 2003). Although various membrane proteins can perform this function in concert with each other, in this study it is shown that Nfasc186 may function as a barrier to prevent lateral diffusion of other molecular components in the AIS cell membrane and may well complement its functions as a guidance molecule for directing synapse formation at this domain.

Furthermore, it cannot be excluded that NrCAM may also perform the same function in conjunction with Nfasc186, by virtue of their mutual interaction (Lustig et al., 2001; Volkmer et al., 1996) as well as with Ankyrin G (Davis et al., 1996)

SUMMARY SECTION 3.2

In agreement with previous findings, Nfasc186, a component of the macromolecular complex found at AIS, is not required to direct assembly of this domain in cerebellar Purkinje neurons. In the absence of Nfasc186, most AIS components are localised, with the exception of NrCAM, which requires Nfasc186 for its delivery and can be equally dispensable for AIS formation.

Nonetheless, Nfasc186 appears to be required for the maintenance of Nav channels, βIV Spectrin and Ankyrin G at AIS.

3.3 The role of the Neurofascin isoforms in assembly of central nodes

The analysis of Neurofascin-null mice has shown that both glial Nfasc155 and neuronal Nfasc186 are required for paranode and node formation in the central nervous system. However, it remains difficult to discern the relative contributions of either isoform in initial assembly of the node. Sherman and collaborators had already shown that the extracellular domain of Nfasc155 could rescue the axoglial junctions in peripheral nerves of Neurofascin-null mice. However, the nodal components Nav channels and NrCAM remained mislocalised, strongly supporting a key role for Nfasc186 in PNS node assembly (Sherman et al., 2005).

Are similar mechanisms of node formation used to concentrate the multimolecular complex at nodes of Ranvier in the CNS? It is likely that peripheral and central nodes are assembled by different mechanisms (Kaplan et al., 2001; Kaplan et al., 1997; Poliak and Peles, 2003; Salzer, 2003; Sherman and Brophy, 2005). For example, their molecular composition is not identical since this study has found that NrCAM is not present at central nodes (see section 3.1.3). Moreover, in the CNS a molecule functionally equivalent to Schwann cell-expressed Gliomedin, which directs targeting of Nfasc186 and NrCAM (Eshed et al., 2005), has not been found yet. In addition, it is still unclear what is the relative contribution of nodal and paranodal constituents in assembly of central nodes.

Therefore, to address whether Nfasc155 and Nfasc186 might play similar roles in CNS node assembly as those in the PNS, this study made use of transgenic lines expressing either isoform on a null background.

3.3.1 Nfasc186 rescues the nodal complex

Transgenic mice were generated using the neurofilament light chain (NF-L) promoter (see Materials and Methods section for details), which has been previously shown to drive expression of trangenes exclusively in neurons starting in embryonic life (Abel et al., 2001; Charron et al., 1995). The transgenic mice were viable and bred normally; however, a full characterization of the transgenic line was not performed due to a viral

infection which spread in the animal house and required complete rederivation of all lines.

Nevertheless, a preliminary analysis permittted to ascertain that the promoter drove robust expression of the full length Nfasc18, with a FLAG-tag linked to the extreme cytoplasmic tail, in both peripheral and central nodes of Ranvier (Figure 30).
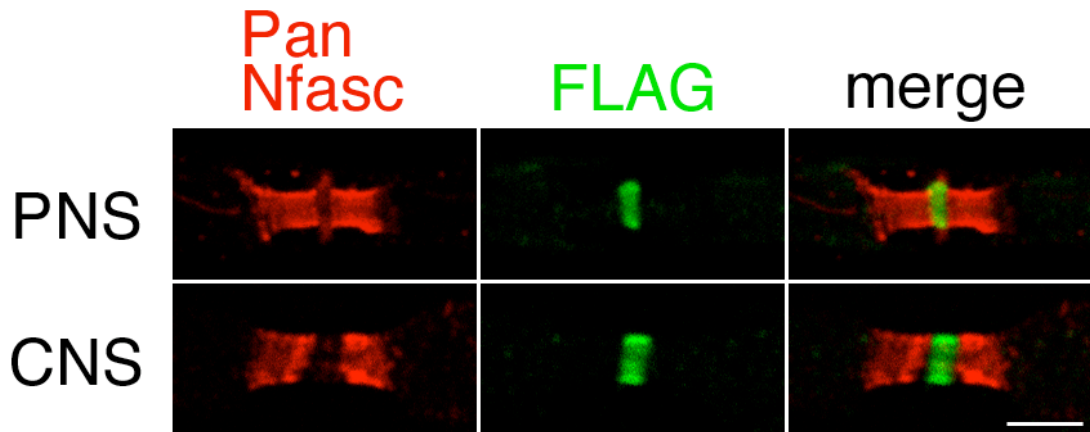
FIGURE 30. FLAG-tagged Nfasc186 is Targeted To Nodes in the PNS and CNS of Transgenic Mice

Immunofluorescence of teased sciatic nerves (PNS) and ventral funiculi (CNS) from 4-week old transgenic mice shows strong endogenous localisation of Nfasc155 at paranodes and, to a lesser extent, of Nfasc186 at nodes, as revealed by a Pan-Neurofascin antibody (red). Immunolabelling with an anti-FLAG antibody (green) shows that FLAG-tagged Nfasc186 (green) expression is restricted to the node of Ranvier.

Expression of FLAG-tagged Nfasc186 was also assessed at AIS of Purkinje cells in the cerebellum, however only endogenous Neurofascin was detected (data not shown). In this regard, it has been previously shown, that C-terminal interactions contribute to Nfasc186 localisation at AIS, possibly via a putative PDZ binding sequence (Dzhashiashvili et al., 2007). Therefore, it is likely that the FLAG-tag at the C-terminus functionally interfered with these interactions thus preventing localisation of Flag-tagged Nfasc186.

One line was chosen to interbreed with *Nfasc*$^{+/-}$ mice to generate *Nfasc*$^{-/-}$/*Nfasc186* transgenic mice. This permitted to test directly whether Nfasc186 could reconstitute the

nodal complex in the CNS of *Nfasc*$^{-/-}$ mice and to unequivocally demonstrate that Nfasc186 is required for node assembly in the PNS.

Indeed, Nfasc186 rescued the nodal complex in both the PNS and CNS (Figure 31A-B), but paranodal Caspr remained mislocalised (Figure 31C). Intriguingly, Ankyrin G in the rescued CNS fibers resumed its normal localisation at both the node and paranode (Figure 31B), suggesting that the transient expression of Ankyrin G at the paranodes does not depend on either Nfasc155 or its axonal partners (Caspr and Contactin).

In the CNS, the extent of rescue of Nav channels at nodes was 96 ± 2% (mean ± SEM) (see Figure 32C). Furthermore, rescuing the nodal complex was functionally significant because *Nfasc*$^{-/-}$*/Nfasc186* mice survived beyond P7, indicating that Nfasc186 is required for viability. These mice were indistinguishable from their littermates up to about P14, when they started to show signs of malnutrition and neurological defects, including tremors, hindlimb clasping and extensor spasms of the lower extremities. They succumbed by P18-19.

The reason why these mice die is currently unknown. However, preliminary observations of myelinated fibers in the spinal cord at P14 indicated that Nav clusters might be mislocalised to paranodes (data not shown) and therefore that nodal function may be compromised in these mice.

Moreover, lethality may result from the absence of intact paranodal axoglial junctions, since Caspr mutants, which lack paranodal junctions in the CNS and PNS, also die between P21 and P33 (Bhat et al., 2001). Moreover, in Caspr mutants Nav channels at CNS nodes disperse over time (Rios et al., 2003), indicating that intact nodes might also be required for viability.

FIGURE 31(Overleaf). Nfasc186 Rescues the Nodal Complex in *Nfasc*$^{-/-}$ Mice

A) Immunofluorescence of teased sciatic nerves from 6-d old *Nfasc*$^{-/-}$ and *Nfasc*$^{-/-}$/*Nfasc186* mice shows that FLAG-tagged Nfasc186 is targeted to the node and can rescue the assembly of the nodal components sodium channels (Nav), βIV Spectrin, Ankyrin G and NrCAM in the PNS. MBP was used as a marker for myelin.

B) Immunofluorescence of teased ventral funiculi of cervical spinal cord from 6-d old *Nfasc*$^{+/+}$/*Nfasc186* mice shows that FLAG-tagged Nfasc186 is correctly targeted to the node and that it can also rescue the nodal complex in the CNS when expressed on a null background (see also Figure 2A). Paranodes, hence the localisation of nodes, were visualised with the Claudin 11 antibody.

C) Immunostaining for Caspr of teased fibers from *Nfasc*$^{+/+}$ and *Nfasc*$^{-/-}$/*Nfasc186* mice shows that the reconstitution of the nodal complex is not accompanied by rescue of the axoglial junction in both the PNS and CNS. All scale bars, 5 μm.
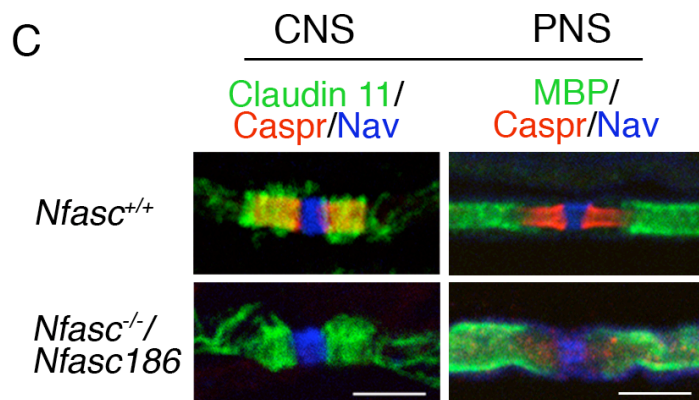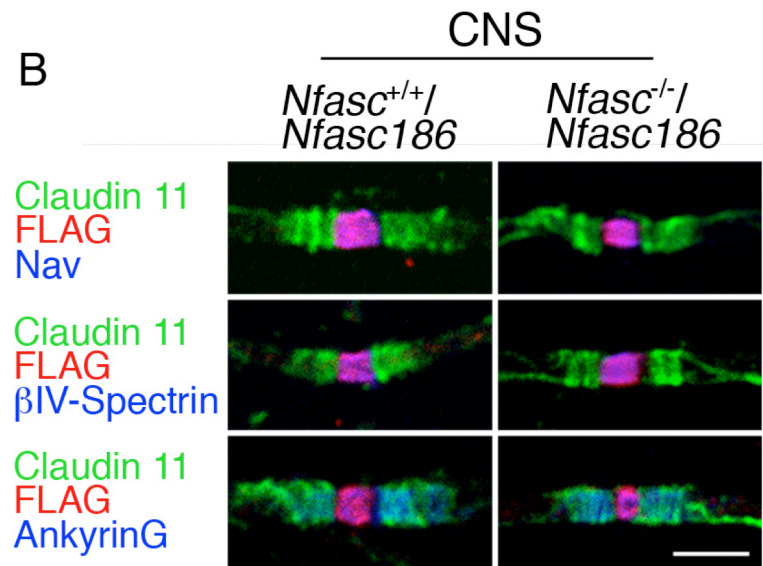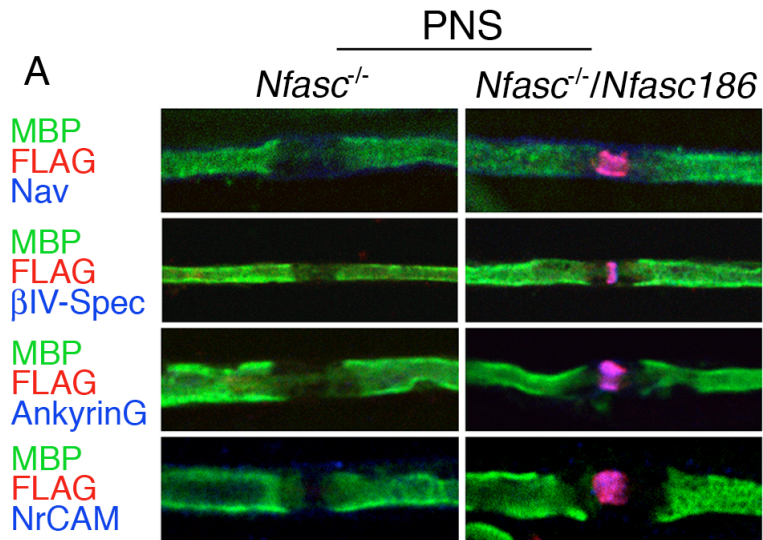
3.3.2 The extracellular domain of Nfasc155 rescues both the axoglial junctions and the nodal complex in the CNS

It has been previously shown that a form of Nfasc155 truncated at the C-terminus (*Nfasc155ΔIC*) is targeted to the paranodal loops of myelinating oligodendrocytes (Sherman et al., 2005). This allowed to test whether this targeting could reconstitute the axoglial junctional complex in the CNS of transgenic mice expressing Nfasc155ΔIC on a null background (Nfasc$^{-/-}$/ *Nfasc155ΔIC*).

Indeed, similarly to what had been observed in the PNS, Nfasc155ΔIC could rescue the localisation of Caspr at paranodes, suggesting that the axoglial junctional complex was reconstituted (Figure 32A). Interestingly, in contrast to the PNS, Nav channels and βIV Spectrin were correctly localised, suggesting that the nodal complex was also rescued (Figure 32B).

Expression of Nfasc155ΔIC on a Neurofascin-null background had a similar effect on the extent of rescue of Nav channels at nodes (91± 4%) (mean ± SEM) as that achieved by expressing Nfasc186 on a Neurofascin-null background (see section 3.3.1 and Figure 32C). This suggests that, in the CNS, an intact axoglial junction might not only be required to promote the migration of oligodendrocyte processes (Figure 7), but it is certainly important for concentrating the constituents of the nodal complex at nascent nodes. Furthermore, the extracellular domain of Nfasc155 appears to be sufficient to stimulate oligodendrocyte process extension and to rescue both the axoglial junction and the nodal complex.

Despite rescuing CNS nodes, the life expectancy of Nfasc$^{-/-}$/Nfasc155ΔIC was not enhanced. This is probably due to the fact that PNS nodes were not rescued.
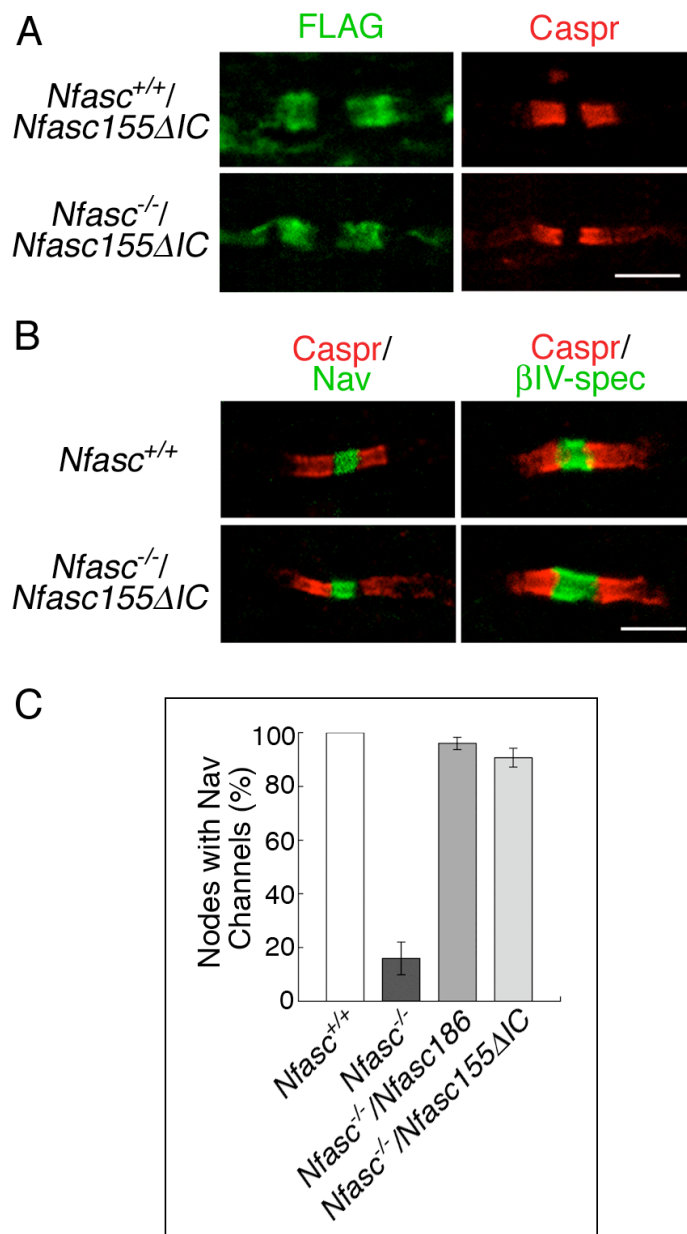
FIGURE 32. Reconstitution of the Axoglial Adhesion Complex Rescues CNS Nodes
A) Immunostaining of longitudinal sections of ventral spinal cord in the CNS shows that FLAG-tagged Nfasc155ΔIC is correctly targeted to paranodes of myelinated fibers and can rescue the Caspr localisation to the paranodal axoglial junctional complex. **B)** In CNS myelinated axons, rescue of Caspr by Nfasc155ΔIC on a null background also reconstitutes the nodal complex, as judged by immunoreactivity to sodium channels (Nav) and βIV Spectrin (βIV-Spec). **C)** In the absence of endogenous Neurofascin, reconstitution of the axoglial adhesion complex by Nfasc155ΔIC and expression of Nfasc186 at nodes were equally effective in rescuing the nodal complex in the CNS (means ± SEM, minimum of 75 nodes, 3 animals per condition). All scale bars, 5 μm.

3.3.3 Cooperative role of the Neurofascins in CNS node assembly: a proposed mechanism

The mechanisms by which central nodes assemble have long remained elusive. Oligodendrocyte soluble factors have been shown to be sufficient for clustering Nav1.2 channels in CNS axons *in vitro* (Kaplan et al., 1997). However, ensheathment of oligodendrocytes is required for clustering Nav 1.6 channels, which are more characteristic of mature nodes (Boiko et al., 2001; Kaplan et al., 2001)

With myelination, proteins become more concentrated at the node (Salzer, 2003). It is possible that the active exclusion of nodal components from the internodes by endocytosis and/or proteolysis and a diffusion barrier associated with the edges of oligodendrocyte processes help to concentrate them as the myelin sheath elongates (Dzhashiashvili et al., 2007; Pedraza et al., 2001; Vabnick et al., 1996). This diffusion barrier could be achieved by the formation of an adhesion complex at the axo-glia interface, which is consistent with the findings that Caspr and Nfasc155 colocalise at the tips of oligodendrocyte converging processes as early as P4. Furthermore, studies have shown that accumulation of Caspr and Nfasc155 at paranodes always precedes detection of nodal components in the CNS (Rasband et al., 1999a; Schafer et al., 2004) and that intact paranodal axoglial junctions prevent dispersal of nodal components (Dupree et al., 1999; Dupree et al., 2005; Ishibashi et al., 2002; Rasband et al., 2003; Rios et al., 2003).

This work has shown that Nfasc155 and Nfasc186 can independently promote assembly of nodes in the CNS. The fact that 16% of CNS nodes in the *Nfasc*$^{-/-}$ nerves displayed immunoreactivity to sodium channels indicates that these channels may be targeted inefficiently or that their stability is compromised. If Nav channels are correctly targeted to nascent nodes independently of the Neurofascins, then one can conclude that both Nfasc155 and Nfasc186 cooperate to stabilise rather than direct the initial assembly of the nodal complex. This conclusion is also in agreement with the proposed role of Nfasc186 at AIS advanced by this work.

Thus, how do CNS nodes assemble? A model proposing how neuronal and glial isoforms of Neurofascin may perform distinct but complementary functions in CNS node assembly and stabilisation is shown in Figure 33.

Previous studies have suggested that Ankyrin G is detected at nascent nodes before other nodal components (Jenkins and Bennett, 2002; Rasband et al., 1999a) and that sodium channel $\alpha-$ and $\beta-$ subunits may be targeted to nodes via an exocytotic pathway (Kaplan et al, 2001). The ability to bind the $\alpha-$ and $\beta 1-$ subunits of sodium channels (Lemaillet et al., 2003; McEwen and Isom, 2004) may enable Ankyrin G to recruit Nav channels to the nodal membrane (Malhotra et al., 2000). This complex then would directly interact with Nfasc186 and βIV Spectrin to form a macromolecular complex, which is stably anchored to the nodal axolemma (Jenkins and Bennett, 2001; Komada and Soriano, 2002; McEwen et al., 2004; Ratcliffe et al., 2001; Yang et al., 2007).

In the absence of Neurofascins, nodal components would still be targeted to the nodes. However, they are likely to diffuse in the lateral plane of the membrane without the anchoring function performed by Nfasc186 and an intact paranodal axoglial junction that serves as a barrier to their further dispersal. By reintroducing Nfasc186, Ankyrin G and sodium channels present at the node may directly associate with it and target its delivery to the plasma membrane (Ratcliffe et al., 2001).

It is likely that, even in the presence of Nfasc186, the nodal complex might eventually disperse over time in the absence of an intact axoglial junction to limit a steady rate of diffusion. This is consistent with previous studies (Rios et al., 2003) as well as with the preliminary observation that nodal clusters were often found to be mislocalised to paranodes in the *Nfasc$^{-/-}$/Nfasc186* mice at P14.

A steady rate of diffusion could also be combined with a reduced rate of synthesis and/or vesicle delivery of nodal components. In this regard, it has been shown that the available pool of vesicle-bound sodium channels decreases as the CNS matures (Schmidt et al., 1985). Hence, although an intact axoglial junction is not required for clustering the nodal complex, its reconstitution reduces the rate at which the nodal components can diffuse away from the node.

An interesting question is why the CNS makes use of two distinct mechanisms to cluster the multimolecular complex necessary for saltatory conduction at nodes of Ranvier?

CNS nodes are structurally different from PNS nodes, not least because oligodendrocytes do not have microvilli that extend into the nodal gap between myelin

segments. It has become evident that Nfasc186 is important for node assembly in the PNS by virtue of its interaction to Schwann cell-expressed Gliomedin.

However, CNS nodes may have evolved to depend on the axoglial junction as a complementary mechanism to that found at PNS nodes, since *cis* interaction of Nfasc186 with nodal components, might not be as efficient as *trans* interactions to ensure the stability of the nodal complex over time. Interestingly, in the absence of intact paranodal axoglial junctions, the tendency for the nodal complex to become more diffuse is more pronounced in the CNS compared to the PNS (Rios et al., 2003), suggesting that axoglial junctions play a more crucial role in maintaining the integrity of CNS nodes than PNS nodes. This is also consistent with the findings of this study in which the axoglial adhesion complex promoted assembly of the CNS nodal complex.

SUMMARY SECTION 3.3

By selectively expressing either Nfasc186 or a truncated version of Nfasc155 on a null background, I have shown that, in marked contrast to the PNS, each of the Neurofascin isoforms can independently rescue the CNS node of Ranvier. Therefore the two Neurofascin isoforms cooperate to assemble functional nodes of Ranvier in the vertebrate CNS.
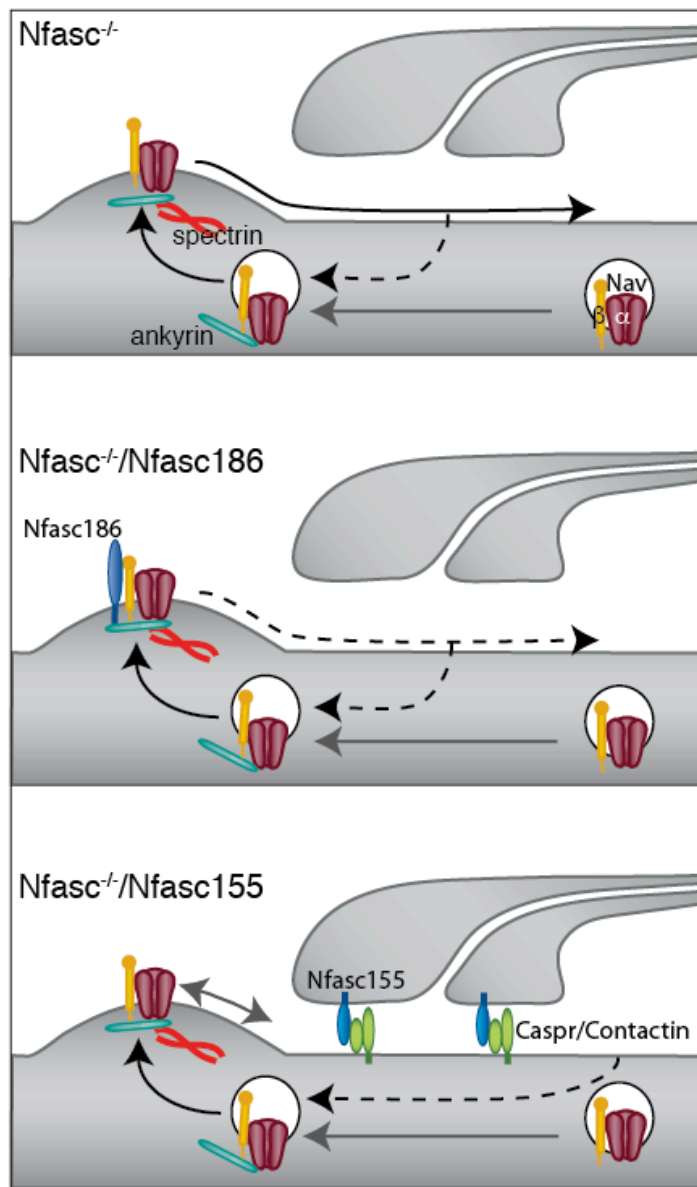
FIGURE 33. Model of the Distinct Roles of Nfasc186 and Nfasc155 in CNS nodes assembly and stabilisation

Top panel: Vesicle-bound sodium channels (α and β subunits) and Ankyrin G associate and are delivered to the nascent node by exocytosis. Ankyrin G then recruits βIV Spectrin which links the complex to the underlying cytoskeleton (not shown). In the absence of both Neurofascin isoforms, the nodal components diffuse laterally away from the nodal membrane and they are cleared by endocytosis and/or proteolysis in the internodes. Vesicles might be recycled if removed by endocytosis.

Middle panel: Expression of Nfasc186 rescues the nodal complex by anchoring sodium channels via direct interaction to their β subunit and to the AnkyrinG/βIV Spectrin complex. However, in the absence of an intact axoglial junction, dispersion of the multimolecular nodal complex can still take place.

Bottom panel: Nfasc155 reconstitutes the axoglial junctional complex at paranodes, hence limiting the rate of diffusion of sodium channels and their associated proteins away from the node.

4.CONCLUSION AND FUTURE WORK

4.1 Concluding remarks

The development of nodes of Ranvier provides an outstanding example of how neuron-glia interactions actively shape the form and function of the nervous system.

Recently, there has been tremendous progress in our understanding of the initial events leading to the organization of the node and its environs along myelinated axons of the PNS and CNS. It has become increasingly clear that myelination actively regulates the localization and kinds of channels that occur in axons and that are required to establish saltatory conduction (Boiko et al., 2001; Kaplan et al., 2001; Schafer et al., 2006).

This work adds substantial new evidence on the role of CAMs in the formation and stability of nodes of Ranvier and AIS in the central nervous system. Glial Nfasc155, due to its location at a point of close contact with axonal partners, is shown not only to facilitate the extension of myelinating processes but also to contribute to the restricted distribution of components at nodes of Ranvier. This is accomplished by establishing a paranodal adhesion complex that functions as a physical barrier to the lateral diffusion of the nodal multimolecular complex. In this regard, this work provides the first direct evidence of the role of axoglial interactions in CNS node assembly and stabilisation.

At the node (and AIS), neuronal Nfasc186 functions as an attachment site for ion channels and scaffolding proteins and as a stabiliser of the multimolecular complex assembled at the nodal (and AIS) axonal membrane.

Hence, both Neurofascins independently promote assembly of central nodes, but are both required for their maintenance. Interestingly, this cooperative role of Neurofascins has been demonstrated in tissue from patients with Multiple Sclerosis, which is caused by inflammatory damage to CNS axons (Howell et al., 2006). In newly forming and established lesions, which are characterised by demyelination and inflammation, early disruption of Nfasc155 expression, and hence of the paranodal structures, appeared to precede alteration of the node itself, as judged by Nav channel and Nfasc186 immunoreactivity, suggesting that Nfasc155 is an early and sensitive marker of myelin damage associated with axonal pathology in MS.

However, Nfasc186- and Nav-positive clusters were still observed in the absence of intact myelin profiles, further supporting a mechanism by which CNS nodes assemble

independently of paranodal axoglial junctions. These results point to a pivotal role for both Neurofascins in the disruption and restoration of central nodes, which is in agreement with the findings of this work.

Moreover, in remyelinating lesions, Nfasc155 was observed in close association with Nav channel clusters at heminodes, indicative of a restricted distribution of Nav clusters at the tips of closely converging remyelinating processes (Howell et al., 2006). This suggest that the axoglial adhesion complex found at the tips of elongating myelin internodes might also represent an actively dynamic molecular sieve, in addition to the more passive diffusion barrier found at paranodes (Pedraza et al., 2001).

How are the Neurofascins targeted to their respective sites? Previous work has shown that the extracellular domain of Nfasc155 and Nfasc186 is sufficient for their respective targeting at paranodes (Sherman et al., 2005) and nodes (Dzhashiashvili et al., 2007).

In the PNS, Nfasc186 targeting is probably mediated by its binding to Gliomedin expressed on the Schwann cell microvilli (Eshed et al., 2005), whereas interactions of Nfasc155 with axonal partners (i.e. Caspr-Contactin complex) may help to concentrate the tripartite complex at the tips of myelinating processes, in both PNS and CNS.

But what about Nfasc186 targeting at CNS nodes? More generally, how are proteins specifically targeted to their respective domains and excluded from others? At central nodes and AIS, are there trafficking signals depending on the interaction with Ankyrin G, βIV Spectrin or some other as yet unidentified components responsible for targeting proteins at these domains? Moreover, what intracellular signalling, transcription factors, micro (mi) RNA or other factors, control their developmentally regulated expression?

The answer to these questions is currently unknown and will continue to keep researchers focused in their effort to determine how neurons establish polarised domains necessary for neuronal excitability and nervous system function.

4.2 Future directions

Future work should extend the analysis of the Nfasc155 rescue in at least two ways: a direct quantitative comparison of inter-heminodal gaps between *Nfasc^-/-^/Nfasc155ΔIC* and *Nfasc* null animals, combined with the analysis of the amount of myelin proteins, should demonstrate unequivocally that Nfasc155 facilitates the advancement of converging myelinating processes and therefore increase the overall myelination state of axons. In addition, measurements of interheminodal gaps in rescued CNS fibers in the *Nfasc^-/-^/Nfasc186* at P6 could further support the conclusion that an intact axoglial junction is required for oligodendrocyte process extension.

As mentioned earlier, *Nfasc^-/-^/Nfasc186* mice survive until P18-19, thus providing an extended time-window for further analysis. This should include the measurements of interheminodal gaps before P18-19 to determine whether the advancing of oligodendrocyte processes is either halted or retarded.

In addition, it would be important to study the developmental localisation of juxtaparanodal markers, such as Kv channels, Caspr2 and TAG along myelinated fibers. The prediction would be that in *Nfasc^-/-^/Nfasc186* mice juxtaparanodal components are mislocalised, similarly to what has been found for mutants lacking paranodal axoglial junctions (Bhat et al., 2001; Boyle et al., 2001; Dupree et al., 1999; Ishibashi et al., 2002).

A second developmentally-regulated event worth investigating is the upregulation of sodium channels of the Nav1.6 type. Rios and colleagues (2003) reported that paranodal interactions regulate expression of sodium channel subtypes, since in the *Caspr* mutant the switch from Nav1.2 to Nav1.6 did not occur. Therefore, one could ask whether this developmentally-regulated switch still occurs in *Nfasc^-/-^/Nfasc186* mice where axoglial-junctions are absent.

Moreover, a quantitative comparison of nodal length and pixel intensity between *Nfasc^-/-^/Nfasc186* mice and controls could confirm my preliminary observations that nodal components might be in the process of dissipating and to what extent. Electrophysiology on wild type and mutant peripheral nerves, before and after the display of an overt clinical phenotype, would also provide further evidence on the physiological relevance of an intact axoglial junction for nerve impulse propagation.

My work on the role of Nfasc186 at AIS could be extended to include electrophysiology of Purkinje cells in cultured cerebella in order to determine the physiological properties of these cells in the mutant compared to wild-type.

As mentioned previously, in the *Nfasc⁻/⁻/Nfasc186* the transgene is targeted to nodes, which are rescued, but not to AIS. This could be used to investigate the role of Nfasc186 at AIS *in vivo* beyond P6. More specifically, we can ask whether Nfasc186 might be required for the stability of AIS and confirm my *in vitro* results.

Since the FLAG-tag at the extreme C-terminus interfered with the targeting of Nfasc186 to AIS, a new transgenic line could be engineered expressing Nfasc186 with a FLAG-tag at the N-terminus, right after the signal peptide, which is required for translocation across the membrane of the endoplasmic reticulum. Hence, transgenic expression of Nfasc186 on a null background at AIS should permit us to rescue the phenotype of mutant Purkinje cells.

Future applications of the transgenic rescue strategy, by expressing either isoforms with deletions of unique exon sequences, should permit us to identify the protein-protein interactions by which Nfasc186 and Nfasc155 cooperate in the assembly of the node of Ranvier. It will also be interesting to test whether the function of the Neurofascins is interchangeable, for example by expressing Nfasc155 in neurons and Nfasc186 in glia.

Finally, a conditional knock-out strategy could allow to switch on and off in a temporal and tissue-specific manner the expression of either Neurofascin isoform, thus extending the *in vivo* analysis beyond the first week of life and permitting the further dissection of their functions in orchestrating assembly and maintenance of domains along myelinated axons.

5. REFERENCES

Abel, A., Walcott, J., Woods, J., Duda, J., and Merry, D.E. (2001). Expression of expanded repeat androgen receptor produces neurologic disease in transgenic mice. Human molecular genetics *10*, 107-116.

Alessandri-Haber, N., Paillart, C., Arsac, C., Gola, M., Couraud, F., and Crest, M. (1999). Specific distribution of sodium channels in axons of rat embryo spinal motoneurones. The Journal of physiology *518 (Pt 1)*, 203-214.

Altevogt, B.M., Kleopa, K.A., Postma, F.R., Scherer, S.S., and Paul, D.L. (2002). Connexin29 is uniquely distributed within myelinating glial cells of the central and peripheral nervous systems. J Neurosci *22*, 6458-6470.

Ango, F., di Cristo, G., Higashiyama, H., Bennett, V., Wu, P., and Huang, Z.J. (2004). Ankyrin-based subcellular gradient of neurofascin, an immunoglobulin family protein, directs GABAergic innervation at purkinje axon initial segment. Cell *119*, 257-272.

Arroyo, E.J., and Scherer, S.S. (2000). On the molecular architecture of myelinated fibers. Histochemistry and cell biology *113*, 1-18.

Arroyo, E.J., Xu, T., Grinspan, J., Lambert, S., Levinson, S.R., Brophy, P.J., Peles, E., and Scherer, S.S. (2002). Genetic dysmyelination alters the molecular architecture of the nodal region. J Neurosci *22*, 1726-1737.

Baumann, N., and Pham-Dinh, D. (2001). Biology of oligodendrocytes and myelin in the mammalian central nervous system. Physiol Rev *81*(2),871-927

Baba, H., Akita, H., Ishibashi, T., Inoue, Y., Nakahira, K., and Ikenaka, K. (1999). Completion of myelin compaction, but not the attachment of oligodendroglial processes triggers K(+) channel clustering. Journal of neuroscience research *58*, 752-764.

Barbin, G. *et al.*(2004). Axonal-cell adhesion molecule L1 in CNS myelination. Neuron Glia Biology, *1*: 65-72.

Barres, B.A., and Raff, M.C. (1993). Proliferation of oligodendrocyte precursor cells depends on electrical activity in axons. Nature *361*, 258-260.

Barres, B.A., and Raff, M.C. (1999). Axonal control of oligodendrocyte development. The Journal of cell biology *147*, 1123-1128.

Barton, W.A., Liu, B.P., Tzvetkova, D., Jeffrey, P.D., Fournier, A.E., Sah, D., Cate, R., Strittmatter, S.M., and Nikolov, D.B. (2003). Structure and axon outgrowth inhibitor binding of the Nogo-66 receptor and related proteins. The EMBO journal *22*, 3291-3302.

Bellen, H.J., Lu, Y., Beckstead, R., and Bhat, M.A. (1998). Neurexin IV, caspr and paranodin--novel members of the neurexin family: encounters of axons and glia. Trends in neurosciences *21*, 444-449.

Bennett, V., and Lambert, S. (1999). Physiological roles of axonal ankyrins in survival of premyelinated axons and localization of voltage-gated sodium channels. Journal of neurocytology *28*, 303-318.

Berghs, S., Aggujaro, D., Dirkx, R., Jr., Maksimova, E., Stabach, P., Hermel, J.M., Zhang, J.P., Philbrick, W., Slepnev, V., Ort, T., and Solimena, M. (2000). betaIV spectrin, a new spectrin localized at axon initial segments and nodes of ranvier in the central and peripheral nervous system. The Journal of cell biology *151*, 985-1002.

Bhat, M.A., Rios, J.C., Lu, Y., Garcia-Fresco, G.P., Ching, W., St Martin, M., Li, J., Einheber, S., Chesler, M., Rosenbluth, J.*, et al.* (2001). Axon-glia interactions and the domain organization of myelinated axons requires neurexin IV/Caspr/Paranodin. Neuron *30*, 369-383.

Black, M.M., and Lee, V.M. (1988). Phosphorylation of neurofilament proteins in intact neurons: demonstration of phosphorylation in cell bodies and axons. J Neurosci *8*, 3296-3305.

Boiko, T., Rasband, M.N., Levinson, S.R., Caldwell, J.H., Mandel, G., Trimmer, J.S., and Matthews, G. (2001). Compact myelin dictates the differential targeting of two sodium channel isoforms in the same axon. Neuron *30*, 91-104.

Boiko, T., Vakulenko, M., Ewers, H., Yap, C.C., Norden, C., and Winckler, B. (2007). Ankyrin-dependent and -independent mechanisms orchestrate axonal compartmentalization of l1 family members neurofascin and l1/neuron-glia cell adhesion molecule. J Neurosci *27*, 590-603.

Boiko, T., Van Wart, A., Caldwell, J.H., Levinson, S.R., Trimmer, J.S., and Matthews, G. (2003). Functional specialization of the axon initial segment by isoform-specific sodium channel targeting. J Neurosci *23*, 2306-2313.

Boiko, T., and Winckler, B. (2003). Picket and other fences in biological membranes. Developmental cell *5*, 191-192.

Boyle, M.E., Berglund, E.O., Murai, K.K., Weber, L., Peles, E., and Ranscht, B. (2001). Contactin orchestrates assembly of the septate-like junctions at the paranode in myelinated peripheral nerve. Neuron *30*, 385-397.

Brady, S.T., Witt, A.S., Kirkpatrick, L.L., de Waegh, S.M., Readhead, C., Tu, P.H., and Lee, V.M. (1999). Formation of compact myelin is required for maturation of the axonal cytoskeleton. J Neurosci *19*, 7278-7288.

Bronstein, J.M., Popper, P., Micevych, P.E., and Farber, D.B. (1996). Isolation and characterization of a novel oligodendrocyte-specific protein. Neurology *47*, 772-778.

Brophy, P.J. (2001). Axoglial junctions: separate the channels or scramble the message. Curr Biol *11*, R555-557.

Brummendorf, T., Kenwrick, S., and Rathjen, F.G. (1998). Neural cell recognition molecule L1: from cell biology to human hereditary brain malformations. Current opinion in neurobiology *8*, 87-97.

Brummendorf, T., and Rathjen, F.G. (1996). Structure/function relationships of axon-associated adhesion receptors of the immunoglobulin superfamily. Current opinion in neurobiology *6*, 584-593.

Caldwell, J.H., Schaller, K.L., Lasher, R.S., Peles, E., and Levinson, S.R. (2000). Sodium channel Na(v)1.6 is localized at nodes of ranvier, dendrites, and synapses. Proceedings of the National Academy of Sciences of the United States of America *97*, 5616-5620.

Chang, B.J., Cho, I.J., and Brophy, P.J. (2000). A study on the immunocytochemical localization of neurofascin in rat sciatic nerve. Journal of veterinary science (Suwon-si, Korea) *1*, 67-71.

Charles, P., Tait, S., Faivre-Sarrailh, C., Barbin, G., Gunn-Moore, F., Denisenko-Nehrbass, N., Guennoc, A.M., Girault, J.A., Brophy, P.J., and Lubetzki, C. (2002). Neurofascin is a glial receptor for the paranodin/Caspr-Contactin axonal complex at the axoglial junction. Curr Biol *12*, 217-220.

Charron, G., Julien, J.P., and Bibor-Hardy, V. (1995). Neuron specificity of the neurofilament light promoter in transgenic mice requires the presence of DNA unwinding elements. The Journal of biological chemistry *270*, 25739-25745.

Ching, W., Zanazzi, G., Levinson, S.R., and Salzer, J.L. (1999). Clustering of neuronal sodium channels requires contact with myelinating Schwann cells. Journal of neurocytology *28*, 295-301.

Collinson, J.M., Marshall, D., Gillespie, C.S., and Brophy, P.J. (1998). Transient expression of neurofascin by oligodendrocytes at the onset of myelinogenesis: implications for mechanisms of axon-glial interaction. Glia *23*, 11-23.

Colman, D.R., Pedraza, L., and Yoshida, M. (2001). Concepts in myelin sheath evolution. In Jessen, K.R., and Richardson, W.D. (Eds.), *Glial Cell Development*. 2nd Edition: Oxford University Press.

Coman, I., Barbin, G., Charles, P., Zalc, B., and Lubetzki, C. (2005). Axonal signals in central nervous system myelination, demyelination and remyelination. Journal of the neurological sciences *233*, 67-71.

Custer, A.W., Kazarinova-Noyes, K., Sakurai, T., Xu, X., Simon, W., Grumet, M., and Shrager, P. (2003). The role of the ankyrin-binding protein NrCAM in node of Ranvier formation. J Neurosci *23*, 10032-10039.

Davids, E., Hevers, W., Damgen, K., Zhang, K., Tarazi, F.I., and Luddens, H. (2002). Organotypic rat cerebellar slice culture as a model to analyze the molecular pharmacology of GABAA receptors. Eur Neuropsychopharmacol *12*, 201-208.

Davis, J.Q., Lambert, S., and Bennett, V. (1996). Molecular composition of the node of Ranvier: identification of ankyrin-binding cell adhesion molecules neurofascin (mucin+/third FNIII domain-) and NrCAM at nodal axon segments. The Journal of cell biology *135*, 1355-1367.

Davis, J.Q., McLaughlin, T., and Bennett, V. (1993). Ankyrin-binding proteins related to nervous system cell adhesion molecules: candidates to provide transmembrane and intercellular connections in adult brain. The Journal of cell biology *121*, 121-133.

de Waegh, S.M., Lee, V.M., and Brady, S.T. (1992). Local modulation of neurofilament phosphorylation, axonal caliber, and slow axonal transport by myelinating Schwann cells. Cell *68*, 451-463.

Demerens, C., Stankoff, B., Logak, M., Anglade, P., Allinquant, B., Couraud, F., Zalc, B., and Lubetzki, C. (1996). Induction of myelination in the central nervous system by electrical activity. Proceedings of the National Academy of Sciences of the United States of America *93*, 9887-9892.

Denisenko-Nehrbass, N., Faivre-Sarrailh, C., Goutebroze, L., and Girault, J.A. (2002). A molecular view on paranodal junctions of myelinated fibers. Journal of physiology, Paris *96*, 99-103.

Denisenko-Nehrbass, N., Oguievetskaia, K., Goutebroze, L., Galvez, T., Yamakawa, H., Ohara, O., Carnaud, M., and Girault, J.A. (2003). Protein 4.1B associates with both Caspr/paranodin and Caspr2 at paranodes and juxtaparanodes of myelinated fibres. The European journal of neuroscience *17*, 411-416.

Devaux, J., Alcaraz, G., Grinspan, J., Bennett, V., Joho, R., Crest, M., and Scherer, S.S. (2003). Kv3.1b is a novel component of CNS nodes. J Neurosci *23*, 4509-4518.

Devaux, J.J., Kleopa, K.A., Cooper, E.C., and Scherer, S.S. (2004). KCNQ2 is a nodal K+ channel. J Neurosci *24*, 1236-1244.

Dugandzija-Novakovic, S., Koszowski, A.G., Levinson, S.R., and Shrager, P. (1995). Clustering of Na+ channels and node of Ranvier formation in remyelinating axons. J Neurosci *15*, 492-503.

Dupree, J.L., Girault, J.A., and Popko, B. (1999). axoglial interactions regulate the localization of axonal paranodal proteins. The Journal of cell biology *147*, 1145-1152.

Dupree, J.L., Mason, J.L., Marcus, J.R., Stull, M., Levinson, R., Matsushima, G.K., and Popko, B. (2005). Oligodendrocytes assist in the maintenance of sodium channel clusters independent of the myelin sheath. Neuron Glia Biol *1*, 1-14.

Dusart, I., Airaksinen, M.S., and Sotelo, C. (1997). Purkinje cell survival and axonal regeneration are age dependent: an in vitro study. J Neurosci *17*, 3710-3726.

Dzhashiashvili, Y., Zhang, Y., Galinska, J., Lam, I., Grumet, M., and Salzer, J.L. (2007). Nodes of Ranvier and axon initial segments are ankyrin G-dependent domains that assemble by distinct mechanisms. The Journal of cell biology *177*, 857-870.

Einheber, S., Zanazzi, G., Ching, W., Scherer, S., Milner, T.A., Peles, E., and Salzer, J.L. (1997). The axonal membrane protein Caspr, a homologue of neurexin IV, is a component of the septate-like paranodal junctions that assemble during myelination. The Journal of cell biology *139*, 1495-1506.

Ekberg, J., and Adams, D.J. (2006). Neuronal voltage-gated sodium channel subtypes: key roles in inflammatory and neuropathic pain. The international journal of biochemistry & cell biology *38*, 2005-2010.

Ellisman, M., Deerinck, T., and Bennett, V. (2001). Structure and formation of the node of Ranvier. In Jessen, K.R., and Richardson, W.D. (Eds.), *Glial Cell Development*. 2nd Edition: Oxford University Press.

Eshed, Y., Feinberg, K., Poliak, S., Sabanay, H., Sarig-Nadir, O., Spiegel, I., Bermingham, J.R., Jr., and Peles, E. (2005). Gliomedin mediates Schwann cell-axon interaction and the molecular assembly of the nodes of Ranvier. Neuron *47*, 215-229.

Faivre-Sarrailh, C., Gauthier, F., Denisenko-Nehrbass, N., Le Bivic, A., Rougon, G., and Girault, J.A. (2000). The glycosylphosphatidyl inositol-anchored adhesion molecule F3/contactin is required for surface transport of paranodin/contactin-associated protein (caspr). The Journal of cell biology *149*, 491-502.

Fannon, A.M., Sherman, D.L., Ilyina-Gragerova, G., Brophy, P.J., Friedrich, V.L., Jr., and Colman, D.R. (1995). Novel E-cadherin-mediated adhesion in peripheral nerve: Schwann cell architecture is stabilized by autotypic adherens junctions. The Journal of cell biology *129*, 189-202.

Fields, R.D., and Itoh, K. (1996). Neural cell adhesion molecules in activity-dependent development and synaptic plasticity. Trends in neurosciences *19*, 473-480.

Foran, D.R., and Peterson, A.C. (1992). Myelin acquisition in the central nervous system of the mouse revealed by an MBP-Lac Z transgene. The Journal of neuroscience, *12*(12): 4890-4897

Furley, A.J., Morton, S.B., Manalo, D., Karagogeos, D., Dodd, J., and Jessell, T.M. (1990). The axonal glycoprotein TAG-1 is an immunoglobulin superfamily member with neurite outgrowth-promoting activity. Cell *61*, 157-170.

Gahwiler, B.H., Capogna, M., Debanne, D., McKinney, R.A., and Thompson, S.M. (1997). Organotypic slice cultures: a technique has come of age. Trends in neurosciences *20*, 471-477.

Garcia-Fresco, G.P., Sousa, A.D., Pillai, A.M., Moy, S.S., Crawley, J.N., Tessarollo, L., Dupree, J.L., and Bhat, M.A. (2006). Disruption of axoglial junctions causes cytoskeletal disorganization and degeneration of Purkinje neuron axons. Proceedings of the National Academy of Sciences of the United States of America *103*, 5137-5142.

Garrido, J.J., Fernandes, F., Moussif, A., Fache, M.P., Giraud, P., and Dargent, B. (2003a). Dynamic compartmentalization of the voltage-gated sodium channels in axons. Biology of the cell / under the auspices of the European Cell Biology Organization *95*, 437-445.

Garrido, J.J., Giraud, P., Carlier, E., Fernandes, F., Moussif, A., Fache, M.P., Debanne, D., and Dargent, B. (2003b). A targeting motif involved in sodium channel clustering at the axonal initial segment. Science *300*, 2091-2094.

Garver, T.D., Ren, Q., Tuvia, S., and Bennett, V. (1997). Tyrosine phosphorylation at a site highly conserved in the L1 family of cell adhesion molecules abolishes ankyrin binding and increases lateral mobility of neurofascin. The Journal of cell biology *137*, 703-714.

Gollan, L., Sabanay, H., Poliak, S., Berglund, E.O., Ranscht, B., and Peles, E. (2002). Retention of a cell adhesion complex at the paranodal junction requires the cytoplasmic region of Caspr. The Journal of cell biology *157*, 1247-1256.

Gollan, L., Salomon, D., Salzer, J.L., and Peles, E. (2003). Caspr regulates the processing of contactin and inhibits its binding to neurofascin. The Journal of cell biology *163*, 1213-1218.

Gow, A., Southwood, C.M., Li, J.S., Pariali, M., Riordan, G.P., Brodie, S.E., Danias, J., Bronstein, J.M., Kachar, B., and Lazzarini, R.A. (1999). CNS myelin and sertoli cell tight junction strands are absent in Osp/claudin-11 null mice. Cell *99*, 649-659.

Gunn-Moore, F.J., Hill, M., Davey, F., Herron, L.R., Tait, S., Sherman, D., and Brophy, P.J. (2006). A functional FERM domain binding motif in neurofascin. Mol Cell Neurosci. *33*, 441-446

Hassel, B., Rathjen, F.G., and Volkmer, H. (1997). Organization of the neurofascin gene and analysis of developmentally regulated alternative splicing. J Biol Chem, *272*, 28742-9

Hedstrom, K.L., and Rasband, M.N. (2006). Intrinsic and extrinsic determinants of ion channel localization in neurons. Journal of neurochemistry *98*, 1345-1352.

Hogan, B., Beddington, R., Costantini, F., and Lacy, R. (1994). *Manipulating the Mouse Embryo: A Laboratory Manual.* 2nd Edition: Cold Spring Harbor Laboratory Press.

Hortsch, M. (1996). The L1 family of neural cell adhesion molecules: old proteins performing new tricks. Neuron *17*, 587-593.

Howell, O.W., Palser, A., Polito, A., Melrose, S., Zonta, B., Scheiermann, C., Vora, A.J., Brophy, P.J., and Reynolds, R. (2006). Disruption of neurofascin localization reveals early changes preceding demyelination and remyelination in multiple sclerosis. Brain *129,* 3173-3185

Ishibashi, T., Dupree, J.L., Ikenaka, K., Hirahara, Y., Honke, K., Peles, E., Popko, B., Suzuki, K., Nishino, H., and Baba, H. (2002). A myelin galactolipid, sulfatide, is essential for maintenance of ion channels on myelinated axon but not essential for initial cluster formation. J Neurosci *22*, 6507-6514.

Isom, L.L. (2001). Sodium channel beta subunits: anything but auxiliary. Neuroscientist *7*, 42-54.

Jenkins, S.M., and Bennett, V. (2001). Ankyrin-G coordinates assembly of the spectrin-based membrane skeleton, voltage-gated sodium channels, and L1 CAMs at Purkinje neuron initial segments. The Journal of cell biology *155*, 739-746.

Jenkins, S.M., and Bennett, V. (2002). Developing nodes of Ranvier are defined by ankyrin-G clustering and are independent of paranodal Caspr-Contactin adhesion. Proceedings of the National Academy of Sciences of the United States of America *99*, 2303-2308.

Jenkins, S.M., Kizhatil, K., Kramarcy, N.R., Sen, A., Sealock, R., and Bennett, V. (2001). FIGQY phosphorylation defines discrete populations of L1 cell adhesion molecules at sites of cell-cell contact and in migrating neurons. Journal of cell science *114*, 3823-3835.

Jessen, K.R., and Mirsky, R. (2005). The origin and development of glial cells in peripheral nerves. Nature reviews *6*, 671-682.

Kandel, E.R., Schwartz, J.H., and Jessell, T.M. (2000), *Principles of Neural Science.* 4th Edition: McGraw-Hill.

Kaplan, M.R., Cho, M.H., Ullian, E.M., Isom, L.L., Levinson, S.R., and Barres, B.A. (2001). Differential control of clustering of the sodium channels Na(v)1.2 and Na(v)1.6 at developing CNS nodes of Ranvier. Neuron *30*, 105-119.

Kaplan, M.R., Meyer-Franke, A., Lambert, S., Bennett, V., Duncan, I.D., Levinson, S.R., and Barres, B.A. (1997). Induction of sodium channel clustering by oligodendrocytes. Nature *386*, 724-728.

Kazarinova-Noyes, K., Malhotra, J.D., McEwen, D.P., Mattei, L.N., Berglund, E.O., Ranscht, B., Levinson, S.R., Schachner, M., Shrager, P., Isom, L.L., and Xiao, Z.C. (2001). Contactin associates with Na+ channels and increases their functional expression. J Neurosci *21*, 7517-7525.

Kizhatil, K., Wu, Y.X., Sen, A., and Bennett, V. (2002). A new activity of doublecortin in recognition of the phospho-FIGQY tyrosine in the cytoplasmic domain of neurofascin. J Neurosci *22*, 7948-7958.

Koch, T., Brugger, T., Bach, A., Gennarini, G., and Trotter, J. (1997). Expression of the immunoglobulin superfamily cell adhesion molecule F3 by oligodendrocyte-lineage cells. Glia *19*, 199-212.

Komada, M., and Soriano, P. (2002). [Beta]IV-spectrin regulates sodium channel clustering through ankyrin-G at axon initial segments and nodes of Ranvier. The Journal of cell biology *156*, 337-348.

Kordeli, E., Lambert, S., and Bennett, V. (1995). AnkyrinG. A new ankyrin gene with neural-specific isoforms localized at the axonal initial segment and node of Ranvier. The Journal of biological chemistry *270*, 2352-2359.

Koroll, M., Rathjen, F.G., and Volkmer, H. (2001). The neural cell recognition molecule neurofascin interacts with syntenin-1 but not with syntenin-2, both of which reveal self-associating activity. The Journal of biological chemistry *276*, 10646-10654.

Koticha, D., Babiarz, J., Kane-Goldsmith, N., Jacob, J., Raju, K., and Grumet, M. (2005). Cell adhesion and neurite outgrowth are promoted by neurofascin NF155 and inhibited by NF186. Mol Cell Neurosci *30*, 137-148.

Koticha, D., Maurel, P., Zanazzi, G., Kane-Goldsmith, N., Basak, S., Babiarz, J., Salzer, J., and Grumet, M. (2006). Neurofascin interactions play a critical role in clustering sodium channels, ankyrin G and beta IV spectrin at peripheral nodes of Ranvier. Developmental biology *293*, 1-12.

Lacas-Gervais, S., Guo, J., Strenzke, N., Scarfone, E., Kolpe, M., Jahkel, M., De Camilli, P., Moser, T., Rasband, M.N., and Solimena, M. (2004). BetaIVSigma1 spectrin stabilizes the nodes of Ranvier and axon initial segments. The Journal of cell biology *166*, 983-990.

Lai, H.C., and Jan, L.Y. (2006). The distribution and targeting of neuronal voltage-gated ion channels. Nature reviews *7*, 548-562.

Lambert, S., Davis, J.Q., and Bennett, V. (1997). Morphogenesis of the node of Ranvier: co-clusters of ankyrin and ankyrin-binding integral proteins define early developmental intermediates. J Neurosci *17*, 7025-7036.

Lemaillet, G., Walker, B., and Lambert, S. (2003). Identification of a conserved ankyrin-binding motif in the family of sodium channel alpha subunits. The Journal of biological chemistry *278*, 27333-27339.

Lubetzki, C., Demerens, C., Anglade, P., Villarroya, H., Frankfurter, A., Lee, V.M., and Zalc, B. (1993). Even in culture, oligodendrocytes myelinate solely axons. Proceedings of the National Academy of Sciences of the United States of America *90*, 6820-6824.

Lustig, M., Zanazzi, G., Sakurai, T., Blanco, C., Levinson, S.R., Lambert, S., Grumet, M., and Salzer, J.L. (2001). Nr-CAM and neurofascin interactions regulate ankyrin G and sodium channel clustering at the node of Ranvier. Curr Biol *11*, 1864-1869.

Malhotra, J.D., Kazen-Gillespie, K., Hortsch, M., and Isom, L.L. (2000). Sodium channel beta subunits mediate homophilic cell adhesion and recruit ankyrin to points of cell-cell contact. The Journal of biological chemistry *275*, 11383-11388.

Marcus, J., Dupree, J.L., and Popko, B. (2002). Myelin-associated glycoprotein and myelin galactolipids stabilize developing axoglial interactions. The Journal of cell biology *156*, 567-577.

Mata, M., Kupina, N., and Fink, D.J. (1992). Phosphorylation-dependent neurofilament epitopes are reduced at the node of Ranvier. Journal of neurocytology *21*, 199-210.

Mathis, C., Denisenko-Nehrbass, N., Girault, J.A., and Borrelli, E. (2001). Essential role of oligodendrocytes in the formation and maintenance of central nervous system nodal regions. Development (Cambridge, England) *128*, 4881-4890.

Matsuda, Y., Koito, H., and Yamamoto, H. (1997). Induction of myelin-associated glycoprotein expression through neuron-oligodendrocyte contact. Brain Res Dev Brain Res *100*, 110-116.

McEwen, D.P., and Isom, L.L. (2004). Heterophilic interactions of sodium channel beta1 subunits with axonal and glial cell adhesion molecules. The Journal of biological chemistry *279*, 52744-52752.

McEwen, D.P., Meadows, L.S., Chen, C., Thyagarajan, V., and Isom, L.L. (2004). Sodium channel beta1 subunit-mediated modulation of Nav1.2 currents and cell surface density is dependent on interactions with contactin and ankyrin. The Journal of biological chemistry *279*, 16044-16049.

Melendez-Vasquez, C.V., Rios, J.C., Zanazzi, G., Lambert, S., Bretscher, A., and Salzer, J.L. (2001). Nodes of Ranvier form in association with ezrin-radixin-moesin (ERM)-positive Schwann cell processes. Proceedings of the National Academy of Sciences of the United States of America *98*, 1235-1240.

Menegoz, M., Gaspar, P., Le Bert, M., Galvez, T., Burgaya, F., Palfrey, C., Ezan, P., Arnos, F., and Girault, J.A. (1997). Paranodin, a glycoprotein of neuronal paranodal membranes. Neuron *19*, 319-331.

Michailov, G.V., Sereda, M.W., Brinkmann, B.G., Fischer, T.M., Haug, B., Birchmeier, C., Role, L., Lai, C., Schwab, M.H., and Nave, K.A. (2004). Axonal neuregulin-1 regulates myelin sheath thickness. Science *304*, 700-703.

Miller, R.H. (2002). Regulation of oligodendrocyte development in the vertebrate CNS. Progress in neurobiology *67*, 451-467.

Moscoso, L.M., and Sanes, J.R. (1995). Expression of four immunoglobulin superfamily adhesion molecules (L1, Nr-CAM/Bravo, neurofascin/ABGP, and N-CAM) in the developing mouse spinal cord. The Journal of comparative neurology *352*, 321-334.

Nakada, C., Ritchie, K., Oba, Y., Nakamura, M., Hotta, Y., Iino, R., Kasai, R.S., Yamaguchi, K., Fujiwara, T., and Kusumi, A. (2003). Accumulation of anchored proteins forms membrane diffusion barriers during neuronal polarization. Nature cell biology *5*, 626-632.

Nave, K.A., and Salzer, J.L. (2006). Axonal regulation of myelination by neuregulin 1. Current opinion in neurobiology *16*, 492-500.

Ogawa, Y., Schafer, D.P., Horresh, I., Bar, V., Hales, K., Yang, Y., Susuki, K., Peles, E., Stankewich, M.C., and Rasband, M.N. (2006). Spectrins and ankyrinB constitute a specialized paranodal cytoskeleton. J Neurosci *26*, 5230-5239.

Oohashi, T., Hirakawa, S., Bekku, Y., Rauch, U., Zimmermann, D.R., Su, W.D., Ohtsuka, A., Murakami, T., and Ninomiya, Y. (2002). Bral1, a brain-specific link protein, colocalizing with the versican V2 isoform at the nodes of Ranvier in developing and adult mouse central nervous systems. Mol Cell Neurosci *19*, 43-57.

Pan, Z., Kao, T., Horvath, Z., Lemos, J., Sul, J.Y., Cranstoun, S.D., Bennett, V., Scherer, S.S., and Cooper, E.C. (2006). A common ankyrin-G-based mechanism retains KCNQ and NaV channels at electrically active domains of the axon. J Neurosci *26*, 2599-2613.

Pedraza, L., Huang, J.K., and Colman, D.R. (2001). Organizing principles of the Caspr-Contactin apparatus. Neuron *30*, 335-344.

Peles, E., Nativ, M., Lustig, M., Grumet, M., Schilling, J., Martinez, R., Plowman, G.D., and Schlessinger, J. (1997). Identification of a novel contactin-associated transmembrane receptor with multiple domains implicated in protein-protein interactions. The EMBO journal *16*, 978-988.

Peles, E., and Salzer, J.L. (2000). Molecular domains of myelinated axons. Current opinion in neurobiology *10*, 558-565.

Poliak, S., Gollan, L., Martinez, R., Custer, A., Einheber, S., Salzer, J.L., Trimmer, J.S., Shrager, P., and Peles, E. (1999). Caspr2, a new member of the neurexin superfamily, is localized at the juxtaparanodes of myelinated axons and associates with K+ channels. Neuron *24*, 1037-1047.

Poliak, S., Gollan, L., Salomon, D., Berglund, E.O., Ohara, R., Ranscht, B., and Peles, E. (2001). Localization of Caspr2 in myelinated nerves depends on axon-glia interactions and the generation of barriers along the axon. J Neurosci *21*, 7568-7575.

Poliak, S., and Peles, E. (2003). The local differentiation of myelinated axons at nodes of Ranvier. Nature reviews *4*, 968-980.

Poliak, S., Salomon, D., Elhanany, H., Sabanay, H., Kiernan, B., Pevny, L., Stewart, C.L., Xu, X., Chiu, S.Y., Shrager, P.*, et al.* (2003). Juxtaparanodal clustering of Shaker-like K+ channels in myelinated axons depends on Caspr2 and TAG-1. The Journal of cell biology *162*, 1149-1160.

Pruss, T., Kranz, E.U., Niere, M., and Volkmer, H. (2006). A regulated switch of chick neurofascin isoforms modulates ligand recognition and neurite extension. Mol Cell Neurosci *31*, 354-365.

Pruss, T., Niere, M., Kranz, E.U., and Volkmer, H. (2004). Homophilic interactions of chick neurofascin in trans are important for neurite induction. The European journal of neuroscience *20*, 3184-3188.

Rasband, M.N. (2004). It's "juxta" potassium channel! Journal of neuroscience research *76*, 749-757.

Rasband, M.N., Park, E.W., Zhen, D., Arbuckle, M.I., Poliak, S., Peles, E., Grant, S.G., and Trimmer, J.S. (2002). Clustering of neuronal potassium channels is independent of their interaction with PSD-95. The Journal of cell biology *159*, 663-672.

Rasband, M.N., Peles, E., Trimmer, J.S., Levinson, S.R., Lux, S.E., and Shrager, P. (1999a). Dependence of nodal sodium channel clustering on paranodal Caspr-Contactin contact in the developing CNS. J Neurosci *19*, 7516-7528.

Rasband, M.N., and Shrager, P. (2000). Ion channel sequestration in central nervous system axons. The Journal of physiology *525 Pt 1*, 63-73.

Rasband, M.N., Taylor, C.M., and Bansal, R. (2003). Paranodal transverse bands are required for maintenance but not initiation of Nav1.6 sodium channel clustering in CNS optic nerve axons. Glia *44*, 173-182.

Rasband, M.N., Trimmer, J.S., Peles, E., Levinson, S.R., and Shrager, P. (1999b). K+ channel distribution and clustering in developing and hypomyelinated axons of the optic nerve. Journal of neurocytology *28*, 319-331.

Rasband, M.N., Trimmer, J.S., Schwarz, T.L., Levinson, S.R., Ellisman, M.H., Schachner, M., and Shrager, P. (1998). Potassium channel distribution, clustering, and function in remyelinating rat axons. J Neurosci *18*, 36-47.

Ratcliffe, C.F., Westenbroek, R.E., Curtis, R., and Catterall, W.A. (2001). Sodium channel beta1 and beta3 subunits associate with neurofascin through their extracellular immunoglobulin-like domain. The Journal of cell biology *154*, 427-434.

Rathjen, F.G., Wolff, J.M., Chang, S., Bonhoeffer, F., and Raper, J.A. (1987). Neurofascin: a novel chick cell-surface glycoprotein involved in neurite-neurite interactions. Cell *51*, 841-849.

Richardson, W. (2001). Oligodendrocyte development. In Jessen, K.R., and Richardson, W.D. (Eds.), *Glial Cell Development*. 2nd Edition: Oxford University Press.

Rios, J.C., Melendez-Vasquez, C.V., Einheber, S., Lustig, M., Grumet, M., Hemperly, J., Peles, E., and Salzer, J.L. (2000). Contactin-associated protein (Caspr) and contactin form a complex that is targeted to the paranodal junctions during myelination. J Neurosci *20*, 8354-8364.

Rios, J.C., Rubin, M., St Martin, M., Downey, R.T., Einheber, S., Rosenbluth, J., Levinson, S.R., Bhat, M., and Salzer, J.L. (2003). Paranodal interactions regulate expression of sodium channel subtypes and provide a diffusion barrier for the node of Ranvier. J Neurosci *23*, 7001-7011.

Rosenbluth, J., Dupree, J.L., and Popko, B. (2003). Nodal sodium channel domain integrity depends on the conformation of the paranodal junction, not on the presence of transverse bands. Glia *41*, 318-325.

Salzer, J.L. (1997). Clustering sodium channels at the node of Ranvier: close encounters of the axon-glia kind. Neuron *18*, 843-846.

Salzer, J.L. (2003). Polarized domains of myelinated axons. Neuron *40*, 297-318.

Sanbrook, J., and Russell, D.W. (2001). *Molecular cloning: A laboratory manual*. 3rd Edition: Cold Spring Harbor Laboratory Press.

Sanchez, I., Hassinger, L., Paskevich, P.A., Shine, H.D., and Nixon, R.A. (1996). Oligodendroglia regulate the regional expansion of axon caliber and local accumulation of neurofilaments during development independently of myelin formation. J Neurosci *16*, 5095-5105.

Schachner, M., and Bartsch, U. (2000). Multiple functions of the myelin-associated glycoprotein MAG (siglec-4a) in formation and maintenance of myelin. Glia *29*, 154-165.

Schafer, D.P., Bansal, R., Hedstrom, K.L., Pfeiffer, S.E., and Rasband, M.N. (2004). Does paranode formation and maintenance require partitioning of neurofascin 155 into lipid rafts? J Neurosci *24*, 3176-3185.

Schafer, D.P., Custer, A.W., Shrager, P., and Rasband, M.N. (2006). Early events in node of Ranvier formation during myelination and remyelination in the PNS. Neuron Glia Biol *2*, 69-79.

Schafer, D.P., and Rasband, M.N. (2006). Glial regulation of the axonal membrane at nodes of Ranvier. Current opinion in neurobiology *16*, 508-514.

Scherer, S.S., and Arroyo, E.J. (2002). Recent progress on the molecular organization of myelinated axons. J Peripher Nerv Syst *7*, 1-12.

Scherer, S.S., and Salzer, J.L. (2001). Axon –Schwann cell interactions during peripheral nerve degeneration and regeneration. In Jessen, K.R., and Richardson, W.D. (Eds.), *Glial Cell Development*. 2nd Edition: Oxford University Press.

Schmidt, J., Rossie, S., and Catterall, W.A. (1985). A large intracellular pool of inactive Na channel alpha subunits in developing rat brain. Proceedings of the National Academy of Sciences of the United States of America *82*, 4847-4851.

Sherman, D.L., and Brophy, P.J. (2005). Mechanisms of axon ensheathment and myelin growth. Nature reviews *6*, 683-690.

Sherman, D.L., Tait, S., Melrose, S., Johnson, R., Zonta, B., Court, F.A., Macklin, W.B., Meek, S., Smith, A.J., Cottrell, D.F., and Brophy, P.J. (2005). Neurofascins are required to establish axonal domains for saltatory conduction. Neuron *48*, 737-742.

Simons, M., and Trajkovic, K. (2006). Neuron-glia communication in the control of oligodendrocyte function and myelin biogenesis. Journal of cell science *119*, 4381-4389.

Squinto, S.P., Aldrich, T.H., Lindsay, R.M., Morrissey, D.M., Panayotatos, N., Bianco, S.M., Furth, M.E., and Yancopoulos, G.D. (1990). Identification of functional receptors for ciliary neurotrophic factor on neuronal cell lines and primary neurons. Neuron *5*,757-766

Starr, R., Attema, B., DeVries, G.H., and Monteiro, M.J. (1996). Neurofilament phosphorylation is modulated by myelination. Journal of neuroscience research *44*, 328-337.

Stevens, B., and Fields, R.D. (2000). Response of Schwann cells to action potentials in development. Science *287*, 2267-2271.

Stevens, B., Porta, S., Haak, L.L., Gallo, V., and Fields, R.D. (2002). Adenosine: a neuron-glial transmitter promoting myelination in the CNS in response to action potentials. Neuron *36*, 855-868.

Suzuki, A., Hoshi, T., Ishibashi, T., Hayashi, A., Yamaguchi, Y., and Baba, H. (2004). Paranodal axoglial junction is required for the maintenance of the Nav1.6-type sodium channel in the node of Ranvier in the optic nerves but not in peripheral nerve fibers in the sulfatide-deficient mice. Glia *46*, 274-283.

Tait, S., Gunn-Moore, F., Collinson, J.M., Huang, J., Lubetzki, C., Pedraza, L., Sherman, D.L., Colman, D.R., and Brophy, P.J. (2000). An oligodendrocyte cell adhesion molecule at the site of assembly of the paranodal axoglial junction. The Journal of cell biology *150*, 657-666.

Taveggia, C., Zanazzi, G., Petrylak, A., Yano, H., Rosenbluth, J., Einheber, S., Xu, X., Esper, R.M., Loeb, J.A., Shrager, P*., et al.* (2005). Neuregulin-1 type III determines the ensheathment fate of axons. Neuron *47*, 681-694.

Traka, M., Dupree, J.L., Popko, B., and Karagogeos, D. (2002). The neuronal adhesion protein TAG-1 is expressed by Schwann cells and oligodendrocytes and is localized to the juxtaparanodal region of myelinated fibers. J Neurosci *22*, 3016-3024.

Trapp, B.D. (1990). The myelin-associated glycoprotein: location and potential functions. In Colman, D., Duncan, I., and Skoff, R. Eds., *Myelination and Dysmyelination*. The New York Academy of Sciences, New York.

Trapp, B.D., and Kidd, G.J. (2000). axoglial septate junctions. The maestro of nodal formation and myelination? The Journal of cell biology *150*, F97-F100.

Trapp, B.D., Nishiyama, A., Cheng, D., and Macklin, W. (1997). Differentiation and death of premyelinating oligodendrocytes in developing rodent brain. The Journal of cell biology *137*, 459-468.

Tuvia, S., Garver, T.D., and Bennett, V. (1997). The phosphorylation state of the FIGQY tyrosine of neurofascin determines ankyrin-binding activity and patterns of cell segregation. Proceedings of the National Academy of Sciences of the United States of America *94*, 12957-12962.

Uemoto, Y., Suzuki, S.I., Terada, N., Ohno, N., Ohno, S., Yamanaka, S., and Komada, M. (2006). Specific role of the truncated beta IV-spectrin I6 in sodium channel clustering at axon initial segments and nodes of Ranvier. The Journal of biological chemistry.

Vabnick, I., Novakovic, S.D., Levinson, S.R., Schachner, M., and Shrager, P. (1996). The clustering of axonal sodium channels during development of the peripheral nervous system. J Neurosci *16*, 4914-4922.

Volkmer, H., Leuschner, R., Zacharias, U., and Rathjen, F.G. (1996). Neurofascin induces neurites by heterophilic interactions with axonal NrCAM while NrCAM requires F11 on the axonal surface to extend neurites. The Journal of cell biology *135*, 1059-1069.

Volkmer, H., Zacharias, U., Norenberg, U., and Rathjen, F.G. (1998). Dissection of complex molecular interactions of neurofascin with axonin-1, F11, and tenascin-R, which promote attachment and neurite formation of tectal cells. The Journal of cell biology *142*, 1083-1093.

Walsh, F.S., and Doherty, P. (1997). Neural cell adhesion molecules of the immunoglobulin superfamily: role in axon growth and guidance. Annual review of cell and developmental biology *13*, 425-456.

Wang, H., Kunkel, D.D., Martin, T.M., Schwartzkroin, P.A., and Tempel, B.L. (1993). Heteromultimeric K+ channels in terminal and juxtaparanodal regions of neurons. Nature *365*, 75-79.

Witt, A., and Brady, S.T. (2000). Unwrapping new layers of complexity in axon/glial relationships. Glia *29*, 112-117.

Wood, P.M., Schachner, M., and Bunge, R.P. (1990). Inhibition of Schwann cell myelination in vitro by antibody to the L1 adhesion molecule. J Neurosci *10*, 3635-3645.

Xu, X., and Shrager, P. (2005). Dependence of axon initial segment formation on Na+ channel expression. Journal of neuroscience research *79*, 428-441.

Yang, Y., Lacas-Gervais, S., Morest, D.K., Solimena, M., and Rasband, M.N. (2004). BetaIV spectrins are essential for membrane stability and the molecular organization of nodes of Ranvier. J Neurosci *24*, 7230-7240.

Yang, Y., Ogawa, Y., Hedstrom, K.L., and Rasband, M.N. (2007). {beta}IV spectrin is recruited to axon initial segments and nodes of Ranvier by ankyrinG. The Journal of cell biology *176*, 509-519.

Yin, X., Crawford, T.O., Griffin, J.W., Tu, P., Lee, V.M., Li, C., Roder, J., and Trapp, B.D. (1998). Myelin-associated glycoprotein is a myelin signal that modulates the caliber of myelinated axons. J Neurosci *18*, 1953-1962.

Yu, F.H., and Catterall, W.A. (2003). Overview of the voltage-gated sodium channel family. Genome biology *4*, 207.

Zhang, X., and Bennett, V. (1998). Restriction of 480/270-kD ankyrin G to axon proximal segments requires multiple ankyrin G-specific domains. The Journal of cell biology *142*, 1571-1581.

Zhang, X., Davis, J.Q., Carpenter, S., and Bennett, V. (1998). Structural requirements for association of neurofascin with ankyrin. The Journal of biological chemistry *273*, 30785-30794.

Zhou, D., Lambert, S., Malen, P.L., Carpenter, S., Boland, L.M., and Bennett, V. (1998). AnkyrinG is required for clustering of voltage-gated Na channels at axon initial segments and for normal action potential firing. The Journal of cell biology *143*, 1295-1304.
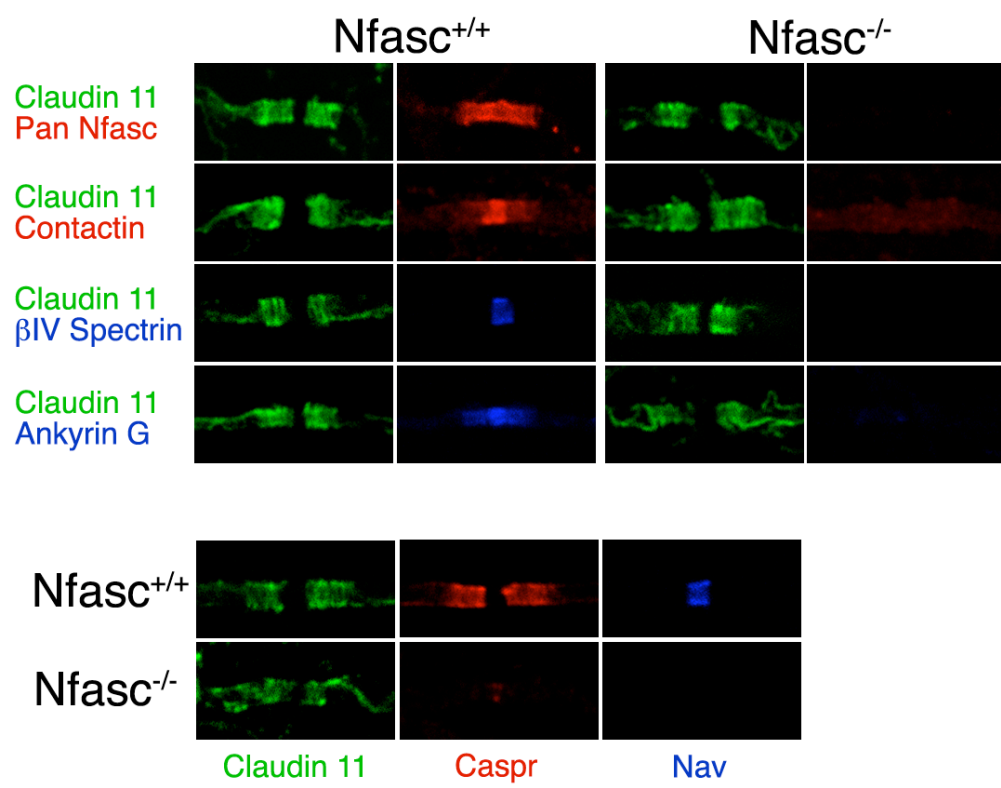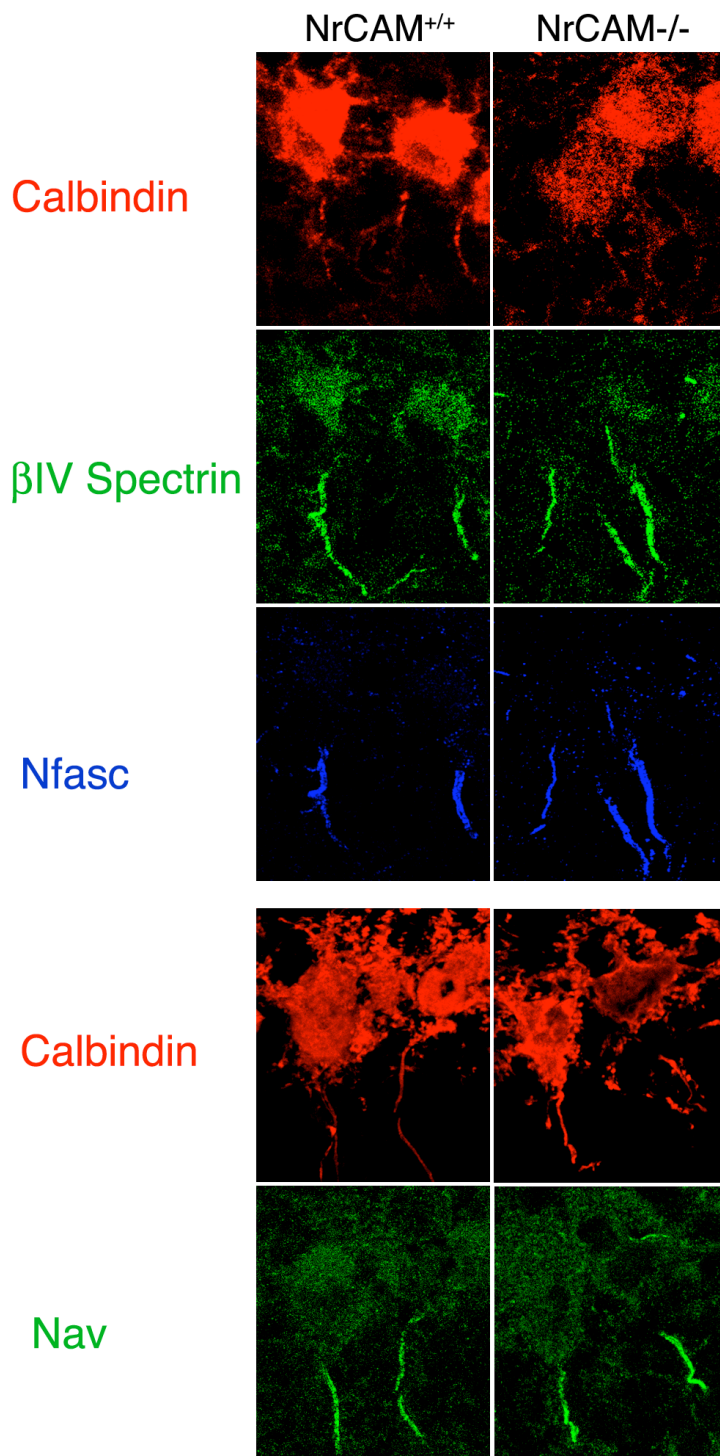
6. SUPPLEMENTARY FIGURES
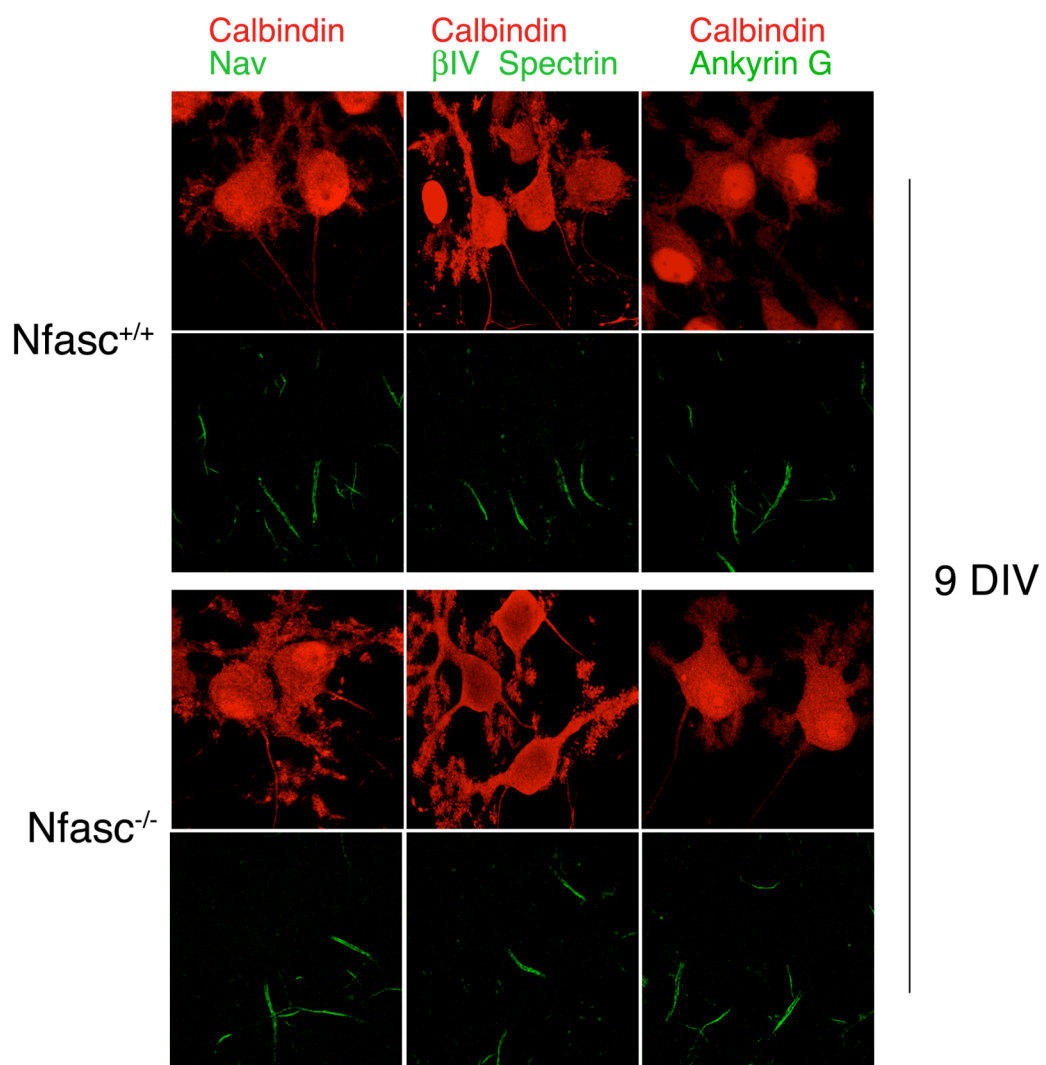
FIGURE S1

FIGURE S2

FIGURE S3-a

FIGURE S3-b

15 DIV